1960

Heat capacity and magnetic susceptibility of thulium ethylsulfate

Bernard Clemence Gerstein
Iowa State University

Mic 60-5879

GERSTEIN, Bernard Clemence. HEAT CAPACITY AND MAGNETIC SUSCEPTIBILITY OF THULIUM ETHYLSULFATE.

Iowa State University of Science and Technology
Ph.D., 1960
Chemistry, physical

University Microfilms, Inc., Ann Arbor, Michigan

HEAT CAPACITY AND MAGNETIC SUSCEPTIBILITY OF THULIUM ETHYLSULFATE

by

Bernard Clemence Gerstein

A Dissertation Submitted to the
Graduate Faculty in Partial Fulfillment of
The Requirements for the Degree of
DOCTOR OF PHILOSOPHY

Major Subject: Physical Chemistry

Approved:

Signature was redacted for privacy.

In Charge of Major Work

Signature was redacted for privacy.

Head of Major Department

Signature was redacted for privacy.

Dean of Graduate College

Iowa State University
Of Science and Technology
Ames, Iowa

1960

TABLE OF CONTENTS

INTRODUCTION

Theorists have a great deal of success in calculating, from first principles, the energy levels of simple gaseous atoms and in correlating these states with many physical properties of gases. When the atom is in the condensed state such as a crystalline solid, it is subjected to electromagnetic fields due to neighboring atoms which profoundly effect the energy states of the system. Also many quantum effects, such as interatomic electronic exchange, which may be neglected in gases, become very important in the condensed state. In attempting to solve the symbolic equations as applicable to the solid state, the theorists have made various simplifying assumptions, and considerable controversy exists in the literature concerning their validity. One such assumption called the crystal field, or ligand field approximation, neglects the finite structure of neighboring electric dipoles, and the exchange interaction between the unpaired electrons of the atom in question and electrons of neighboring atoms. The electric field due to these dipoles is then treated as a perturbation (1) on the atomic energy levels of the atom in question, where these energy levels have been calculated using atomic wave functions. The neglect of the exchange interaction implies that the electric field satisfies Laplace's equation in the region of the atom whose energy levels are being calculated. If the wave functions of the

neighboring dipole systems and the electrons being perturbed by the electric field did over-lap, then the electric field would no longer satisfy Laplace's equation in the region in question. In this case, molecular rather than atomic wave functions would have to be used to obtain a solution to the problem.

Using the crystal field approximation in practice, one does not usually solve the problem from first principles, because the calculation involves an exact knowledge of radial wave functions. Instead, the solution is separated into angular and radial contributions, and the radial contributions are fed into the calculation as experimentally determined parameters. The number of parameters is always small compared to the number of levels one calculates, so the calculation is not trivial. This approximation has led to results which are in fair agreement with experiment in the case of some magnetically dilute cubic salts of the iron group (2) and in good agreement with the splittings of the basic level of the ground term in magnetically dilute rare earth salts (3). Very seldom, however, has an attempt been made to correlate the so called crystal field splittings of all of the term values for any given rare earth salt, or even all of the splittings of the basic term (4).

The rare earth salts, whose 4f electrons are partially shielded by the 5s and 5p shells from exchange interaction, present the ideal physically limiting case in which to test

the validity of the crystal field approximation in its entirety. It is generally inferred from physical evidence (5) that the 4f electrons of the rare earths do not take part in chemical bonding unless first promoted to outer subshells, and it has been established (6) that the sharp absorbtion line spectra of the rare earths at low temperatures is due to transitions within the 4f shell. While the energy states of rare earth ions arise from all the electrons and atoms in the solid, the differences in the energy levels arise from interactions involving only the $4f^n$ electrons, since any contributions from neighboring atoms and other electrons are assumed to be nearly the same for the initial and final states. Therefore, in most calculations involving these levels, one needs only consider the electrons in the incomplete 4f shell. Hund has shown (6) that at room temperatures, the behavior of these levels can be predicted to a good approximation by making the calculation for the gaseous ion. The crystal field splitting must therefore be able to be treated as a perturbation of the L·S coupling, and this is the starting point of the calculation in the rare earths.

Certain physical properties such as the magnetic susceptibility and the magnetic contribution to the specific heat may be calculated once the energy levels of a system are known. It is the purpose of this work to determine experimentally, for the nine hydrated ethylsulfate of thulium, these

properties in a temperature range in which they may be expected to be dependent on the energy level structure. Once these data have been obtained, they can be compared with the presently published experimental work, and theoretical work involving the crystal field approximation. Elsewhere in the Ames Laboratory the energy levels of rare earth salts are being determined from absorbtion spectra, and once a complete identification of observed lines has been made, precise calculations can be made for comparison with thermal, magnetic and spectral data.

The nine hydrated ethylsulfate of Tm, hereafter referred to as TmE.S., was chosen for four reasons as the salt to measure. The first was that the crystal structure was known, and the salt was sufficiently magnetically dilute to allow one to make the assumption that no direct exchange interaction would occur between magnetic atoms (7), (8). The second was that the crystal field matrix elements have been calculated in terms of four crystal field parameters (9), (10), (11), (12), and the energy level calculation is relatively simple. The third was that this is one of the salts whose absorbtion spectra is presently being investigated in this laboratory, and the fourth was that paramagnetic resonance data have given no information concerning the crystal field splittings in this salt, except the negative inferrence that the ground state of the basic term is a singlet.

The procedure for obtaining C_m, the magnetic specific heat of TmE.S., was to measure the heat capacities of TmE.S. and LuE.S. and to make a reasonable assumption concerning the difference in the lattice contributions of the two salts such that C_m could be obtained by the proper subtraction. The magnetic susceptibility was obtained by measuring the change in mutual inductance due to the presence of the sample in a mutual inductance coil. Single crystals were used for the measurement, so that a susceptibility could be obtained parallel and perpendicular to the c axis of the crystal.

REVIEW OF LITERATURE

This review will consist of six sections: spectra, magnetic properties, specific heat measurements, crystal field theory, paramagnetic resonance work, and quantum mechanical calculations of configuration energies. Each section will be reviewed chronologically. The breakdown is necessarily somewhat artificial, since many pieces of work correlate two or more of the above sections. It is felt that the separation will be to the advantage of the reader, however, because of the great amount of material covered. The order of presenting the sections was chosen to approximately follow the chronological order of the development of our knowledge concerning the energy structure of rare earth ions in salts. This too must obviously be an unrealistic ordering because of the simultaneous development of theory and experimental work. The ordering is somewhat interesting, however, because it accentuates how in some cases the experimental work was carried out long after the quantitative theory was developed, and no recourse to anything resembling a quantitative calculation was made by some experimentalists.

Spectra

A few definitions will be needed to avoid confusion concerning terminology used in this review and throughout this work. A "term" is taken to mean the $(2S + 1)(2L + 1)$ states

belonging to a given configuration. An example would be ^3H associated with a $4f^{12}$ configuration. Here, S is 1 and L is 5. "Term intervals" will be taken to mean energy differences between terms. An example would be the energy differences between ^3H and ^3F. "Term splittings" will refer to energy differences between states of a given term, where here "state" means a term symbol with a given J value. An example of a term splitting would be the splitting of ^3H into the $^3H_6$, $^3H_5$, and $^3H_4$ states. "Crystal field splittings" will refer to the splitting of a state into two or more of its 2J + 1 components.

Becquerel, (13 to 22) was one of the first observers to realize that the bands observed in the absorbtion spectra of the rare earths could be sharpened with decreasing temperature and moved with a magnetic field. Herzfeld (23) suggested that these lines were caused by a Stark effect on the vibrating rare earth atoms penetrating the electric field of neighboring atoms. Bequerel (24) later made a similar suggestion. Hund (6) first calculated the magnetic moments at room temperature with the assumption that the rare earth atom existed as the free ion, and Freed and Spedding (25), (26) were one of the first to attempt to correlate Hund's work with the spectra of the salts. Freed (27) followed this with further measurements on the ethyl sulfates of Ce, Pr, Nd, and Gd, and suggested that the transitions for all but Ce were within the 4f shell. At about the same time, Spedding and Nutting (28) measured the

spectra of various salts of Gd and found similar term splittings of the various states with different anions. Spedding (29), and Freed and Spedding (30) suggested that the lines in Gd at low temperatures were caused by the electric field within the crystal. Uzmasa (31) also observed the shift in spectral lines of rare earths in solution with change in anion and suggested the shift was due to the anions. Further qualitative work of this type was carried out by Freed (32), and Spedding and Bear (33).

Prandtl (34) measured the absorbtion spectra of $TmCl_3$, in solution and reported term splittings, but no crystal field splitting. Ellis (35) noted that the rare earths may be the first case of electronic transitions causing color in solids. In 1937, Bethe and Spedding (36) definitely established that the absorbtion spectra of hydrated thulium sulfate could be attributed to transitions within the 4f shell, and in the same year the absorbtion spectra and crystal field splitting of $Nd_2(SO_4)_3.8H_2O$ was measured by Spedding, et al. (37). Merz (38) noted that the properties of free rare earth ions are not shifted greatly in compounds, and Joos and Ewald (39) speculated that the lines in rare earth spectra might be caused by a vibratory type interaction between the metal atom and surrounding atoms. Spedding, et al. (40) found three low lying levels in octa hydrated praesodymium sulfate that were not in disagreement with the crystal field calculations of

Penny and Schlapp (41). Van Vleck (42) calculated the properties of the rare earths using the free ion model, and suggested that the spectral lines were caused by transitions in states not involving a change in electron configuration. Spedding (43) correlated the spectral and magnetic work on $NdCl_3$ and found good or bad agreement with the work of Penny and Schlapp (41) depending upon whose magnetic data were used. Spedding and Hamlin (44) then measured the splitting of the ground state of $NdCl_3.6H_2O$. Merz (45) carried out measurements of absorbtion spectra on rare earth ethylsulfates, and some further work was accomplished by Ewald (46). Meehan and Nutting (47) measured absorbtion spectra of octa hydrated Er, Dy, Ho, and Tm sulfates and stated that the sharp lines were due only to transitions within the 4f shell. Freed, et al. (48) measured the spectra of Eu in some co-ordination compounds and explained their results using the symmetry of the electric field within the crystals.

A review of the emission spectra of the rare earths was made by Meggers (49) in 1942. Broer, et al. (50) obtained term splittings of trivalent Pr, Tm and Yb, and Broer (51) later gave a qualitative discussion of rare earth absorbtion spectra using the results of Bethe (1) who 15 years previous to this, had set up the quantitative basis for the calculations involved. Most of the above work has been reviewed in context by Yost, Russel, and Garner (52). Work on the

absorbtion spectrum of Er has been carried out by Severin (53), (54). Hoonschagen and Gorter (55) have obtained term splittings for trivalent Er from the absorbtion spectrum of erbium nitrate in solution, but made no mention of crystal field splitting. Gobrecht (56) measured the absorbtion spectrum of octahydrated thulium sulfate and obtained term splittings essentially in agreement with Bethe and Spedding (36). Freed and Hochanadel (57) measured the spectra of some rare earth salts which remained fluid at 78°K, but no quantitative statements were made concerning the results. Work on the absorbtion spectrum and crystal field splittings of ground and excited terms of trivalent Eu in the hydrated chloride and bromate was carried out by Hellwege and Kahle (58) and Geisler and Hellwege (59) who calculated the matrix elements of the crystal field potential in terms of the splitting that was observed. Hellwege and Hellwege (60) found three lines in the spectra of trivalent Pr which were attributed to the crystal field splitting of the ground state, $^3H_4$. The Zeeman splittings of single crystals of praesodymium magnesium nitrate and neodymium zinc nitrate were measured by Brochard and Hellwege (61) and were quantitatively interpreted in terms of a crystal field of C_{3v} symmetry with fair success. The g factors were experimentally determined rather than calculated from first principles. Theoretical work on thulium sulfate octahydrate was carried out by Paskin and Keller (62) in an

attempt to understand the spectral data, and the magnetic susceptibility of the salt was calculated. Dieke and Heroux (63) carried out further spectral measurements on salts of neodymium, and interpreted the two lowest Zeeman splittings in terms of the crystal electric field. They essentially used the data to calculate the wave functions for the split states.

Absorbtion spectra of the hydrated fluoride and chloride of Pr were qualitatively interpreted by Freed and Sayre (64) in terms of crystal fields of C_{2v} and C_{3h} symmetry, respectively, and Jørgensen (65) carried out the same type of work on $Nd(BrO_3)_3.9H_2O$. The absorbtion spectrum of hexahydrated holmium and erbium chlorides was measured by Kahle (66) and the results explained on the basis of a crystal field having C_2 symmetry. Jørgensen (67) also measured the spectrum of erbium in solution, but was able to give no quantitative information concerning assignments of L, S, and J quantum numbers for the bands observed. The absorbtion spectrum of $PrCl_3.6H_2O$ was reported by Judd (68), who quantitatively interpreted the results in terms of a calculation involving a crystal field of C_{3h} symmetry, and a partial breakdown of Russell Saunders coupling for the excited levels. He was able to obtain good agreement between theory and experiment for the splittings of the basic state, $^3H_4$. Cook and Dieke (69) measured the absorbtion spectrum of trivalent Gd and obtained term assignments, but mentioned no crystal field splitting.

The absorbtion spectra of thulium ethylsulfate was measured by Johnsen (70) who picked up transitions from the basic to higher states, and a splitting of the ground state at 33 cm^{-1}. Measurements on Nd solutions and salts were carried out by Krumholz (71) who, even as late as 1958, was content to report that a similarity existed between the salt and solution bands. Carlson and Dieke (72) obtained term splittings, and splitting of the ground state of neodymium chloride from fluorescence spectra. No attempt was made to correlate the data with the crystal field approximation. The fluorescence spectra of an Yb impurity in a CaF_2 crystal was measured and analyzed by Feofilov (73). Term intervals and splittings, and crystal field splittings were determined for ions of Ce, Pr, Nd, Sm, Eu, Gd, Tb, Dy, Ho, Er, Tm, and Yb from an analysis of the fluorescence spectra of rare earth activated phosphorous by Keller (74), and Keller and Pettit (75). The crystal field splittings were not quantitatively correlated with current crystal field theory. Kahle (76) has recently measured the spectra of Eu in the bromate and chloride salts and correlated the results with the crystal field approximation. He essentially evaluated the crystal field matrix elements of the lowest states from the spectral data. Gruber and Conway (77) have measured the absorbtion spectrum of thulium ethylsulfate and picked up splittings of the ground state at 33, 195 and 321 cm^{-1}. They also calculated term splittings and intervals and

compared them, to within 200 cm^{-1}, with the lines that they observed. They found that one must consider intermediate, rather than pure Russel Saunders coupling, for a reasonable agreement between calculated and experimental term splittings.

Magnetic Properties

In 1921, Wedekind (78) was one of the first to plot effective magneton number versus atomic number for the rare earths and obtain the curve, later published by Van Vleck (5), with maxima at Nd and Dy. The work prior to 1930 by Cabrera, Meyer, Duperier, Zernicke and James, Decker, and Williams has been tabulated and discussed by Van Vleck (5). The result of this work is that all the rare earths with the exception of Sm and Eu, have magnetic moments at room temperature which are in fair accord with the lowest J value calculated assuming Russell Saunders coupling.

The theoretical and experimental work, by Kramers and co-workers, on the magnetic properties of rare earth salts, has recently been collected and published, along with the rest of Kramers' work, by the North Holland Publish Co. (79). Kramers succeeded in setting up the theory relating the energy structure of the rare earth ions to their magneto optical properties, but the experimental work on the Faraday effect was such, that at the time no extensive definitive conclusions were reached concerning the detailed relationships between energy levels and magneto optical rotary power. Most of the later

workers turned to the spectra for a more straight-forward approach to the problem.

In 1931, Gorter (80) tabulated the theoretical work of Hund, Laport and Sommerfeld, and Bose and Steiner for comparison. All authors agreed roughly that the magnetic moments of the rare earths at room temperature could be obtained from a free ion type calculation. Klemm, et al. (81) measured the room temperature magnetic moments of La, Ce, Pr, Nd, and Sm hexaborides, and found that the magnetic moments were consistent with the free ion value. Williams (82) found that some Gd and Nd salts obeyed a Curie-Weiss law near room temperatures, and tabulated values for the Curie-Weiss Δ. The same type work was carried out on the octahydrated sulfates of Tb, Dy, Ho, and Er by Velayos (83), and on Nd_2O_3 and Pr and Nd sulfates by Cabrera, et al. (84). The magneto-rotary power of nine hydrated ethylsulfates of Pr, Nd, Dy and Er was measured by Becquerel (85) in 1935, who found that the ratio between the magnetic moment and the rotation of plane polarized light through the crystal was a constant. In the same year, Fereday and Wiersma (86) measured the principle susceptibilities of single crystals of Ce, Pr, Nd, and Er ethylsulfate nine hydrate, and found the parallel susceptibility to be greater than the perpendicular susceptibility in the range 14-200°K for all except Pr ethylsulfate, the only one having an even number of 4f electrons. A year later, Mazza and Botti (87) reported

the room temperature susceptibility of a mixture of Sm_2O_3 and Gd_2O_3. Cabrera (88) reported susceptibility measurements on a number of rare earth salts and found that all could be fitted with a Curie-Weiss curve. Some single crystal work on octahydrated neodymium sulfate was done by Krishnan and Mookherji (89) in 1938 and the anisotrophy of the crystals interpreted in terms of a non-cubic crystal field. In 1939 Jackson (90) measured the susceptibility of a single crystal of octahydrated neodymium sulfate in the range 14-300°K, and found excellent agreement with Krishnan and Mookherji's data. He made no calculations, however, to relate the results to the electric field in the crystal. In the same year, Penny and Kynch (91) attempted to reconcile the spectral and magnetic data on $Nd_2(SO_4)_3.8H_2O$ using a cubic crystal field, but were unsuccessful in doing so. Freed (92) made some more qualitative statements concerning the relation between the magnetic properties of rare earth ions in salts and solutions, and the symmetry of the surrounding crystal field. Most of the important magnetic work on the rare earths prior to 1941 has been summarized by Yost, Russell, and Garner (52).

In 1942, Van den Handel (93) measured the perpendicular and parallel susceptibilities of neodymium ethylsulfate and found deviations from Curie's law below 200°K, but did not interpret the results as caused by a trigonal crystal field. Subsequently, in 1953, Elliot (4) calculated the susceptibility

of this salt and found excellent agreement between the calculations made by Elliot and Stevens, and Van den Handel's results. The Elliot-Stevens crystal field calculations will be reviewed under "Review of Literature, Crystal Field Theory".

Some single crystal susceptibility measurements on magnetically dilute salts of Ce, Pr, Nd, and Sm were carried out by Mukherji in 1949 (94). He found that the axis along which the maximum susceptibility was measured varied as a function of temperature. The maximum variation was found to be 63° in the case of $Pr_2Mg_3(NO_3)_{12}\cdot 24H_2O$ and was of the order of 10° for similar salts of Ce and Nd. No variation was reported in the Sm salts which were measured.

In 1955, Satten and Young concluded from susceptibility measurements on octahydrated sulfates of rare earths (95) that the crystal field in these salts was not cubic, as had been previously supposed. The results of the Faraday effect on ethylsulfates of Ce, Pr, Sm, Gd, Dy, and Er were reviewed by Van den Handel (96) in 1956, but no crystalline field interpretation was given. In 1959 the susceptibilities of Pr_2O_3 and Tb_2O_3 were measured from 100 to 600°K by Vickery and Ruben (97) and it was observed that the Curie-Weiss law was obeyed, and that the magnetic moments corresponded to that of the free ions. In the same year, Mookherji and Neogy (98) discussed the assymetry of the crystal field of $Eu_2(SO_4)_3\cdot 8H_2O$ as evidenced by the magnetic anisotropy that they found in the

crystal. They too concluded that the crystal field in this type of compound was not cubic.

Ayant and Thomas (99) calculated the magnetization of Yb in ytterbium iron garnet assuming the Yb ion to be in a cubic crystal field, and found good agreement between theory and experiment. The susceptibilities of gallates of Pr, Nd, and Er were measured from 4-300°K by Cohen and Ducloz (100), who reported that Curie's law was not followed at low temperatures.

Specific Heat Measurements

Relatively little work has been reported on calorimetric measurements of the specific heats of rare earth salts, possibly because of the difficulty involved in separating a large lattice contribution from a small electronic contribution. The method of paramagnetic resonance (101), however, has been recently used in some cases to obtain ground state splittings from which specific heat curves have been calculated.

The first attempt to obtain Schottky type anomalies which agreed with previous crystal field splitting data for rare earth salts was made by Ahlkberg and Freed (102). These workers measured Cp of octahydrated samarium sulfate in the range 14-300°K, and obtained a peak at 100°K which agreed with the ground term splittings measured by Spedding and Bear (33). The heat capacity of octahydrated gadolinium sulfate (103), (104) was used to obtain the lattice contribution of the Sm

salt. Later, Ahlkberg, et al. (105) measured the heat capacities of octahydrated Sm sulfate and octahydrated Nd sulfate from 3-40°K and found no evidence of an electronic transition in the Sm salt, but evidence of the 77 cm^{-1} level found by Spedding, et al. (37) in the Nd salt.

In 1953, Daniels (106) gave formulae relating the susceptibility and entropy of a paramagnetic salt, which could be used once the dipole-dipole interaction between magnetic ions was known. The formulae appeared to work quite well for Nd ethylsulfate below 4°K, but not for Ce ethylsulfate, implying that exchange effects were coming into play in the Ce salt at low temperatures. The magnetic heat capacities of Nd and Ce ethylsulfates were obtained from the paramagnetic resonance data of Bleany, et al. (107) and Cooke, et al. (108). Subsequently Cooke, et al. (109) measured the paramagnetic resonance of Ce magnesium nitrate from 104°K and were able to satisfactorily account for the specific heat obtained from the observed splitting in terms of magnetic dipole-dipole interactions. It would thus appear that the more magnetically dilute crystals of $Ce_2Ng_3(NO_3)_{12}.24H_2O$ do not undergo magnetic exchange type interactions as does $Ce(C_2H_5SO_4)_3.9H_2O$ below 4°K. The relationship between strong magnetic exchange interactions and inter-magnetic dipole distances has recently been discussed by Sato and Kikuchi (110) and it might be of interest to correlate the data on these two Ce salts with their conclusions.

The specific heat of Yb ethylsulfate has been measured by Cooke, et al. (111) and the statement was made that no Schottky type contribution existed below 20°K. Horst Meyer and P. L. Smith (112) measured the heat capacities of La, Pr, Nd, Dy, Yb, and Y ethylsulfates in the range 1.3-20°K and found the thermal data to agree well with results obtained from paramagnetic resonance data and the crystal field theory of Elliot and Stevens, which will subsequently be reviewed.

Goldstein, et al. (113) measured the specific heats of La_2O_3 and Nd_2O_3 and reported evidence of a bump in the Nd oxide. No interpretation was given. The specific heats of $PrCl_3.6H_2O$ and $LaCl_3.6H_2O$ were measured by Hellwege, et al. (114), in the range 4.8-280°K, and the magnetic contribution of the Pr salt was obtained by assuming that the lattice contribution was the same for both salts. A Schottky type bump was picked up at 10°K which agreed fairly well with a crystal field splitting calculated for the first excited level above ground in the lowest state of the basic term, $^2F_{5/2}$.

Crystal Field Theory

In 1929, Hans Bethe (1) laid the foundation for the calculation of atomic energy levels using the crystal field approximation, and a year later (115) he somewhat enlarged upon his first paper. All work subsequent to this has been concerned with the application of Bethe's theory to a specific

type of experiment, or specific symmetries.

Jordahl, et al. (116), and Penny and Schlapp (41), (117) followed Bethe's work with calculations of the susceptibilities of Pr, Nd, Ni, Cu, Cr, and Co salts using the crystal field approximation. The magnetic data, however, was only good to about 10 per cent at best, so no definite conclusions could be drawn as to how far a quantitative calculation could be pushed. In 1935 Van Vleck (118) explained the low susceptibilities of iron group salts with qualitative arguments concerned with the energy levels of the salts as split by a cubic, or nearly cubic field. Kynch (119) followed this with calculations of the matrix elements of 4f electrons in a cubic field. Spedding, in 1937, (120) calculated the crystal field splitting for the ground term of trivalent Er for a field of cubic symmetry, and in accordance with the earlier work of Penny and Schlapp (41), calculated the magnetic susceptibility of octahydrated erbium sulfate. Bethe and Spedding (36), in the same year, measured and calculated term intervals and splittings and cubic crystal field splitting for trivalent Tm in the octahydrated sulfate. From the magnitude of the spin-orbit coupling parameter, they came to the conclusion that R-S coupling was far from being followed for this salt. In 1938, Ellis and Hall (121) noted that from Ketelaar's (7) structure determination of the rare earth ethylsulfates, the crystal field splittings of some rare earth ethylsulfates could be determined in terms of the

spherical harmonics Y_2^o and Y_4^o.

There was an absence of work during the years immediately prior to, and during the second world war, but work was resumed in 1948 by Kittel and Luttinger (122) who applied the crystal field approximation to microwave absorbtion experiments on salts having cubic, tetragonal, rhombic, and trigonal symmetries. A year later, DeBoer and Van Lieshout (123) carried out the same type of work. They applied their calculations to the splitting of the ground state of trivalent Gd in a cubic crystal field, and took intermediate coupling into account. The years 1951 through 1953 saw six papers come out by Stevens (9) and Elliot (10), Elliot and Stevens (11), (12), (124), and Scovil and Stevens (125). In these papers, they developed the calculations for applying the crystal field approximation to the rare earth ethylsulfates in terms of the matrix elements of a C_{3h} crystal field for the ground and next higher J value. This work was followed by that of Judd (126), (127), (128) who performed the same calculations for a crystal field of C_{3v} symmetry, which is found in the rare earth double nitrates. In 1952 Kleiner (129), and later Tanabe and Sugano (130) calculated, from first principles, the crystal field splitting parameter for potassium chrome alum, and came out with a result that was not only the wrong order of magnitude, but differed in sign from the experimentally determined parameter for the cubic salt. Their conclusions were that the interactions of the

chromium atom with the finite structure of the surrounding dipoles, which in the crystal field treatment are considered as point dipoles, were the cause of the discrepancy. Recently, however, Phillips (131) has shown that these three workers neglected the orthogonalization of the metal and ligand wave functions with respect to each other, and that the orthogonalization procedure leads to a calculated crystal field parameter which is in agreement with experiment.

In 1957, Lacroix (132) attempted to correlate theory and experiment in the splitting of the ground terms in trivalent Eu and Gd in cubic crystal fields. The paramagnetic resonances of these ions in a cubic lattice of CaF were measured. In the same year, Hellwege, et al. (133) used first order perturbation theory to calculate the Zeeman plus crystal field splittings of the ground term of EuE.S. Sayre, et al. (134) cleared up a few minor disagreements between their work in 1958 and Judd's previous calculations, and Afanas'eva (135) essentially repeated the calculations of Judd, Elliot, and Stevens for the rare earth ethylsulfates and double nitrates. In the same year, Low (136) measured the paramagnetic resonance of trivalent Gd in the cubic crystal field of a CaF lattice. He essentially repeated the work of Lacroix (132), and somewhat more fully developed the theory of splitting of an S state in a cubic field using intermediate coupling. Subsequently Lacroix (137) suggested that the

ground configuration of the trivalent Gd ion was $4f^6(5S^26p^6)6P$ rather than the conventional $4f^7$, in order to account for the difficulty in correlating theory and experiment for this ion in a known cubic field. Statz and Koster (138) in 1959, developed the general theory of Zeeman splittings for crystal fields of all symmetries, and at the same time Jarrett (139) published the formalism for incorporating covalent bonding into the crystal field approximation. Simultaneously, White and Andelin (140) calculated the results of including a magnetic exchange interaction along with the crystal field potential in the Hamiltonian. Satten and Margolis (141) have recently published L•S and crystal field matrix elements for the f^2 configuration in crystal fields of trigonal and octahedral symmetry, to be used in conjunction with Stevens' (9) tables.

Paramagnetic Resonance

The theoretical work relating paramagnetic resonance absorbtion to crystal field splittings in rare earth ethylsulfates and chlorides was essentially carried out by Stevens (9), Elliot (10), Elliot and Stevens (11), (12), (123), (124), (142), (143), Scovil and Stevens (125), and Judd (126), (127), (128) in the years 1951 to 1957. The paramagnetic resonance effect, discovered by Zavoisky (144) in 1945, has been extensively used to determine ground state splittings of paramagnetic salts, and has been discussed by Cooke (101). In 1950, Al'tshuler, *et al.* (145) published results of resonance

experiments of hydrated nitrates and sulfates Pr and Nd, Er $(NO_3)_3 \cdot 5H_2O$, $Ce(CO_3)_3 \cdot 5H_2O$, and Sm_2O_3. The results were interpreted in terms of crystal field splittings of the ground state of the basic term in the trivalent ions.

The paramagnetic resonance work in the Clarendon laboratory (107), (146), (147), (148) has been reviewed by Bleany and Stevens (149), Cooke (3), and Bowers and Owen (150) in the light of the calculations of Stevens, Elliot, and Judd. Hellwege, in 1953 (151) measured the hyperfine splittings of trivalent Pr using the paramagnetic resonance technique. In 1957, Al'tshuler, et al. (152) carried out paramagnetic resonance absorbtion experiments on double nitrates and ethyl sulfates of trivalent Pr, Eu, Tb, Ho, and Tm, but used ultrasonic vibrations instead of an alternating magnetic field in their work. Huchinson, et al. (153) measured the paramagnetic absorbtion of hydrated gadolinium chloride, a crystal with C_{3h} symmetry, and used the calculations made by Elliot and Stevens to interpret their results. Subsequently Huchinson and Wong (154), and Judd and Wong (155) used paramagnetic resonance to determine the splittings of the basic terms in all of the rare earth trichlorides, and Er and Ho magnesium nitrates. The trichlorides have C_{3h} symmetry, and so could be considered in the light of Stevens' and Elliot's theory for the ethylsulfates. The measurements on the magnesium nitrates were interpreted in terms of Judd's earlier work (127) on

matrix elements of a crystal field of ichosohedral symmetry. Ryter (156), in the same year, measured the paramagnetic resonance of Eu and Gd which were introduced as impurities in the cubic lattice of CaF, and found that he was able to account for the results with a cubic crystal field. The same work was carried out at practically the same time by Lacroix (132), (137), and Low (136), but Lacroix, as mentioned in the last section, felt that he could not adequately describe his results with a $4f^7$ configuration for Gd.

Sanadze (157), in 1957, measured the paramagnetic resonance of $Nd(NO_3)_3.6H_2O$, repeating the work that had been done earlier by Al'tshuler (145). In 1958, Matsumura, et al. (158) measured the electron spin resonance of trivalent Eu in cubic CaF, and interpreted their results in terms of the calculations of Kittel (122) and DeBoer (123). Baker and Bleany (159), in the same year, obtained magnetic moments and nuclear spins of Pr^{141}, Tb^{159}, and Ho^{167} using paramagnetic resonance to measure hyperfine splitting. They could pick up no resonance in Tm, which indicated that the ground state was non-degenerate, and they stated that the overall splitting of the ground terms for Tm and Tb should be small relative to the other rare earths because of the magnitude of Stevens' α, β and γ.

Quantum Mechanical Calculations of Configuration Energies

There have been essentially two schools of thought with respect to the calculation of term intervals and term splittings in the rare earths. The first, following Hund's (6) original calculation, and the evidence presented by Van Vleck (5) that the rare earths closely followed the Russell-Saunders case as presented by Conden and Shortley (160), calculated term intervals using the Russell-Saunders (R-S) coupling scheme. The second, and most recent, has taken account of the fact that R-S coupling is not followed exactly by the rare earths, and an accurate calculation must include intermediate and spin-spin coupling.

Gibbs, *et al.* (161), in 1929, published calculated term intervals and splittings for $4f$ electrons following Hund's (6) scheme. Three years later Snow and Rawlins (162) calculated, and measured term splittings for salts of Pr, Nd, Sm, and Eu using the R-S scheme, and found relatively good agreement. Hund (163) in 1936, extended his earlier treatment (6), and in the same year R. J. Lang (164) located terms for trivalent Ce. There were four papers published by Gobrecht (165), (166), (167), (168) in the years 1937-38, in which he discussed multiplet structure for rare earth ions in terms of the R-S coupling scheme.

H. Lang did the same for trivalent Pr and Eu in 1938 (169).

Two years later, Spedding (170) also calculated the term intervals and splittings for trivalent Pr using the methods of Condon and Shortley. He found good agreement between his calculated values and his previous data (40) if he took intermediate coupling into account.

As with the other work, theoretical and experimental, on rare earth metals and compounds, the calculations prior to 1940 have been reviewed by Yost, et al. (52).

Racah (171), (172), (173), (174), in the years 1942 to 1949, published a series of four papers in which he replaced Condon and Shortley's diagonal sum method of calculating matrix elements of e^2/r_{ij} by a more simplified calculation using matrix algebra and tensor operators.

In 1950, Rao (175), (176), (177) calculated the term values for the $4f^4$ configuration, and Ishizdu (178), in the same year, calculated the off-diagonal electrostatic matrix elements for the $4f^3$ configuration using Racah's methods to obtain his results. Two years later, Racah (179) extended his methods to the calculation of term values for the f^3 configuration.

Satten (180) measured the absorbtion spectrum of $Nd(BrO_3)_3 \cdot 9H_2O$, and in addition to experimentally determining all of the crystal field splittings of the ground term $^4I_{9/2}$, he calculated term energies for the f^3 configuration using Slater's diagonal sum method. His results agreed with those

of Racah. He assumed R-S coupling for all terms calculated, and recalculated two terms having J = 1/2 taking into account intermediate coupling. In a later note (181) he discussed an error in his previous paper which has been found by Jørgensen (182). Satten has also discussed the Landé interval rule for the f^3 configuration (183). Reilly (184), also in 1953, calculated the electrostatic matrix elements of the f^7 configuration, and correlated Slater's and Racah's methods for computing term intervals.

Jørgensen (185) in 1955, published a note in which he attributed the opacity of solutions of trivalent Tm in $HClO_4$ to f-d transitions, and noted that Spedding's previous identification (170) of the position of the ^1I term might be in error. Judd, in the same year, (186) calculated term splittings which agreed with spectroscopic data (58), (169) for trivalent Eu. He assumed in his calculation that there was no breakdown of R-S coupling. The same type of calculation was made by Judd in 1956 for trivalent Sm, Dy, Eu, Tb, and Ho (187), but this time he considered deviations from R-S coupling which were caused by spin-spin interactions. His calculations satisfactorily explained the deviations of the above ions from the Landé interval rule.

In 1957 Elliot, Judd, and Runciman (188) used the tensor-operator and group theoretical methods of Racah to examine the coulomb interaction, L·S coupling, and crystal field potential

terms in the Hamiltonian. Their paper, coupled with the earlier work of Stevens (9), Elliot (10), Elliot and Stevens (11), (12), (124), (142), (143), Scovil and Stevens (125), Judd (126, (127), (128), and Racah (171 to 174), forms the most comprehensive statement to date of the formalism and calculations involved in a complete solution of the problem of a rare earth ion in a crystalline solid. They do not include magnetic exchange type of interactions, however, but the treatment of the problem when one adds magnetic exchange, and over-lap of ligand and metal ion orbitals has been set up by Jarrett (139) and White and Andelin (140).

Rao (189) recalculated term splittings in 1958 for the $4f^1$ and $4f^2$ configurations, and in 1959 Gruber and Conway (190) calculated term intervals and splittings for trivalent Tm taking into account intermediate coupling. In 1959, Judd and Louden (191) calculated spin-orbit matrix elements for the f^3 configuration using R-S coupling only, and correlated their results with the earlier experimental work of Dieke and Heroux (63) and Spedding (40). Wybourne (192), in the same year, recalculated term splittings for trivalent Pr and Tm, in agreement with the earlier work of Bethe and Spedding (36), (40). Also in 1959, Runciman (193) published tables classifying the terms in the f^7 configuration. Wybourne has recently calculated terms for trivalent Nd and Er (194). He diagonalized the complete spin orbit matrices for the f^3 and f^{11}

configurations to obtain term energies. The most recent publication to appear has been a calculation by Gruber and Conway (195) of the crystal field splittings of the ground and higher terms of nine hydrated thulium ethylsulfate. Intermediate coupling was taken account of, and the agreement between the calculated and observed splittings of the ground term was much better than that calculated using crystal field constants extrapolated from the work of Elliot and Stevens (11). This point will be treated at the end of this work in the discussion section. The agreement between calculated and observed splittings of excited states, however, left a great deal to be desired.

Summary of Literature Review

A brief glance through the above review might lead one to suspect that the crystal field approximation has been extensively tested and not found lacking, so further experimental work could be considered as frosting on the cake. To the extent that this review has not been a critical one, the criticism is justified. If one intercompares, however, the "good" agreement between experiment and theory obtained by various workers on a given compound, ca. the hexa hydrated chlorides of the rare earths which are now known to belong to the symmetry group C_{3h}, one sees that the early workers obtained "good" agreement using a crystal field of cubic symmetry, whereas the later ones explained their results using

a trigonal field. Clearly the criterion of "good" agreement was different in the two cases. An examination of the results of spectral measurements also reveals that where the splitting of the ground state has been correlated with crystal field calculations, the crystal field splittings of higher states are frequently in complete disagreement with the calculated values, or agree so poorly that there is a definite indication of error somewhere. It might also be mentioned that where various authors have claimed agreement between calculated and experimental term intervals, the possibility exists that the states have been incorrectly identified. This is particularly true where states are moved as much as 10,000 cm^{-1} when intermediate coupling is included, and the identification of the states was made using R-S coupling.

While it is true that the workers at the Clarendon Laboratory have been successful in quantitatively correlating paramagnetic resonance and heat capacity data with splittings of the lowest level of the ground state for the even numbered rare earths, they have only evaluated four pieces of information using four parameters. It would seem that a more extensive quantitative test might be desired, namely, a fitting of at least all of the splittings of the ground state with these four parameters. This is not to underestimate the importance of the calculations of Elliot, Stevens, and Judd, but only to point out that their results have not been

extended as far as they might be.

One does have the feeling, however, that transitions within the $4f$ configuration are largely responsible for the optical, thermal and magnetic properties of the rare earth salts. Also, because of the excellent "partial" fitting between experiment and theory, it would seem that the theoretical calculations might be extended to obtain all of the splittings of the ground plus some higher states for even and odd numbered rare earth salts. By no stretch of the imagination has this yet been accomplished theoretically, and the present experimental data are not yet extensive enough to allow even all ground state splittings to be identified for a homologous series of rare earth salts.

MATERIALS AND APPARATUS

Materials

The $Tm(EtSO_4)_3 \cdot 9H_2O$ and $Lu(EtSO_4)_3 \cdot 9H_2O$ were prepared from 99.9+ per cent pure oxides of Tm and Lu obtained at the Ames Laboratory. The procedure for separation and purification of the rare earths has been discussed by Spedding (196). The procedure for preparation of the salt was as follows: The oxide was dissolved in concentrated HCl at 85°C and allowed to boil down to a thick syrup. The solution was then cooled and about 80 per cent of the remaining water aspirated off at room temperature. The cooling was done to prevent the formation of the insoluble oxychloride which forms at temperatures of the order of 90°C in the presence of air. The almost dry hydrated chloride was then dissolved in absolute ethanol, and mixed with an absolute alcoholic solution of sodium ethylsulfate, an excess of 10 per cent more than the stoichiometric amount of $NaEtSO_4$ needed to combine with the Tm being used. It was found that the solubility of $Tm(EtSO_4)_3 \cdot 9H_2O$ in CH_3CH_2OH was 172 g/l, so 5.82 ml of absolute ethanol was used in the combined solutions for each g of $Tm(EtSO_4)_3 \cdot 9H_2O$ to be prepared. When the alcoholic solutions of the rare earth chloride and sodium ethylsulfate were combined, the majority of the NaCl in the solution was precipitated. The solution plus NaCl precipitate was allowed to stand at room temperature for 24 hours, and the NaCl precipitate then removed by

filtration. Ninety per cent of the alcohol was then removed from the solution at room temperature by aspirating the solution in a filtering flask which was immersed in a constant temperature water bath and attached to a rocking mechanism to prevent supersaturation at the surface of the solution. Enough water to dissolve the ethylsulfate was then added to the alcoholic solution, and the solution aspirated at room temperature, with rocking, down to a thick mush of fine crystals. The crystals were filtered, dissolved, and one recrystallization from H_2O carried out. The resulting crystals were analyzed (197) by titration with E.D.T.A. in the presence of 2-(1,8-dihydroxy-3,6-disulfo-2-naphtylazo)-benzene sulfonic acid and found to contain 99.9 per cent the theoretical amount of rare earth. These crystals were used for the heat capacity measurements.

To obtain the single crystals used for the magnetic susceptibility measurements, some seed crystals about 5mm x 5mm x 2mm were taken from the crystals to be used in the heat capacity measurements, and glued to a plexiglass paddle with plexiglass cement. The paddle was wired to a glass rod with gold wire, and the rod connected to an electric motor which rotated it at about 15 rpm and reversed direction every 10 seconds. The end of the rod to which the crystal was attached was immersed in 150 cc of saturated solution in a beaker which was placed in a dessicator. Dessicant was

placed about the beaker to remove the water from the solution, and it had to be replaced every 36 hours. The crystal growing apparatus is shown in Figure 1. In retrospect it appears that it might have been simpler and less expensive to simply expose the beaker to the atmosphere of the laboratory, and make some arrangement to keep dust out of the solution while stirring.

The crystals grown for the susceptibility measurements were about 3 cm long by 2 cm wide by 1-1/2 cm thick. Under carefully controlled conditions, a crystal this size could be grown in 2 weeks. By "carefully controlled conditions" is meant primarily not allowing the solution to become unsaturated when adding water to dissolve small seed crystals that formed during the evaporation process. This prevention was accomplished by removing the rod plus crystal from the saturated solution, adding water to the solution, and stirring for 10 minutes. If all the small crystals in the solution were not dissolved, it was safe to replace the crystal in the solution and continue its growth.

Apparatus

Heat capacity measurements

The type of low temperature calorimeter and circuits used for heat capacity measurements from 12 to 300°K has previously been described (198), so no overall description will be given of them here. The wiring of the thermocouples, and the calorimeter can are different than in the calorimeter

Figure 1. Apparatus for growing single crystals from aqueous solution

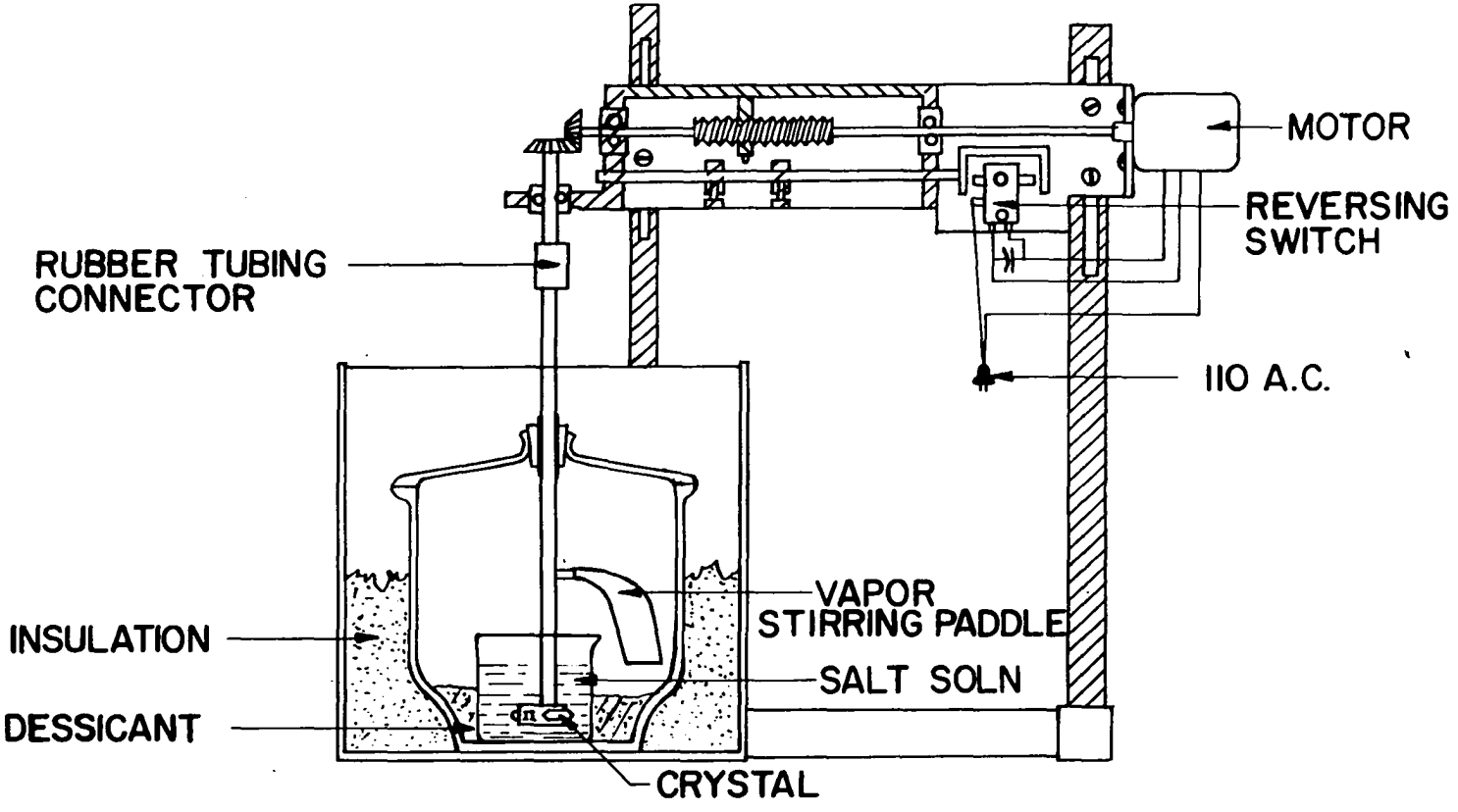
MOTOR
REVERSING SWITCH
RUBBER TUBING CONNECTOR
110 A.C.
VAPOR STIRRING PADDLE
INSULATION
SALT SOLN
DESSICANT
CRYSTAL

referred to above, however, so a short account will be given of them: The absolute and difference thermocouples were copper-constantan, and were arranged as shown schematically in Figure 2. There were 6 difference thermocouples to measure the temperature difference between the 3 components of the sample can and adiabatic shield, the side bottom and top, and between the side and bottom of the shield, the side and top of the shield, and the bottom of the shield and the floating ring. Absolute thermocouples were soldered to the side of the shield and to the lower refrigerant tank. The wires used were No. 32 B. & S. silk insulated copper and No. 34 silk insulated advance constantan. As shown in Figure 2, one copper wire, number 2, served for the can side of the side, bottom and top difference thermocouples.

It was decided to use the one, rather than 3 copper wires for this purpose in order to reduce the thermal conductivity of the bundle of leads between the gold plated sample can and adiabatic shield. That this procedure would lead to no undesirable thermal emfs was shown by a measurement of the thermal emf between gold plated copper and copper which was found to be 3.4 microvolts/220°.

Similarly, one copper wire, number 1, served for the shield side-bottom and shield side-top difference thermocouples, and one constantan wire, number 5, served for both absolute thermocouples. In the ring shield difference thermo-

Figure 2. Thermocouple arrangement in the calorimeter

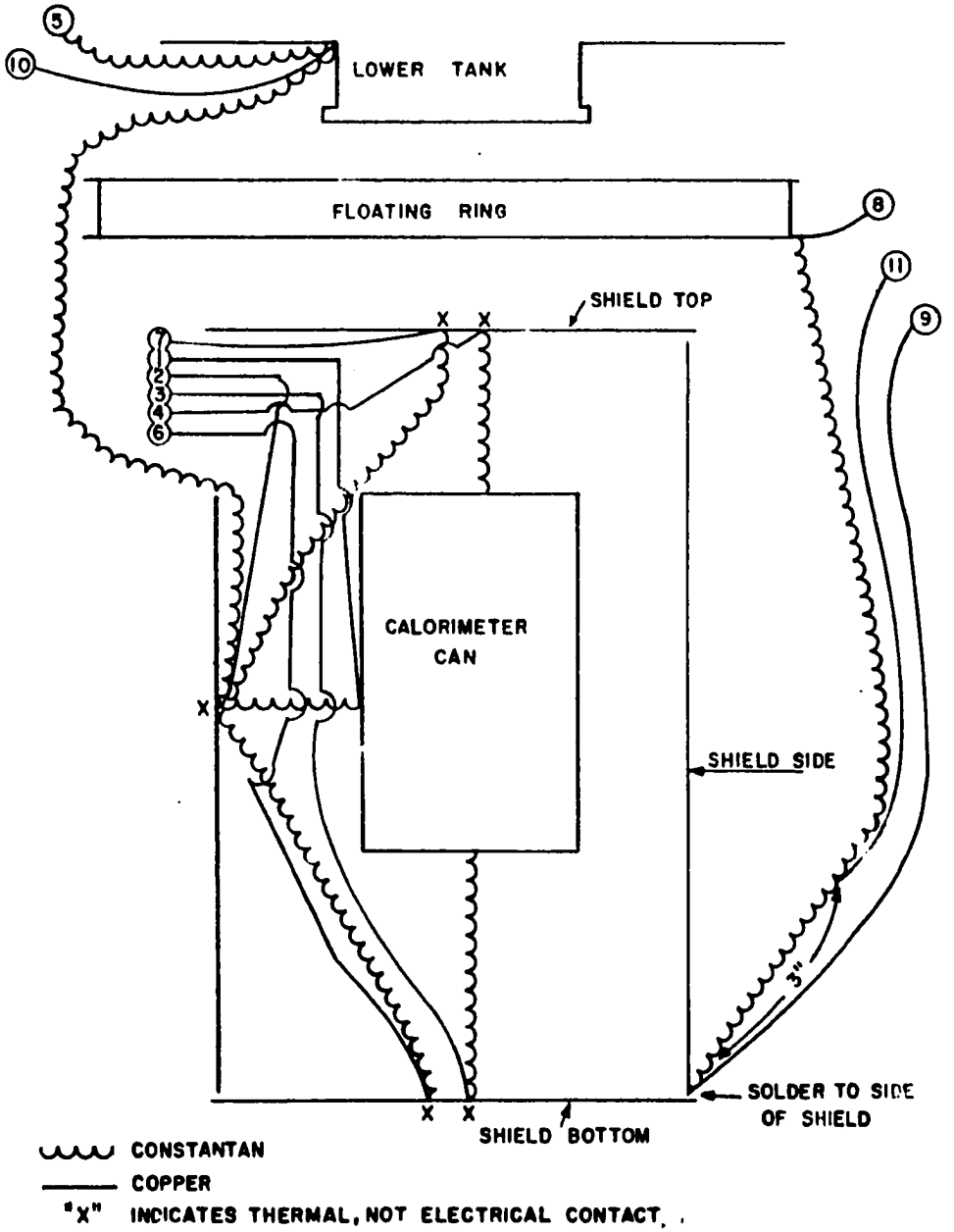
5
10
LOWER TANK
FLOATING RING
8
11
9
SHIELD TOP
1
2
3
4
6
X
X
CALORIMETER CAN
X
SHIELD SIDE
3"
X
X
SHIELD BOTTOM
SOLDER TO SIDE OF SHIELD
CONSTANTAN
COPPER
"X" INDICATES THERMAL, NOT ELECTRICAL CONTACT.

couple designated by wires 8 and 9, one junction was soldered to the side of the shield at its bottom edge, and one junction was tied in among the leads about one inch from the floating ring, between the shield and floating ring. It is felt that this positioning of the thermocouple, and method of attaching both junctions to their respective stations was responsible for reducing the cold temperature drifts of the sample from .001° per minute to less than 10^{-5}° per minute above 200°K.

The difference thermocouple wiring arrangement allowed one to check the difference in temperature between the side, bottom and top of the can, a measurement which could not be made with the wiring arrangement previously described.

It should be mentioned that another factor in keeping the drifts low was the method of wrapping heating wire on the components of the adiabatic shield. Since the edges of the side, bottom, and top of the shield could not be wrapped, the heater wire near the edges was overwound in an amount sufficient to take into account the area not covered with wire and insure more uniform heating of the shield components.

The sample can was constructed to fulfill the following 3 purposes: (1) to allow hydrated salt to be sealed in the can without decomposing or dehydrating it, (2) to provide uniform heating and rapid temperature distribution between the sample and the can during a heating period, and (3) to provide rapid temperature equilibrium throughout the sample

immediately proceeding the heating period. To accomplish (1), the cover of the sample can was constructed as shown in Figure 3. The larger cover was soldered to the can while empty. The salt was then inserted into the can through the hole in the outer cover, the can placed in an ice bath with particular attention being given to the cooling of the junction between the outer cover and side of the can. The inner cover was then soldered on. It was thus possible to solder the can shut and yet not decompose the sample. A silver capillary tube was provided on the cover to pump out air and introduce helium used for a thermal exchange medium. Ordinarily 2 cm pressure of He was introduced into the can at 300°K, and sealed in the can by pinching off and fusing the silver port.

A small container for solder was also provided on the cover. This container allowed one to add or remove solder from a non-vital joint after soldering operations were completed, thus keeping the weight of the solder on the can constant.

To accomplish (2) and (3), the sample heater, which was silk insulated No. 40 B. and S. constantan, was wound on a 0.010 inch thick cylindrical copper shell placed in the can and provided with six 0.010 inch copper radial fins. The shell was not in good thermal contact with the can, but was in good thermal contact with the powdered sample which was packed around it. The can was thus heated through the sample so that

Figure 3. Calorimeter can cover

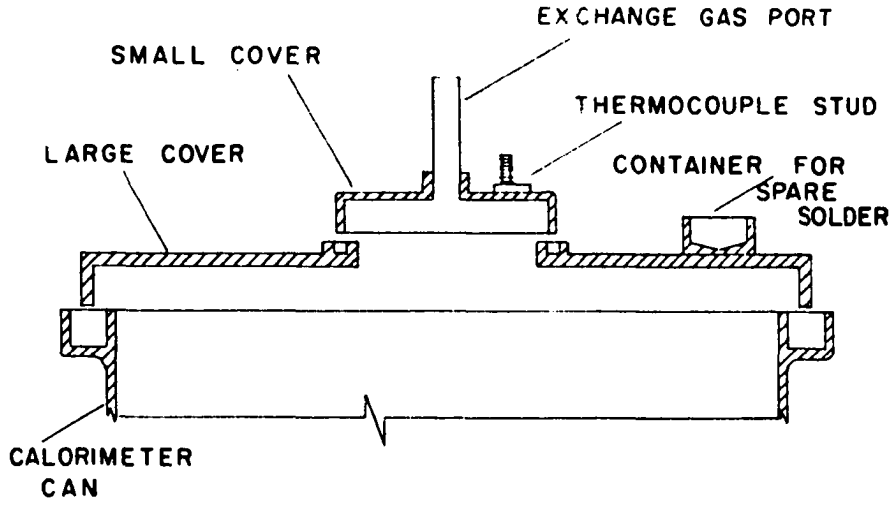
EXCHANGE GAS PORT
SMALL COVER
THERMOCOUPLE STUD
LARGE COVER
CONTAINER FOR SPARE SOLDER
CALORIMETER CAN

FIG 1

no part of the can became hotter than the sample. This arrangement made manual control of the adiabatic shield quite easy since all temperature differences were a slowly changing function of time. The heater leads were brought into the can through a Stupakoff seal in its bottom.

A check of values of heat capacities obtained in the calorimeter used for the salt measurements was made by running the heat capacity of a 99.9 per cent pure sample of benzoic acid supplied by the National Bureau of Standards. It was found that the curve obtained from the benzoic acid measurements in the calorimeter used for the ethylsulfates agreed with the N.B.S. data to within 0.1 per cent from 15 to 300°K, except for the region from 60-90°K where the N.B.S. data are known to deviate from a smooth curve by as much as 0.2 per cent.

Magnetic susceptibility measurements

The magnetic susceptibility apparatus consisted of 2 main groups of equipment; a mutual inductance bridge and related equipment, and a cryostat and related equipment. The bridge group will be discussed first.

The Hartshorn (199) type mutual inductance bridge used in this work was designed and constructed by L. D. Jennings* and has been described by V. H. Hesterman (200), so no detailed account will be given of it here. A discussion will be given,

*Present address, Watertown Arsenal, Watertown, Mass.

however, under "Experimental Procedure" of the circuit equations involved in the balancing of the bridge. L. D. Jennings has recently discussed the principles of design of inductance bridges in general (201), and the reader is referred to his work for a thorough understanding of the important considerations involved. It suffices to say that the smallest unit of inductance on the bridge was approximately 2×10^{-5} henrys. The circuit for measuring susceptibilities is shown in Figure 4. The "primary" half of the circuit consisted of a Hewlett Packard Model 202C oscillator in series with a power amplifier constructed in this laboratory. The power amplifier was in series with the bridge primary, an external variable primary, and the sample primary. The "secondary" half of the circuit consisted of the bridge secondary in series with the external variable secondary, the sample secondary, and a 1:200 gain transformer. The transformer, Model No. KI 1117, was supplied by South Western Industrial Electronics Co. of Houston, Texas. The output of the transformer was fed into a 33 cycle high gain selective amplifier described by Jennings (201), and from thence into the Y terminals of an oscilloscope. The amplifier was designed and built in this laboratory. The X sweep of the oscilloscope was externally synchronized with the oscillator signal, thus allowing one to identify an inductive and resistive component in the amplifier signal. This

Figure 4. Mutual inductance circuit for measuring magnetic susceptibilities

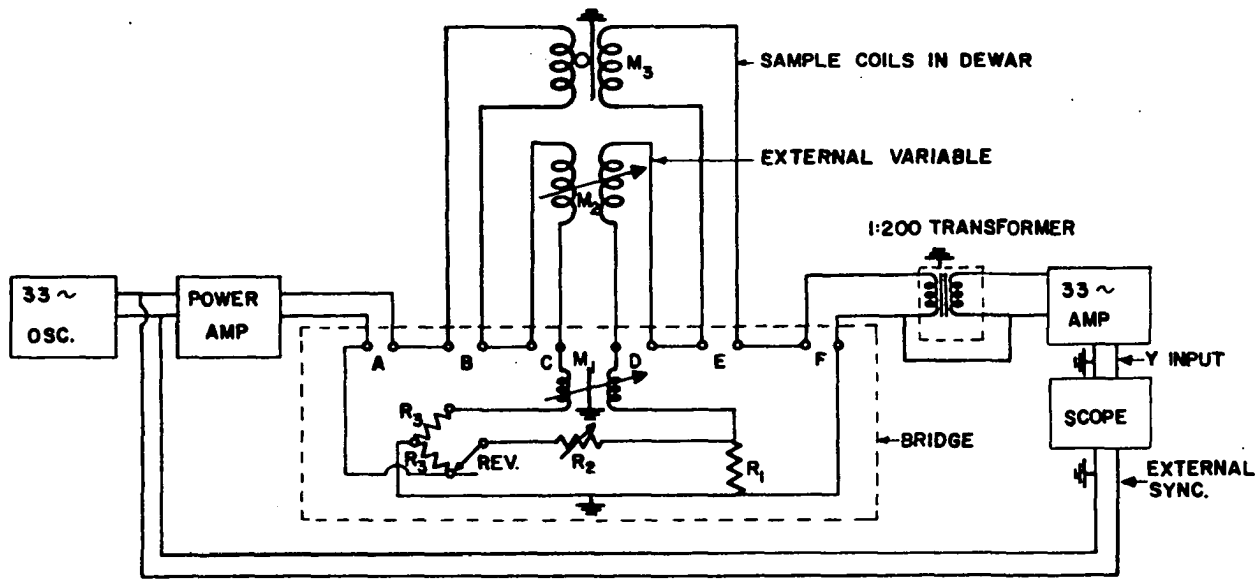

A,B,C,D,E, & F—ARE CO AX CONNECTORS ON THE HOUSING OF THE BRIDGE

R_1 = 0.1 Ω

R_3 = 1Ω

identification will be further discussed. A common side of the primary and secondary, and the case of the transformer were grounded. The bridge and the sample coils were wound as astatic pairs with grounded shields between primary and secondaries to minimize external inductive, and internal capacitive pickup. The external variable described by Hesterman (200) was wound as an astatic pair, but no capacitive pickup shields were used. To minimize external inductive pickup, all leads were coax cable or twisted pairs, where it was not feasible to use coax. The entire circuit was essentially used as a null point instrument, in that the bridge was used to oppose the signal from the sample coils due to the presence of the sample. The external variable was used to place the signal from the sample coils within the limits of the variable inductance available from the bridge. In principle the sample coils were wound as an astatic pair such that the net mutual inductance was zero with the sample absent. In practice the windings were never perfect, and the net signal from the sample coils was compensated for with the external variable.

There were two different sample coils used in the susceptibility measurements. One was used for the measurement of the perpendicular susceptibility, and the other for the measurement of the parallel susceptibility. Since the construction of the two was quite similar, only the coil used for

the perpendicular measurements will be described. An exploded view of the coil, along with the nomenclature and dimensions of the components is given in Figure 5. The number of turns used in the primary and secondary was a result of the formulae given under "Treatment of Data". The dimensions of the coil were arranged to yield a net mutual inductance of zero in the absence of a sample, and were calculated according to published tables of mutual inductance versus coil configuration (202). The 0.001 inch copper foil shown in Figure 5 was grounded and served as a shield to prevent capacitive coupling between the primary and secondary. Slits were made in it, similar to those in the core of a commercial transformer, to reduce eddy currents. The two outer windings of the secondary were wound counter to the center winding to give a net mutual inductance of zero.

The cryostat and related equipment consisted of the cryostat proper, and the following systems: (1) a system for mounting the sample and moving it in and out of the sample coils, (2) a vacuum system to thermally isolate the sample from the bath, (3) a manometer system used to measure temperatures below 4.2°K, (4) a thermocouple-potentiometer circuit to measure temperatures above 4.2°K, (5) a heater circuit to heat the sample, and (6) a pumping system to lower the temperature of the liquid He bath. System 1, above, and part of the cryostat proper are shown in Figure 6. The

Figure 5. Exploded view of sample coils used for perpendicular susceptibility measurements

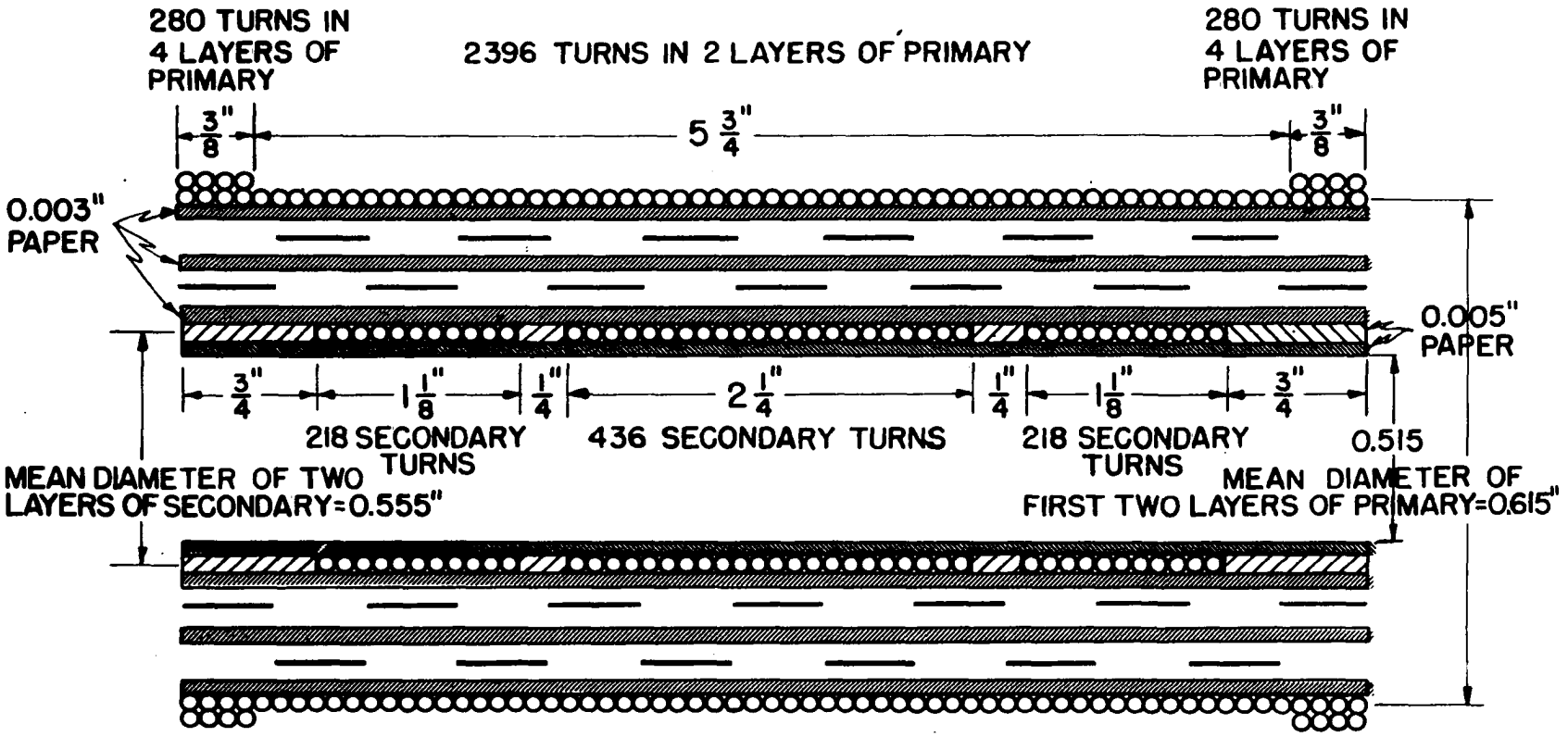

PRIMARY — #36 FORMVAR COVERED COPPER
SECONDARY— #30 FORMVAR COVERED COPPER
oooooooooooooo COIL WINDING
—— —— 0.001" COPPER FOIL

Figure 6. Sample support and dewar system for measuring magnetic susceptibilities

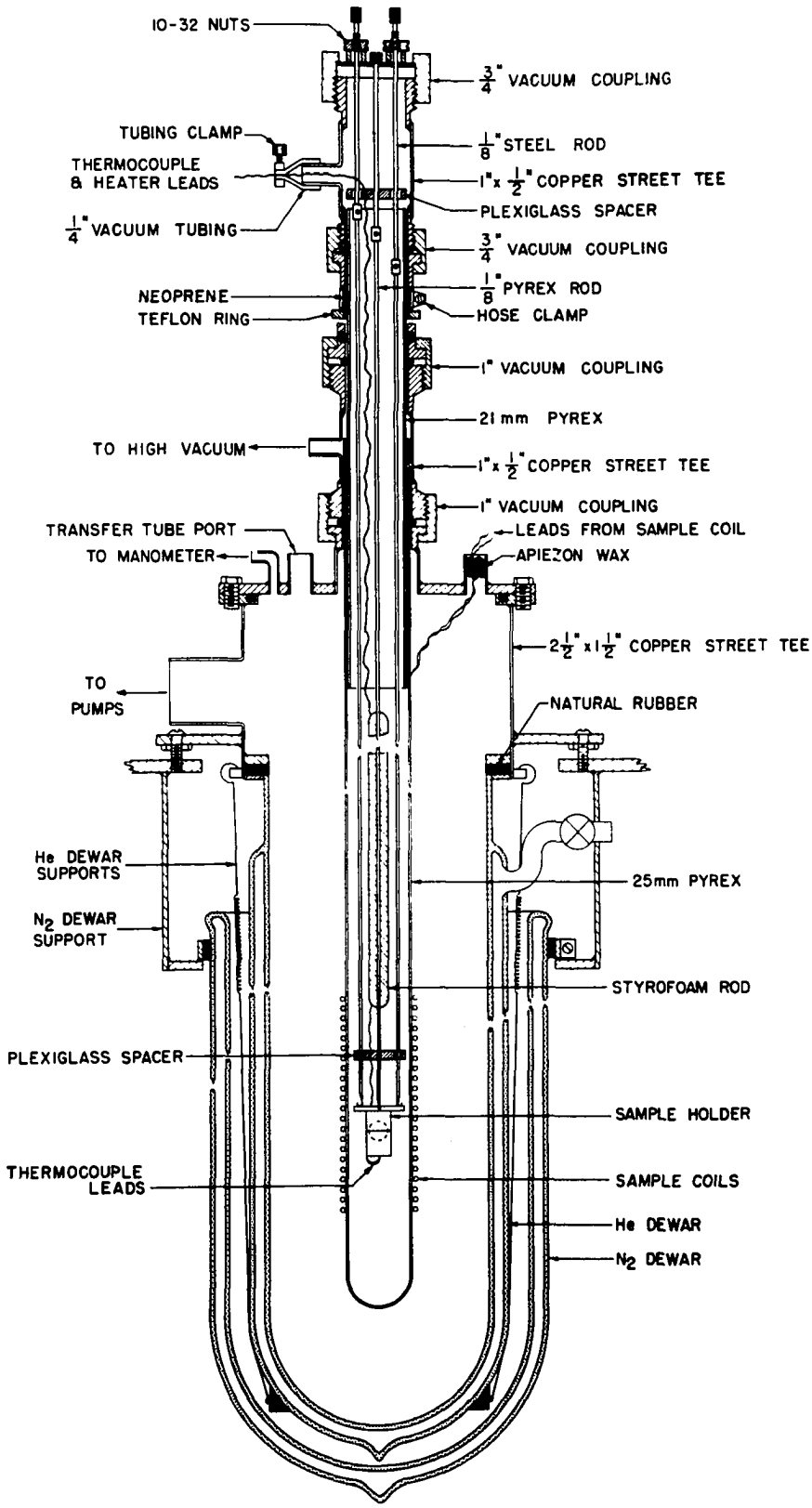
10-32 NUTS
3/4" VACUUM COUPLING
TUBING CLAMP
1/8" STEEL ROD
THERMOCOUPLE & HEATER LEADS
1" x 1/2" COPPER STREET TEE
PLEXIGLASS SPACER
1/4" VACUUM TUBING
3/4" VACUUM COUPLING
1/8" PYREX ROD
NEOPRENE
TEFLON RING
HOSE CLAMP
1" VACUUM COUPLING
21 mm PYREX
TO HIGH VACUUM
1" x 1/2" COPPER STREET TEE
1" VACUUM COUPLING
TRANSFER TUBE PORT
LEADS FROM SAMPLE COIL
TO MANOMETER
APIEZON WAX
2 1/2" x 1 1/2" COPPER STREET TEE
TO PUMPS
NATURAL RUBBER
He DEWAR SUPPORTS
25mm PYREX
N2 DEWAR SUPPORT
STYROFOAM ROD
PLEXIGLASS SPACER
SAMPLE HOLDER
THERMOCOUPLE LEADS
SAMPLE COILS
He DEWAR
N2 DEWAR

cryostat proper consisted of two concentric dewar supports, helium and nitrogen dewars, a sample coil mounting, and pumping lines for systems 2 and 6. The pumping lines were copper pipe which served as two of the three legs of the dewar supports. The entire unit was mounted on a 3/4 inch plywood base to which casters were attached, and was thus mobile. Both dewars were constructed of pyrex tubing and strip silvered in this laboratory by W. Jones of the glassblowing shop. The inner dewar was 33 inches long and had a 1-3/4 inch i.d. and a 2-1/2 inch o.d. The outer dewar was 34 inches long and had a 4 inch i.d. and a 4-3/4 inch o.d. The vacuum chamber of the inner dewar, instead of being pumped out and sealed off, was provided with an 8mm port shown at the top of the dewar in Figure 6. Before each series of measurements, the vacuum chamber was pumped down, through this port, to about 25 microns pressure. When liquid He was introduced into the dewar, the resulting temperature drop would lower the pressure in the vacuum chamber to well below the thermal conducting region. This procedure was used because He diffuses through pyrex, and a permanently sealed system would have had to have been broken, re-evacuated, and re-sealed about every third run. In a typical series of measurements, 5 liters of liquid He were required to fill the He dewar and cool the sample from 78 to 4.2°K. The sample coil mounting was a 25 mm o.d. pyrex tube which made a vacuum seal to the He dewar

support unit through a one inch Cenco vacuum coupling, as shown in Figure 6. The He dewar, in turn, made a vacuum seal to its support by being spring loaded against a natural rubber gasket.

System 1 consisted of a sample holder about which was wrapped the sample heater and thermocouple, and a sample support consisting of three 3 mm glass rods connected to three 1/8 inch steel rods. The lower end of the glass rods were hooked, and the top of the cylindrical sample container was attached to them, at 120° intervals, with cotton thread. The upper half of the unit was housed in a 21 mm o.d. pyrex tube, and suitable O ring vacuum couplings permitted it to be translated with respect to the sample coils. The inside of the sample coil supporting tube will hereafter be referred to as "the sample system". The glass rods were connected to the steel rods by means of small brass cylinders into which both fit snugly. A set screw served to keep the steel rods in the cylinders, and the glass rods were glued in place with Duco cement. The steel rods were brought from the sample system to the outside through a piece of 1/4 inch natural rubber which served as a vacuum seal. The steel rods could be translated with respect to each other, thus allowing rotational orientation of the sample in the coils. The upper ends of two of the steel rods were threaded and fitted with 10-32 nuts to provide fine adjustment of their translational

motion.

The sample holder was a right circular plexiglass cylinder 1 inch long x 0.390 inch in diameter. It was divided into 2 halves, each having a 5/16 inch diameter hemisphere milled in it to accommodate half the sample. The 2 halves were glued together with plexiglass cement. A small plexiglass ring, in which there were 3 holes 120° apart, was fitted to the top of the sample holder. It was through these holes that the supporting glass rods were threaded to the sample container.

The thermocouple, an alloy of Au 2 per cent Co coupled to Au 0.37 per cent Ag, was number 36 enamel covered wire, and wrapped around both halves of the sample container. It was led into the sample cavity through a small hole in the bottom of the sample. The thermocouple wire was supplied by Sigmund Cohn and Corp. of Mt. Vernon, New York. The temperature-e.m.f. curve from 4-250°K of a sample of this thermocouple wire was measured by J. Schirber of this laboratory. The shape of this curve was assumed to be the same for all such wire taken from the same spools, and thus Schirber's data allowed one to obtain a temperature-e.m.f. relationship if one calibration point were available. At first thought, one might think that the Co in the thermocouple would contribute significantly to the magnetic moment of the sample container, but a calculation showed that the amount present was negligible compared to the sample. It was found, however, that some sections of the

wire contributed an unreasonable amount to the inductive signal due to the sample plus container. This contribution must have been caused by a ferromagnetic precipitate of cobalt in the allow. No such wire was used in any of the measurements tabulated in this work.

The sample heater was an alloy of non-insulated number 40 Cu-Be wire, and had a resistance of 7 ohms/foot. This composition was used because it was found to be nonparamagnetic at liquid helium temperatures. The heater was noninductively wrapped over the thermocouple, with a layer of cigarette paper between the two for electrical insulation. Since the heater was not insulated, it was not doubled and wrapped around the sample container as is ordinarily done in noninductive winding. Instead, a layer of number 32 formvar covered copper was wrapped around the container, the Cu-Be was wrapped, turn for turn, beside it, and the pair constituted a noninductive winding. Silver solder was used for all electrical connections which were in the sample coils, because lead-tin solder exhibits a superconducting transition, with associated permeability change, at He temperatures. The heater leads were number 36 formvar covered copper, and were soldered to the number 32 Cu and number 40 Cu-Be near the top of the sample holder. The heater and thermocouple leads were led from the sample system through a tee which made a vacuum coupling with the 21 mm pyrex tube. Between the sample

container and the tee, the leads were wrapped around a 12 inch long x 3/8 inch in diameter styrofoam rod, in order to increase the thermal path between the sample holder and room temperature. A vacuum seal to the outside was made by separating the leads and clamping them in a piece of 1/4 inch vacuum tubing connected to the center arm of the tee. A bit of vacuum grease was smeared inside the clamped portion of the tubing to insure a good vacuum seal.

System 2, the pumping group for the sample chamber, consisted of a Consolidated Electrodynamics Corp. VMF 11 air cooled diffusion pump and a Duoseal forepump, Model 1400 B. The diffusion pump with its blower was mounted on the nitrogen dewar support, and was connected to the sample system with a flexible bellows. The top view of the cryostat and associated parts of system 2 are shown in Figure 7. A 1/2 inch valve, labeled A in Figure 7, was provided between the forepump and diffusion pump. On the diffusion pump side of A, a 1/8 inch toggle valve, B, was provided as a vent and an inlet for He exchange gas. On the forepump side of A, an 1/8 inch vacuum toggle valve, C, was provided to allow pumping on the vacuum chamber of the inner dewar.

The manometer system, 3, was a standard mercury manometer in parallel with an oil manometer. The two had a common low vacuum side to the bath in the inner dewar. Each was provided with a glass scale marked in mm units. The oil manometer was

Figure 7. Top view of cryostat and associated parts of magnetic susceptibility apparatus

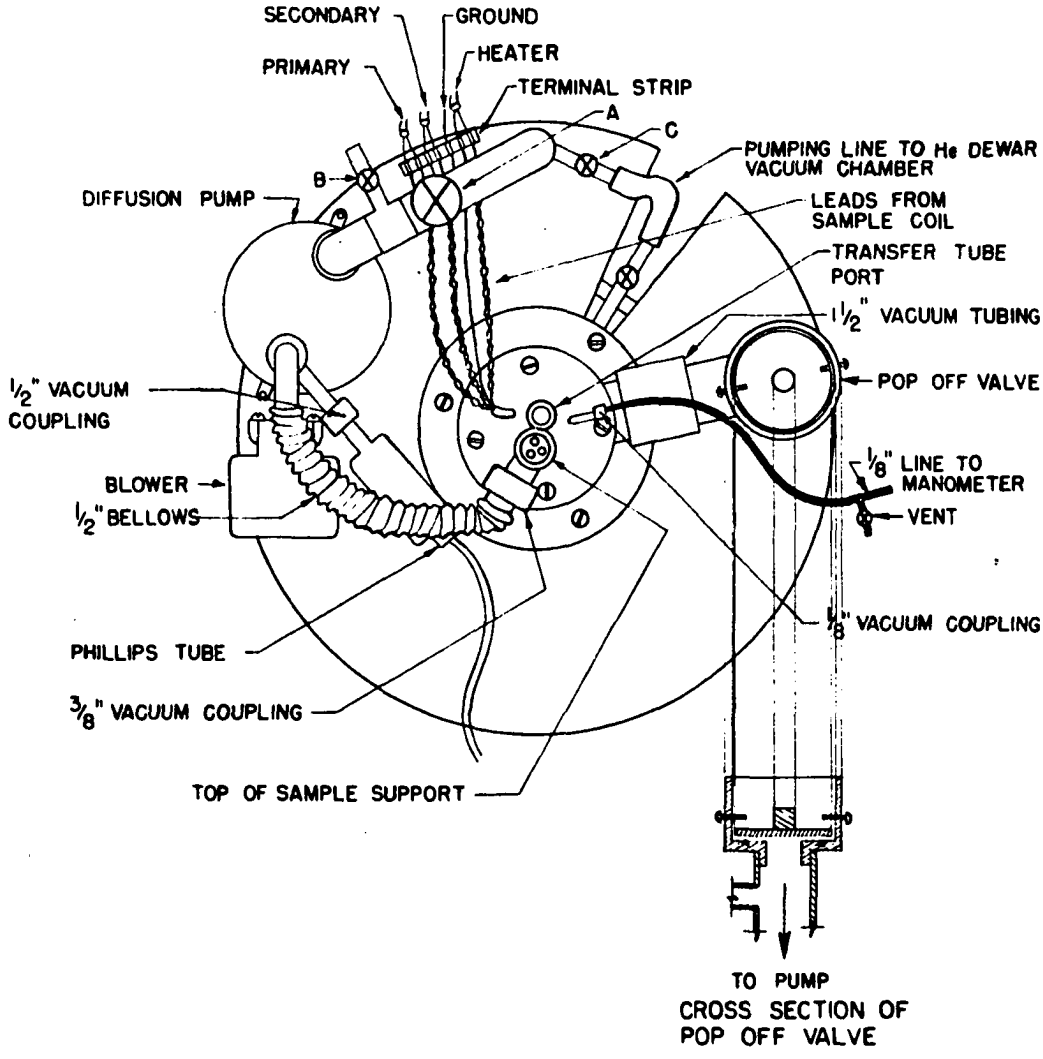
SECONDARY
GROUND
PRIMARY
HEATER
TERMINAL STRIP
A
C
B
PUMPING LINE TO He DEWAR VACUUM CHAMBER
DIFFUSION PUMP
LEADS FROM SAMPLE COIL
TRANSFER TUBE PORT
1½" VACUUM TUBING
½" VACUUM COUPLING
POP OFF VALVE
⅛" LINE TO MANOMETER
BLOWER
½" BELLOWS
VENT
⅛" VACUUM COUPLING
PHILLIPS TUBE
⅜" VACUUM COUPLING
TOP OF SAMPLE SUPPORT
TO PUMP
CROSS SECTION OF POP OFF VALVE

provided with a valve between its two arms, so it could be used as a differential manometer. Pressures over the He bath were read on the Hg manometer from 760 to 50 mm. The oil manometer was used below 50 mm Hg. The oil to Hg density ratio was found to be 1/13.00. A safety system was provided in the oil manometer to prevent pressures higher than 6 cm Hg from being introduced, thus preventing the random external lubrication of all equipment within a 6 foot radius of the manometer. Eighth inch copper tubing was used to connect the manometer with the manometer port on the cryostat, and provision was made to introduce He gas into this line in order to bring the pressure in the inner dewar up to that of the laboratory.

A Rubicon Type B potentiometer, catalog number 2780, was used to measure the e.m.f. of the thermocouple. The galvanometer was a Leeds and Northrup catalog number 2430A, and had a sensitivity of 4.7 microvolts per cm.

The sample heater circuit system, 5, consisted of 30 ohms of the Cu-Be wire described above, 2 variable resistors, and a 12 volt source of current. The heater was in series with a 200 ohm, 1/2 watt helipot variable resistor, and the center and an end tap of a 1200 ohm, 1/2 watt helipot variable resistor. The 2 end taps of the 1200 ohm variable were connected to two 6 volt Willard cells in series. By varying the position of the center tap of the 1200 ohm resistor, one could continuously vary the voltage across the heater from

zero to 12 volts. The 200 ohm variable provided a fine control of the heater current. An on-off switch was provided to open and close the battery circuit.

The pump used to reduce the pressure over the bath in the inner dewar was a Kinney DVM 12814, and was connected to the cryostat with 40 feet of 2 inch copper pipe. At the site of the cryostat, a 2 inch vacuum valve in parallel with a 1/8 inch needle valve was provided in the 2 inch line from the pump. The needle valve permitted relatively fine adjustment of the pumping speed down to a pressure of about 70 mm Hg, and the 2 inch valve was used for lower pressures. This arrangement permitted control of the bath temperature, in the case of liquid He, to $\pm$ 0.005° and was satisfactory for the measurements in this work. For work where the susceptibility might be a rapidly varying function of temperature below 4°K, however, some type of manostat which would permit finer control would have to be used. C. A. Swenson of the Ames Laboratory has recently assembled an instrument which permits control of He bath temperatures to $\pm$ 0.0005° in the range of 1.2-4°K, and the reader is referred to him for further details. With the pump and pumping line described above, a temperature of 1.3°K could be attained.

A pop-off valve, shown in Figure 7, was provided as a safety pressure release between the inner dewar and the valves in the pumping line. After finishing pumping on the bath, one

could close the valves to the pump and allow the system to come to atmospheric pressure without fear of the system warming and blowing apart, since any excess pressure would be relieved through the pop-off.

EXPERIMENTAL PROCEDURE AND TREATMENT OF DATA

Experimental Procedure

Heat capacity measurements

The procedure for making heat capacity measurements in this laboratory has been described by Skochdopole (203), and with the exception of a few differences will not be reiterated in detail. In principle one has a sample in a suitable container, called the calorimeter can, surrounded by a shield which he endeavors to keep at the same temperature as the can, thus "adiabatically" isolating the sample. The shield is referred to as the adiabatic shield. A measured amount of electrical energy is introduced into the sample, and the resulting temperature rise of the system is measured. A calibrated platinum resistor is ordinarily used as a thermometer in the temperature range 12-350°K. The raw data for the heater and thermometer readings are voltage measurements across the resistor in question, and across a known resistance in series with it. The desired currents and resistances are then obtained using Ohm's law. The voltage measurements in this laboratory are made with a White double potentiometer to an absolute accuracy of one microvolt. Temperatures are measured to an accuracy of 0.01°K, and temperature differences may be measured to 0.001°.

The differences between the method of collecting data in

Skochdopole's work and the present research were the following: (1) during the rating periods, i.e., the periods during which temperature drifts were being determined, the voltage across the standard resistor in series with the thermometer was adjusted to read 9999 on the White potentiometer dials. This voltage was obtained by adjusting the resistance in a 10 K decade resistor box in series with the thermometer. The purpose of this procedure was to facilitate calculation of temperatures; (2) in each of the series of heat capacity measurements made on the sample, in a region where no anomalies are known to be present, a few points were taken to check $\Delta Q/\Delta T$ of the sample plus can as a function of ΔT, and of heater current. The method of making these checks was to reduce the time of a heating period by a factor of 4, having previously taken at least 4 points with the length of the heating periods long enough so that 1/4 the time of one of them would not be less than 300 seconds. This would reduce the ΔT by a factor of 4. After 2 points had been taken at 1/4 the time of the previous heating period, 2 points were taken with the heating current reduced by a factor of 2 and the time of the heating period increased by a factor of 4. Thus the ΔT was kept the same as in the previous 2 points. The reason for making these checks was to determine whether or not the calorimeter was functioning correctly. For instance, it might be possible that when the sample heater current exceeds a

certain value, parts of the sample container become superheated enough to conduct some of the energy supposedly being supplied to the sample back through the heater leads into the adiabatic shield. In this case one would expect $\Delta Q/\Delta T$ of the sample plus sample container to increase with increasing current. In one case, when running the heat capacity of $Lu(EtSO_4)_3 \cdot 9H_2O$, it was actually found that $\Delta Q/\Delta T$ was a function of ΔT. When the circuits were checked, it was found that the thermometer leads might have had a high resistance "short" among them. Separating and re-insulating the leads removed the effect.

Magnetic susceptibility measurements

Prior to measuring the susceptibility of single crystals of TmE.S., the crystals were machined into 5/16 inch diameter spheres, and oriented in the sample container such that the c axis would be parallel, or perpendicular to the rotational axis of the sample coils.

The machining was done with a precision metal lathe. Essentially, a plexiglass mandril was placed in the chuck of the lathe, and a crystal glued to the end of it with plexiglass cement. Half the crystal was machined by taking longitudinal and transverse cuts about 0.002 inch deep such that the envelope of the cuts on the surface of the crystal was a hemisphere. The crystal and mandril were then removed from the lathe, and a new mandril having a 5/16 inch diameter hemisphere milled in its end was placed in the lathe. The crystal was removed from

first mandril, and the hemispherical section glued into the matching cavity in the second mandril. The second half of the crystal was then machined into a hemisphere. The spherical crystal was covered with a thin film of collodian for protection against surface decomposition. Five such crystals, labeled crystals numbers 1, 2, 3, 4 and 5 were prepared, and their weights were 0.5107 g, 0.4748 g, 0.5179 g, 0.4601 g, and 0 .5432 g, respectively.

An approximate determination of the orientation of the c axis of each of the hexagonal crystals was made with the use of a polarizing microscope. In most cases, the determination was good to 5° at best. A small line was scribed on the surface of the crystals to indicate the plane perpendicular to the c axis.

The crystals used for each series of measurements were placed, with the desired orientation, in the cylindrical plexiglass sample container, and the two halves of the sample container were glued together with plexiglass cement. The sample with its support system was then placed in the 25 mm pyrex sample coil support, and the sample system and the dewar were cooled to 78°K with the liquid nitrogen in the outer dewar. Liquid helium was then transferred into the inner dewar and the system was ready for susceptibility measurements. For the parallel susceptibility measurements, the rotational orientation of the crystal was adjusted with the sample support

rods such that a minimum inductance reading was obtained. It was assumed that the minimum corresponded to the field of the primary coils being parallel to the crystal c axis. Since a relatively small orientational adjustment was required when the crystal was first aligned using a polarizing microscope, there was no reason to believe that the extremum in the inductive signal did not correspond to the field being parallel or perpendicular to the crystalline c axis.

The process of making susceptibility measurements essentially consisted of measuring the mutual inductance of the sample coils with the sample in, and with the sample out of the coils. This procedure was carried out with the sample at a known temperature as determined by vapor pressure or thermocouple e.m.f. data. The measurements may be categorized into two parts; below, and above 4.2°K. Each will be discussed separately.

Below 4.2°K, the vapor pressure over the liquid He bath was used as a thermometer. Ordinarily a vapor pressure bulb immersed in the liquid He bath is used for accurate temperature determination, but the bath vapor pressure is sufficient when only 0.01° accuracy is desired. The parallel and perpendicular susceptibilities of TmE.S. are slowly enough varying functions of temperature below 4°K that 0.01° accuracy was sufficient. The sample was cooled to 4.2°K with liquid He in the inner dewar, and 25 microns pressure of He exchange gas in the sample

system. An "in" reading, with the sample in the coils, was taken of the bridge inductance and resistive components, and the vapor pressure over the bath. The sample was then raised out of the coils far enough so that a one inch translation up or down did not affect the signal from the bridge circuit. An "out" reading was then taken of inductance, and resistance. The pressure over the bath was the same for the "in" and "out" reading. The pressure was then reduced over the He bath by opening the valve connecting the bath to its pumping line, and "in" and "out" readings were taken at 0.2° intervals from 4.2 to 1.3°K. A steady state pressure was attained for each point. Because the temperature of the bath, and thus the configuration of the sample coils, was changing, the "out" readings below 4.2°K were a function of temperature. Usually one "out" reading was taken for every four "in" readings, and the intermediate "out" readings were obtained by interpolation. This procedure was used because taking an "out" reading would warm the upper components of the sample system. A few tenths of a liter of He was then evaporated every time the sample was replaced back into the coils for the next "in" reading. Since only three liters of He were available in the dewars, a finite number of "out" readings could be taken before the level of the He dropped below the top of the sample coils.

When the lowest attainable temperature was reached, the He exchange gas was pumped from the sample system. At this

point, the temperature of the sample would start to rise. The temperature gradients along the thermocouple wire would then change rapidly, giving rise to varying thermal e.m.f.'s, until the pressure in the sample system was below 0.2 microns. The thermocouple was thus useless as a thermometer for a short time while the sample was warming. By the time the pressure was low enough to permit the use of the thermocouple as a thermometer, the sample had usually warmed to greater than 4°K. He vapor pressure was thus the only thermometer below 4°K.

In order to obtain a calibration point for the thermocouple, the inductance versus temperature curve was plotted from 1.3 to 4.2°K, and the first few inductance points taken using the thermocouple as a thermometer were placed on a smooth extrapolation of this curve. Thus e.m.f. versus temperature points were obtained for the thermocouple. The process of using these calibration points to obtain a temperature-e.m.f. curve for the thermocouple will be discussed under "Treatment of Data, Magnetic susceptibility measurements".

As the sample warmed, thermocouple and bridge readings were taken, usually by two operators, at one degree intervals to 20°K; two degree intervals to 40°K; five degree intervals to 100°K; and ten degree intervals to 210°K. The sample began to lose water under vacuum above 210°K, so readings were concluded at this temperature. The sample would warm at a reasonable rate, ca. 0.5° per minute, to about 20°K. Above this tempera-

ture, the sample heater had to be used to warm the sample. It was found that too rapid a heating rate would cause the temperature of the sample to lag behind that of the thermocouple, and would yield data with a large amount of scatter. The heating rate was thus adjusted so that when the heater was shut off, the time for the thermocouple reading and the bridge reading to reach constant values was less than 10 seconds. This procedure resulted in a minimum of scatter. No improvement in the scatter of the data could be made if, instead of a constant slow heating rate, points were taken with the heater adjusted to give zero heating rate. Both methods were used, however, in different runs, in order to check the consistency of the data thus obtained.

The "out" readings were relatively constant for all points taken after the bath had been pumped to the lowest attainable temperature, because the coil configuration was not changing. Enough "out" readings were therefore initially taken to establish that they were indeed constant, and then an "out" reading was taken every 10 points, or so.

A special set of measurements of the parallel susceptibility, discussed under "RESULTS, Magnetic Susceptibility Measurements", were taken using liquid H_2, N_2, CH_4, and C_3H_8 as coolant baths and vapor pressure thermometers. These measurements were taken because of an irreproducibility in the measurements below 20°K using the sample container wired with

a heater and thermocouple. The scatter was attributed to a closed circuit around the sample holder due to a short in the thermocouple or heater leads. An unwired sample container was constructed, and measurements were taken from 1.3-4, 13-20, 63-78, 90-100, and 165-205°K using the above mentioned liquid gases as heat sinks and thermometers. In these measurements, an in and out reading was taken for every point.

A short discussion of the equation of the circuit in Figure 6 will now be given to show that the unbalanced signal to the scope consists of an inductive and a resistive component and these are 90° out of phase with respect to each other. The problem of balancing the circuit when the sample is absent, thus obtaining "bridge readings", will then be discussed. The circuit equations with the sample present will be discussed under "Treatment of Data". The procedure for balancing of the circuit is the same in the absence or presence of a sample.

Referring to Figure 6, M_1 and M_2 will be considered as one variable inductor, M_1' with associated resistance proportional to ρ_1. M_3 has an associated resistance proportional to ρ_2. The a.c. statement that the secondary voltage be zero is:

$$\left\{jwM_1' + \rho_1 + jwM_2 + \rho_2 - R_3 \left[\frac{d}{R_2 + d + R_3}\right]\right\} ip = 0 \quad (1)$$

where $d = \frac{R_1 R_2}{R_1 + R_4}$, R_4 is the resistance associated with ρ_1 and ρ_2, ip is the primary current, j is the square root of -1, and

w is the frequency. Collecting imaginary and real components, we see that

$$M_1' = -M_2 \quad \text{(imaginary)} \tag{2}$$

and

$$\mathcal{E}_1 + \mathcal{E}_2 = \frac{R_3 d}{R_2 + d + R_3} \simeq \frac{R_3 d}{R_2} \quad \text{(real)} \tag{3}$$

if d and R_3 are small compared to R_2. For this bridge, R_1 = 0.1 ohm, R_3 = 1 ohm, and R_2 is variable from 0-1.8 meg ohms. R_2 was usually of the order of 200 ohms for the circuit used in this work, so the approximation made in (5) is valid to about 1 per cent. One therefore has two components to balance in order to make the signal from the secondary zero, and these are 90° out of phase with respect to each other. The inductive component is balanced with the variable inductance of the bridge, M_1', and the resistive component is balanced by varying R_2. Each unit of bridge inductance corresponds to approximately 2×10^{-7} henrys. Note that the magnitude of the resistive component is inversely proportional to R_2. Now it may be that the phase of the resistive component to be balanced is the same as that of the voltage pickup in the secondary obtained by varying R_2. The reversing switch, Rev., is thus provided to change the phase of the primary component tapped into the secondary.

As mentioned above, externally synchronizing the X sweep of the scope with the oscillator signal allows identification of inductive and resistive components. The reason for this is

that the external sync from the oscillator has the effect of making the phase angle constant between the X and Y sweeps, thus allowing a "locking" of the signal at a desired position on the scope screen. Once the signal is locked, an approximate null may be obtained by randomly varying inductive and resistive components. Usually the initial off balance signal will be large enough to saturate the amplifier, so the initial balancing is carried out with the amplifier gain turned low enough to obtain an unsaturated signal. Once a rough balance has been obtained, the gain of the amplifier may be increased and M_1' and R_2 randomly varied to obtain a fine balance. With the signal balanced to approximately zero, the position of the inductive out of balance signal is identified by unbalancing the signal with M_1'. The resistive out of balance signal will then be 90° out of phase with this signal.

At the start of a susceptibility run, a fine balance was obtained, using the above method, with the sample in and out of the sample coils. Once this was achieved, the amplifier gain could be turned up to its maximum value, approximately 10^6 referred to the input, and a fine balance obtained for each reading by adjusting the inductive, or resistive components. Which component to adjust was obvious from the position of the signal on the scope screen, since positions for inductive, and resistive off balance had previously been identified.

Treatment of Data

Heat capacity measurements

The treatment of the raw data in the heat capacity measurements was the same as described by Skochdopole (203), but the calculations were programmed to be carried out on the IBM 650 computer by D. R. Fitzwater and L. D. Jennings of this laboratory. Essentially the computer would calculate a heat input and an initial and final temperature from the thermometer and heater voltage data, and then calculate the ratio of the energy input to the temperature difference. Specifically, the computer would fit the temperature-time points of the rating periods to a straight line using the method of least squares. After all the drifts had been calculated, the machine would look at the mean deviation from the least squares temperature-time line for the points of each rating period. If the deviation exceeded a value which would lead to an error in the ΔT of greater than half the expected experimental error, the drifts of two rating periods on each side of the rating period in question were fitted to a least squares straight line of drift versus temperature and the drift in question re-evaluated to fit the line. The criterion for whether or not a point should be re-evaluated could be varied. Provision was also made to correct drifts for the initial and final points of a set of readings. All the drifts were corrected if the readings were such that the ΔT's were small.

Magnetic susceptibility measurements

The individual measuring a physical property with an eye towards correlating theoretical and experimental work must ask: (1) What have I measured? (2) What have I calculated? (3) What is the relationship between the two? These questions are so obvious that they are sometimes overlooked, and the reason for stating them here is the ease with which confusion can result from failure to ask them about the type of susceptibility measurement described in this work.

In principle, one places a paramagnetic sample in a mutual inductance coil and measures the change in mutual inductance due to the presence of the sample. This procedure is carried out with the sample at various temperatures, and the raw data obtained are mutual inductance "in" and "out" readings, and vapor pressure measurements over the coolant bath, or thermocouple e.m.f. readings. The problem of relating pressure or e.m.f. readings to temperature is relatively straightforward. The problem of relating a change in mutual inductance to a calculated susceptibility is one in which particular care must be exercised in answering question 3, above.

For a paramagnetic material,

$$\vec{M} = \chi \vec{H} \mu_0 \qquad (4)$$

where M is the magnetic moment per unit volume, μ_0 is 4π x 10^{-7} henrys/meter in M.K.S. units, χ, the magnetic

susceptibility, is a symmetric dyadic, and H is the magnetic field intensity vector. In an isotropic solid, or along one of the principal axes of a single crystal, M and H are parallel. The problem of relating a measured change in inductance, hereafter referred to as ΔI, to a calculated susceptibility, is the question of what is H. The problem arises because one is attempting to relate a property of an atom to a macroscopically measurable entity. For certain simple geometrical configurations, the H related to the macroscopic χ is exactly calculable, and equals $Ho/1 + N\chi/\mu_o$. This statement is equivalent to $H = Ho - NM$. Here, Ho is the external field, and N is the so-called demagnetization factor which physically arises from the surface magnetization of the material in question, and mathematically arises from the boundry conditions involved in a magnetostatic treatment of the problem. N turns out to be zero for an infinitely long needle aligned parallel to H, and one for a very thin disc whose axis of rotation is parallel to H. For a sphere, it is equal 1/3. Thus far, the magnetostatic treatment of the problem involves no ambiguity because a macroscopic χ has been considered in a macroscopic treatment. One ordinarily is interested, however, in calculating χ from atomic (microscopic) considerations and in relating a macroscopic to microscopic χ by using the discipline of statistical mechanics. In this case, H is the field on the atomic system

in question, rather than the effective field on the sample as a whole. One must therefore include, along with the external field and the demagnetization field, the so-called dipole field due to the magnetic dipoles surrounding the magnetic dipole whose moment we are interested in. The difference between the microscopic and macroscopic treatment of the problem is thus the taking into account of the dipole field. The dipole field has been the subject of much misunderstanding, and the reader is referred to Van Vleck (204) for a summary of past work, and the Van Vleck solution. The important point for this work is that the magnitude of the dipole field is approximately that of the magnetization of the sample, and the direction is opposite to that of the demagnetization field, so the two tend to cancel. The external field and the field at the atom in question, therefore, may be approximated as being equal. This approximation becomes poor as the magnitude of the susceptibility approaches unity. How poor it becomes will in general depend on how poorly the demagnetization field is canceled by the dipole field. For the remainder of this discussion, it will be assumed that the external field is equal to the field at the site of the individual magnetic dipoles. It will be seen that the error involved in the assumption is less than the total experimental error.

The following reasoning is involved in a rough calculation relating ΔI to χ :

1. The mutual inductance between a primary and a secondary is defined as the flux linkage per unit primary current.

2. The total flux goes as the total magnetic induction, B.

3. The total B due to a sample is approximately the total M of the sample, which in turn equals $\chi\mu_0 HV$, where V is the volume of the sample in the system of units one is using.

4. Since the H that the sample sees is ni where n is the turns per length of primary in the presence of the sample, the flux picked up by the secondary will go as $nm'\chi V\mu_0 i$. Here m' is turns per length of sample, i.e., the number of "effective" turns of the secondary that pick up the flux due to the sample. ΔI due to the sample will therefore go as $nm'\chi V\mu_0$, which dimensionally has units of inductance. If the volume of the sample is recognized as the length, l', times an average area, A, then one may say $\phi = nm'\chi Al'\mu_0 i$, where the proper identification between the flux and B times an area is made. Thus $\Delta I = \beta\chi V$, (6) where β is a geometrical factor.

Using standard alternating current theory, the statement that the magnetic moment of the sample need not be exactly in phase with the primary current is $\chi = \chi' - j\chi''$. χ' and χ'' are called the real and imaginary components, respectively, of the dynamic susceptibility. Referring to the circuit equations

discussed under experimental procedure, magnetic susceptibility measurements, we see that the following is obtained:

$$\{jw\Delta I_1 - jwV\beta(\chi' - j\chi'') + R_3\Delta R_2 d/R_2^2\}\, ip = 0 \qquad (5)$$

where ΔI is the change in M_1, and ΔR_2 is the change in R_2, respectively, needed to balance the signal from the bridge circuit due to the sample in the sample coils. Therefore

$$\chi' = \Delta I_1/\beta V \qquad (6)$$

$$\chi'' = R_3\Delta R_2 d/R_2^2\beta V w \qquad (7)$$

and

$$\chi''/\chi' = R_3\Delta R_2 d/R_2^2 w\Delta I. \qquad (8)$$

The easiest way to accurately determine β is to calibrate the sample coils with a material of known susceptibility.

A sample of ferric ammonium alum was used to calibrate the coil used for the perpendicular susceptibility measurement and the perpendicular susceptibility of TmE.S. was used to calibrate the coil used in the parallel susceptibility measurements. The alum sample had approximately the same volume as the TmE.S. crystals. Ferric ammonium alum is known to follow Curie's law to 1°K (203) and has a magnetic moment corresponding to a spin of 5/2. Thus, to convert ΔI to χ' for a given sample, ΔI is multiplied by the reciprocal of an experimentally determined constant times the sample volume. Ordinarily χ'' is small compared to χ' above 1°K, so in effect, $\chi = \Delta I_1/\beta V$. A measurement of 4°K showed that χ''/χ' was less than 0.001. This measurement was made by suspending the sample, in a plexiglass sample holder, by a thread and measuring ΔR_2. This

datum could not be obtained from a measurement of ΔR_2 of the sample in its wired sample holder because the thermocouple and heater wires contributed a.c. losses which added to the signal from the sample.

β^{-1} was found to be 1.369×10^{-3} for the coil used in the perpendicular susceptibility measurements, and 2.654×10^{-3} for the coil used in the parallel susceptibility measurements, where the volumes of the crystals were taken to be in the units of cm^3. A pycnometric measurement of the density of TmE.S. gave the value of 2.004 g $(cm^3)^{-1}$. This value agreed, to within 0.1 per cent, with the value obtained by extrapolating a smooth curve of density versus atomic number for the rare earth ethylsulfates from LaE.S. to ErE.S. For a given crystal of mass m, therefore, the conversion of ΔI to χ is made by multiplying ΔI by $2.004(\beta m)^{-1}$. For the perpendicular susceptibility measurements, the conversion was $\chi_\perp = 2.743 \times 10^{-3} \Delta I/m$. For the parallel susceptibility measurements, the conversion was $\chi_{\parallel} = 5.319 \times 10^{-3} \Delta I/m$.

Note that the reason the density of the sample is involved is that the desired result is a "text book" dimensionless χ; i.e., the standard text book treatment of magnetic susceptibilities yields a formula which, for a single atomic moment, has dimensions of volume. Upon multiplication of this formula by the number of atoms per unit volume, a dimensionless number is obtained. This procedure is aesthetically pleasing because

from our definition of χ as the magnetic moment divided by the field, both of which have the same dimension, we expect χ to be dimensionless. If, however, the atomic susceptibility is multiplied by Avagadro's number rather than the number of atoms per unit volume, a molar χ is obtained which has dimensions of volume. Since the measured entity is really a susceptibility per gram, the calculated and measured results are related by the molecular weight, which is known to a higher accuracy than the densities. In order to conform with text book practice and thereby reduce the amount of confusion to the uninitiated reader, however, dimensionless susceptibilities will be used in this work, and a knowledge of densities is necessary.

Vapor pressure measurements over the liquid He and over liquid H_2 and N_2 baths were converted to temperatures on the 1948 International Temperature Scale through the use of the tables published by C. T. Linder (205). In the check measurements on $\chi_{\parallel}$ of TmE.S., temperature versus vapor pressure data on the CH_4 and the C_3H_8 liquid baths were obtained, to within 2°K on the 1927 International Temperature Scale, from data published by R. I. Copson and Per K. Frolich (206).

The Au-Co, Au-Ag thermocouple was used for measurements above 4.2°K. A few calibration points of e.m.f. versus temperature were taken, as described under "Experimental Procedure, Magnetic susceptibility measurements", and the

e.m.f. versus temperature curve was assumed to have the same shape as Shirber's curve, mentioned in the description of the susceptibility apparatus. Once a temperature-e.m.f. relationship was established for one temperature, a difference in e.m.f. between this thermocouple and Shirber's, for a given temperature, was known. It was also known that the difference between the e.m.f.'s of the two thermocouples was zero at 273.15°K. Thus two fixed calibration points were established, and the difference in e.m.f. between the two thermocouples was assumed to vary linearly between zero at the ice point and the value obtained at the first calibration point above 1.3°K. Once this difference, as a function of temperature, was known, e.m.f.'s on the thermocouple used in this work could be converted to e.m.f.'s, and thus temperatures on Shirber's scale.

RESULTS

Heat Capacity Measurements

The results of the heat capacity measurements of LuE.S. and TmE.S. plus the calorimeter are tabulated in Tables 1 and 2, respectively. The experimental points deviated from a smoothed curve by greater than 0.1 per cent above 30°K in a few isolated cases. Note that there are three series of measurements, a, b, and c for each salt. These were taken for the following reason: In the initial runs on the Lu salt a bump was observed in the $\Delta Q/\Delta T$ versus T curve of the sample plus the can in the region 220-275°K. Since the can had been previously measured and no such anomaly found in it alone, and since no anomaly was expected in the Lu salt, it was assumed that the salt had an impurity present. After preparing and rerunning of a new sample of the $Lu(EtSO_4)_3 \cdot 9H_2O$, it was concluded that the impurity could be nothing but water occluded in, or adsorbed on the salt particles. Vapor pressure measurements of the equilibrium $Lu(EtSO_4)_3 \cdot 9H_2O(s) \rightleftharpoons Lu(EtSO_4)_3 \cdot xH_2O(s) + H_2O(g)$ at 25°C showed the pressure of H_2O over the salt to be 1.8 mm, quite concievably lower than the partial pressure of water in the laboratory atmosphere at room temperature, so one would expect the salt to adsorb water under laboratory conditions. At first it was thought that sealing the salt in the calorimeter can and removing H_2O from it until the pressure was lowered to the equilibrium value of

Table 1. Experimental values of $\Delta Q/\Delta T$, in joules $(deg)^{-1}$, for $Tm(C_2H_5SO_4)_3 \cdot 9H_2O$ plus the calorimeter can

ΔT	Mean T (°K)	$\Delta Q/\Delta T$	ΔT	Mean T (°K)	$\Delta Q/\Delta T$
	Series A		0°C = 273.15°K		
	Run 1			Run 2	
3.7829	15.416	3.726	4.4569	14.247	3.108
2.9882	19.864	6.360	2.7602	17.866	5.022
3.4209	24.081	9.118	2.8613	20.682	6.803
5.4738	28.538	12.504	5.2313	28.579	12.535
7.4645	35.006	17.850	7.4923	34.951	17.811
6.6437	42.061	23.855	9.2536	43.327	24.926
5.4587	48.114	28.996	7.2230	51.568	31.860
6.0730	53.882	33.753	6.1647	58.263	37.266
6.7928	60.316	38.909	5.4851	64.092	41.830
6.0247	66.726	43.776			
	Run 3			Run 4	
6.7713	49.461	30.110	5.9886	55.592	35.125
5.7773	55.737	35.252	8.5562	62.868	40.854
5.1363	61.194	39.598	7.4679	70.883	46.680
6.7715	67.150	44.073	6.7515	77.995	51.552
7.7826	74.429	49.148	7.4324	85.092	56.210
7.0545	81.849	54.135	8.2283	92.926	60.812
6.5319	88.645	58.413	6.4288	100.257	64.779
6.1510	94.988	61.966	6.1147	106.531	68.034
5.8798	101.006	65.137	5.8516	112.517	71.025
7.3202	107.611	68.613	7.8213	119.355	74.305
6.9501	114.749	72.150	10.5605	128.549	78.523
10.9329	123.693	76.352	9.9816	138.823	82.963
10.4119	134.368	81.095	11.3651	149.501	87.320
9.7197	144.437	85.293	10.8181	160.596	91.625
9.2968	153.946	89.087	8.6644	170.341	95.224
4.1718	160.684	91.692	8.3867	178.869	98.285
4.1012	164.824	93.252	8.1387	187.132	101.197
1.0175	166.778	93.899	9.4742	195.939	104.229
1.0143	167.795	94.185	10.7009	206.034	107.560
8.8307	172.718	96.067	10.3585	216.571	111.012
10.1956	182.232	99.482	10.0344	226.770	114.490
9.8383	192.256	102.982	1.0139	231.283	
9.5384	201.944	106.167	9.7324	235.639	117.827
9.2566	211.342	109.310	4.5855	242.786	124.956

Table 1. (Cont.)

ΔT	Mean T (°K)	ΔQ/ΔT	ΔT	Mean T (°K)	ΔQ/ΔT
Run 3 (Cont.)			Run 4 (Cont.)		
8.7232	230.663	115.810	4.5719	247.343	125.289
8.4164	239.229	119.954	4.3750	251.797	130.882
8.0168	247.434	125.855	3.6657	255.802	156.154
6.7384	254.792	149.646	3.8957	259.592	146.897
7.4618	261.895	135.076	4.4365	263.748	128.954
8.9759	270.105	130.918	4.3864	268.156	130.386
8.7692	278.960	133.922	8.6187	274.646	132.658
8.5426	287.601	137.387	8.4342	283.178	135.479
8.3535	296.062	140.423	8.2454	291.498	138.490
			8.0610	299.625	141.584
Series B					
Run 1			Run 2		
9.6771	212.373	108.465	5.7742	60.150	38.421
9.4082	221.911	111.462	5.2021	65.638	42.594
9.1793	231.193	114.142	6.0317	71.256	46.540
4.5040	238.207	116.236	5.5533	77.049	50.477
4.4054	242.656	118.793	6.7601	83.207	54.530
4.3654	247.033	119.838	7.1106	90.144	58.742
4.2905	251.352	121.888	7.9568	97.680	62.852
4.1301	255.549	126.580	7.4686	105.394	66.963
4.0816	259.654	128.045	9.3615	113.810	71.024
4.1871	263.766	124.781	8.8185	122.902	75.290
4.1437	267.916	126.054	8.3825	131.504	79.100
8.1594	274.050	127.958	7.6778	139.536	82.485
9.3153	282.773	130.673	7.3971	147.074	85.543
9.1097	291.972	133.530	2.4100	151.978	87.454
			2.3840	154.376	88.382
			7.0898	159.114	90.187
			6.8803	166.099	92.782
			8.3458	173.713	95.520
			9.6850	182.728	89.665
			9.3672	192.253	101.895
			9.0862	201.480	104.942
			8.8331	210.440	107.851
			9.4564	220.029	110.893
			9.2041	229.353	113.825
			8.9615	238.425	116.814

Table 1. (Cont.)

ΔT	Mean T (°K)	ΔQ/ΔT	ΔT	Mean T (°K)	ΔQ/ΔT
				Run 2 (Cont.)	
			8.6982	247.241	120.257
			8.2442	255.698	126.791
			8.3634	263.982	124.900
			8.1931	272.241	127.410
			8.0336	280.337	129.860
			7.8873	288.268	132.354
			7.7231	296.049	134.910
	Run 3			Run 4	
2.8823	17.990	5.215	2.4320	17.437	4.721
2.3881	20.860	6.771	5.0982	21.195	7.036
4.6713	24.410	9.284	4.4969	25.990	10.416
3.9560	28.722	12.511	4.7945	30.634	14.037
9.0074	35.199	17.836	9.2965	37.680	19.905
6.5675	43.000	24.406	6.9026	45.780	26.757
5.4330	49.000	29.458	5.7588	52.112	32.021
5.8126	54.624	34.040	5.0656	57.526	36.358
		Series C			
	Run 1			Run 2	
3.6425	24.937	9.614	4.1910	27.721	11.690
4.6295	29.081	12.755	5.2120	32.419	15.455
7.5384	35.164	17.748	6.5942	38.322	20.396
5.7212	41.796	23.329	6.8634	45.050	26.078
6.2612	47.787	28.373			
	Run 3			Run 4	
9.6172	204.092	104.098	6.8022	85.743	56.026
9.2009	213.500	108.719	8.5982	93.445	60.439
8.9639	222.598	111.476	7.9852	101.781	64.875
8.7478	231.443	114.130	9.5915	110.572	69.315
8.5302	240.073	116.940	9.0003	119.871	73.746
8.3276	248.492	119.695	8.5266	128.636	77.730
8.0516	256.671	123.713	10.4899	138.151	81.778
7.9976	264.685	124.556	9.4139	148.107	85.789
7.8419	272.591	126.828	8.3574	156.993	89.208

Table 1. (Cont.)

ΔT	Mean T (°K)	ΔQ/ΔT	ΔT	Mean T (°K)	ΔQ/ΔT
Run 3 (Cont.)			Run 4 (Cont.)		
8.9612	280.975	129.384	8.7244	165.533	92.367
8.7714	289.828	132.079	8.4346	174.110	95.447
8.5868	298.485	134.816			

Table 2. Experimental values of ΔQ/ΔT, in joules (mole-deg)$^{-1}$, for $Lu(C_2H_5SO_4)_3 \cdot 9H_2O$ plus the calorimeter can

ΔT	Mean T (°K)	ΔQ/ΔT	ΔT	Mean T (°K)	ΔQ/ΔT
Series A 0°C = 273.15°K					
Run 1					
5.6065	202.841	105.965			
9.3884	210.328	108.422			
9.1330	219.585	111.353			
9.9052	228.596	114.113			
8.6959	237.416	116.770			
8.4957	245.993	119.443			
9.2912	254.374	122.306			
8.0319	262.526	126.167			
7.9703	270.516	127.074			
9.1333	278.434	129.264			
Series B					
Run 1			Run 2		
3.6175	17.814	5.791	0.6064	20.920	7.735
2.7852	21.011	7.530	1.5026	21.975	8.371
2.7825	23.782	9.590	1.3456	23.403	9.349

Table 2. (Cont.)

ΔT	Mean T (°K)	ΔQ/ΔT	ΔT	Mean T (°K)	ΔQ/ΔT
	Run 1 (Cont.)			Run 2 (Cont.)	
3.2623	26.796	11.792	3.0412	25.597	10.880
3.6108	30.232	14.458	3.3086	28.770	13.309
5.0522	34.559	18.027	4.1010	32.486	16.314
5.0834	39.632	22.306	4.4877	36.781	19.902
5.7763	45.058	26.929	3.8096	40.931	23.417
6.7493	51.323	33.195	2.0787	43.876	25.926
5.8165	57.604	37.331	1.9496	45.891	27.644
5.2018	63.115	41.700	1.8413	47.787	29.267
4.7783	68.107	45.374	1.7514	49.585	30.763
5.6829	73.340	49.015	1.6730	51.298	32.199
6.0354	78.252	52.317	1.6052	52.937	33.554
6.7349	84.639	56.501	1.5474	54.515	34.798
6.2935	91.156	60.362	1.4918	56.036	36.089
6.6680	97.640	63.859	1.4450	57.505	37.249
6.3238	104.139	67.232	6.9538	61.706	40.584
6.0426	110.325	70.290	0.7825	62.969	41.570
5.8034	116.249	73.124	0.7704	63.747	42.231
5.5958	121.952	75.776	0.7602	64.514	42.803
7.5400	128.522	78.666	0.9789	65.385	43.439
7.2440	135.916	81.808	2.7505	67.251	44.778
6.9901	143.036	84.708	2.6358	69.947	46.673
6.7687	149.918	87.415	2.3662	77.067	51.553
6.5744	156.592	89.937	2.2942	79.399	53.156
6.3993	163.080	92.337	2.2307	81.664	54.630
6.2426	169.401	94.601	2.1736	83.868	56.043
6.0998	175.574	96.761	2.1205	86.017	57.424
5.9692	181.610	98.824	2.0765	88.117	58.676
7.4914	188.291	101.094	2.0351	90.174	59.871
9.7128	196.891	103.888	1.9970	92.192	60.997
9.4256	206.453	106.971	1.9625	94.174	62.054
9.1651	215.743	109.931	1.9290	96.121	63.111
8.6861	224.663	112.713	1.9015	98.039	64.097
8.7223	233.358	115.362	1.8808	99.931	64.815
8.5196	241.972	118.033			
8.3280	250.387	120.678			
8.0717	258.579	124.441			
7.9933	266.594	125.608			
7.8466	274.502	127.881		Run 1 (Cont.)	
7.7035	282.258	130.190			
7.5648	289.874	132.509	7.4420	297.354	134.600

Table 2. (Cont.)

ΔT	Mean T (°K)	ΔQ/ΔT	ΔT	Mean T (°K)	ΔQ/ΔT
	Run 3			Run 4	
2.1446	20.359	7.300	0.6147	19.698	6.931
2.2500	22.549	8.795	0.7160	20.360	7.327
1.9409	24.651	10.203	0.8751	21.151	7.812
1.7191	26.479	11.526	0.8166	21.996	8.375
2.0101	28.341	12.954	0.9403	22.870	8.979
2.1412	30.417	14.598	0.6393	23.520	9.423
2.6550	32.815	16.560	1.0489	24.364	9.997
2.3543	35.321	18.676	0.9772	25.379	10.733
			0.9196	26.328	11.411
			0.8692	27.221	12.077
			1.3001	28.304	12.924
		Series C			
	Run 1			Run 2	
0.3223	11.855	2.609	0.2775	11.861	2.576
0.4011	12.212	2.699	0.3100	12.157	2.786
0.6189	12.720	3.055	0.8871	12.758	3.029
0.5598	13.307	3.379	0.7779	13.581	3.456
0.8190	14.005	3.686	0.8638	14.405	3.936
0.7308	14.783	4.134	0.7874	15.228	4.321
0.9336	15.617	4.532	0.9252	16.070	4.797
1.1008	16.627	5.103	0.8427	16.950	5.269
0.9860	17.663	5.700	1.0204	17.883	5.806
0.8978	18.614	6.262	1.2376	19.035	6.501
0.9623	20.768	7.618	0.8407	20.073	7.182
0.8964	21.697	8.181	0.7931	20.892	7.616
			0.7423	21.659	8.140

1.8 mm would be sufficient to insure that the excess water had been removed from the sample. This was not the case, however, as the salt still had a bump in the heat capacity in the range 220-275°K when this method was used. Apparently the

equilibrium was not established in the time allowed. It was finally decided to use the heat capacity measurements themselves as analysis of the water in the sample. With an unknown amount of water in the sample, the heat capacity was run in the range 12-300°K, and the enthalpy under the bump in the range 220-275°K evaluated. These runs are called Series A. A given amount of water was then pumped off the sample, the heat capacity in the high temperature range re-run, and the difference in enthalpy under the bump obtained in the first and second runs evaluated. The second runs are called Series B. Assuming that the water removed was proportional to this difference, enough water was then removed from the sample to bring the enthalpy under the bump to zero. These measurements are labeled Series C. In practice, the enthalpy under the bump was never completely removed, but enough was removed to insure that further removal would not lower the heat capacity of the sample by more than 1/3 of the experimental error.

For example, in the "Lu salt A" runs, the enthalpy under the bump was 260 joules. Then 0.593 g of H_2O was removed from the sample and the enthalpy under the bump lowered by 217 joules. The lowering of the heat capacity at 100 and 200°K was 0.9 and 1.1 per cent, respectively. Then $43 \times 0.593/217 = 0.12$ g of H_2O should have been removed from the sample in order to reduce the bump to zero. Actually, about 0.10 g of H_2O was pumped from the sample, and the enthalpy under the bump

reduced to 13 joules. The heat capacity between runs B and C was lowered 0.1 per cent at 200°K, which is the experimental accuracy in the measurement of $\Delta Q/\Delta T$. Further removal of water to lower the bump to zero would not have lowered the heat capacity by more than 0.03 per cent. The reason for the indeterminateness in the amount of water pumped from the sample is that in the pumping process a small amount of salt was also removed, and only the weight of the salt plus the water removed could be measured.

Since in runs B on the Lu salt the heat capacity of the salt plus excess H_2O had been accurately determined in the range 15-300°K, the entire temperature range was not covered in runs C. Instead, some points were taken in the range of 15-30, 55-100, and 150-220°K. The heat capacity of the salt in C was then determined over the range 12-200°K by plotting the difference between a smooth curve through the points in B and the points in C as a function of temperature, interpolating the curve through the temperature range not covered in C and performing the required subtraction.

The water in the $Tm(EtSO_4)_3.9H_2O$ was removed in the same manner as in the Lu salt. A run, Series A, was made in the range 200-280°K and the enthalpy under the bump found to be 30.1 joules. It was assumed that the excess enthalpy per gram of water was the same for the Tm salt as for the Lu salt and enough water was removed from the salt to reduce the bump

sufficiently such that further removal of water would result in no appreciable change in the heat capacity below 200°K. When the salt was re-run (Series B) through this range, it was found that the bump containing 14 joules still remained. This was somewhat fortuitous, since the difference in the heat capacities of the two salts was the desired quantity, and the errors introduced by the excess water would tend to cancel, particularly as nearly the same number of moles of each salt were measured. Series B covered the range from 12-300°K. After Series B was completed, it was found that the resistance of the leads from the thermometer to the measuring circuit was not infinite, even when the measuring circuit was disconnected. The actual resistance was found to be on the order of 10^5 ohms, measured on a Simpson meter. The cause was traced to an electrical contact between all of the thermometer leads due to the presence of soldering salts. These salts had been used for soldering the leads from the thermometer to a bank of knife switches, but had not been completely cleaned off of the panel to which the knife switches were attached. Since this effect on the heat capacity measurements would be small in any case, but larger below 20°K, where small ΔT's were taken, than in the high temperature region, it was decided to re-run the Tm salt in the region 12-30°K after cleaning the knife switches. The results, labeled Series C, were a few tenths of a per cent higher and not as erratic as the measurements in Series B below

20°K, but agreed with B above 20°K to within experimental error. For this reason, the results of Series B were neglected below 20°K, but were used above 20°K since the effect was not appreciable.

The magnetic heat capacity of thulium ethylsulfate was then obtained from the raw data with the use of the following considerations: The raw data give $\Delta Q/\Delta T$ of 1/7.994 moles of LuE.S. plus the calorimeter can, and $\Delta Q/\Delta T$ of 1/7.981 moles of TmE.S. plus the calorimeter can. Care was taken to make $\Delta Q/\Delta T$ of the can the same for both salts, and to make the number of moles of each salt nearly the same for both sets of measurements. These precautions were taken to minimize the error involved in subtracting out the contribution of the can.

There were 0.0016 more moles of TmE.S. than LuE.S. in the $\Delta Q/\Delta T$ measurements. The magnetic contribution of the Tm will therefore be given by

$$C_m = 7.981 \left[(\Delta Q/\Delta T \text{ TmE.S. plus can}) - 1.0016\ (\Delta Q/\Delta T \text{ LuE.S. plus can}) + (0.0016\ \Delta Q/\Delta T \text{ can}) - \frac{\Delta C(T)}{7.981}\right] \quad (9)$$

where $\Delta C(T)$ is the difference in the lattice heat capacities of TmE.S. and LuE.S. The third term in the brackets is to take into account that 0.0016 too much of the $\Delta Q/\Delta T$ of the can was subtracted out in the second term. Note that the only place the contribution of the can alone comes into the calculation of C_m is the third term above. Since $\Delta Q/\Delta T$ of the can was

about 1/3 that of the can plus sample, a knowledge of the can values to within 10 per cent was sufficient to insure that the can term would contribute less than experimental error in the above formula.

The problem is now one of making a reasonable assumption concerning $\Delta C(T)$ such that the magnetic entropy lies near the value of R Ln(2J + 1) which, for Tm $^3H_6$, is 21.26 joules(mole)$^{-1}$. As one goes to higher atomic numbered rare earths, there are 2 opposing effects in the lattice contribution of the salts. The first is the lowering of the characteristic frequencies of the rare earth atom associated with an increase in mass across the series. The second is the shrinking of the unit cell, and more particularly, the contraction of the metal-water distances. Fitzwater and Rundle (8) have shown that the unit cell dimensions decrease a few hundreths of an angstrom from PrE.S. to ErE.S., but the metal-water distances decrease by 0.1 A. One might therefore expect that the increased mass of the metal atom would be compensated for by the higher stretching frequencies associated with the smaller metal-water distances, and that the higher vibrational frequencies of the waters in the smaller unit cells would be the predominating effect. Even if the compensation of the stretching frequency versus mass effect for the metal atoms were neglected, the total effect due to the metal atom would be on the order of 1/9 of that due to the waters because of

the ratio of metal atoms to water molecules. In summary, one would expect a lowering of the lattice heat capacities of the rare earth ethylsulfates as one goes to heavier rare earths.

During the time that this work was in progress, Horst Meyer and P. L. Smith (112) published the heat capacities of 7 rare earth ethylsulfates, including LaE.S., in the range 1.3-20°K. The lattice contributions decrease as the atomic number of the rare earth increases.

Meyer's data, together with my LuE.S. data at 20°K, give a reasonably smooth curve from which the lattice contribution of TmE.S. at 20°K may be obtained. The curve is shown as the solid line in Figure 8. The temperature 20°K was chosen at which to correlate Meyer's and my data, because my results become less accurate at lower temperatures due to the decreasing sensitivity of the platinum resistance thermometer. $\Delta C(20°K)$ may be obtained from this curve.

Since my measurements extend to 300°K, and the bump associated with the excess water only extends to about 270°K, there is a 30° interval above 270°K in which to evaluate the difference in the heat capacities of the TmE.S. and LuE.S. If the assumption is made that the magnetic contribution of the Tm salt is fully developed above 270°K, the differences in the lattice heat capacities of the 2 salts can be obtained to the extent that the difference in the $C_p - C_v$ correction is neglected. For 2 isomorphous salts such as these, one would

Figure 8. C_L^{20} versus T for the rare earth ethylsulfates

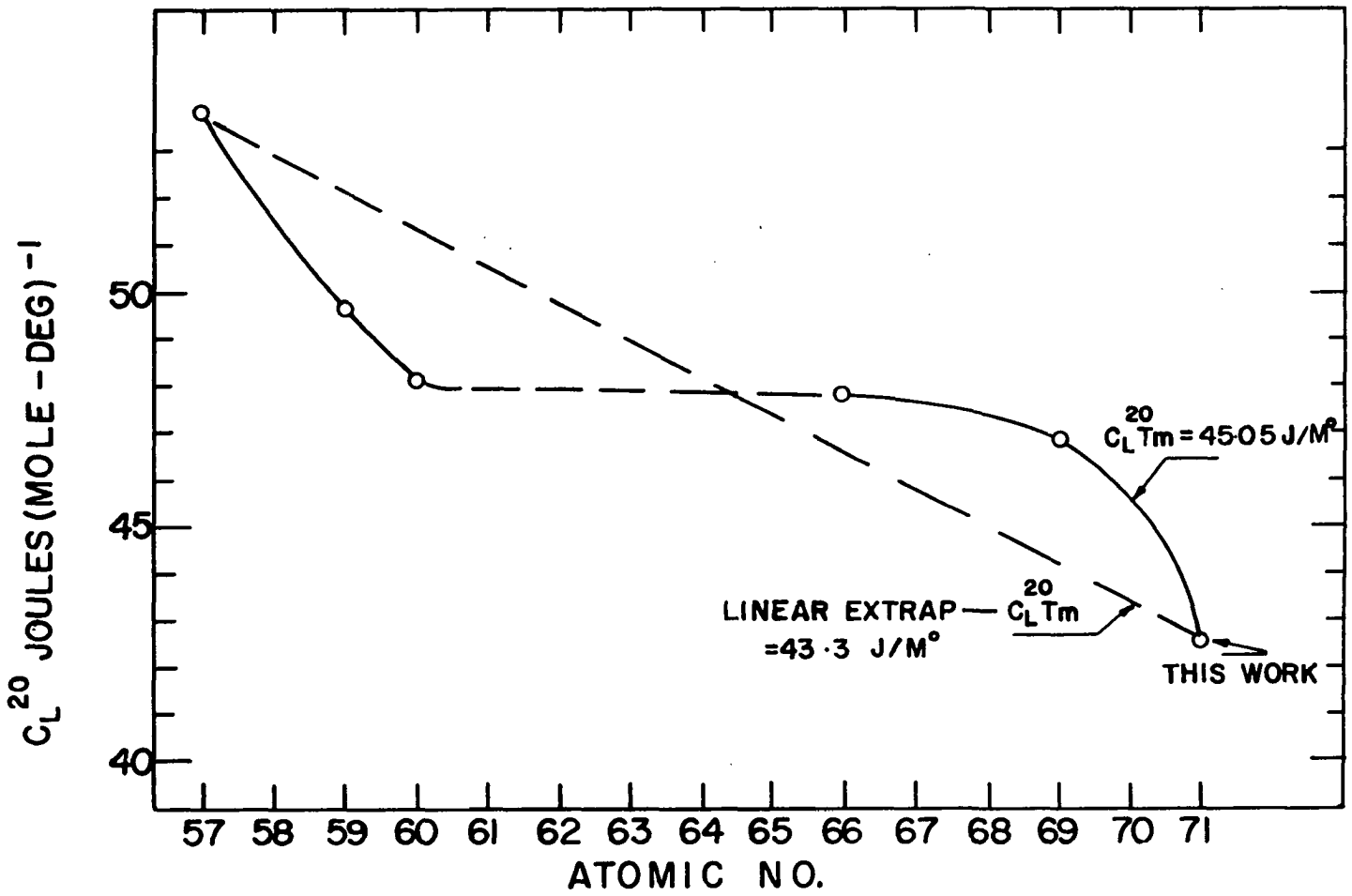
C_L^{20} JOULES (MOLE - DEG)$^{-1}$
50
45
40
57 58 59 60 61 62 63 64 65 66 67 68 69 70 71
ATOMIC NO.
$C_L^{20}Tm = 45.05$ J/M°
LINEAR EXTRAP — $C_L^{20}Tm$
=43.3 J/M°
THIS WORK

expect the $C_p - C_v$ difference to be negligible compared to the observed difference in the lattice heat capacities. $\Delta C(300°K)$ may be there obtained from my data.

In summary, the following information concerning $\Delta C(T)$, the difference in lattice heat capacities of TmE.S. and LuE.S., is available: (1) $\Delta C(20°K)$ from Horst Meyer's and my data. (Assumption involved: Magnetic contributions of Pr, Nd, Dy, and Yb ethylsulfates have been correctly evaluated.) (2) $\Delta C(300°K)$ from my data. (Assumption involved: The magnetic contribution of TmE.S. is fully developed at this temperature, and the difference in dilatation corrections is negligible.)

If one assumes these two $\Delta C(T)$'s to be correct, the problem of how $\Delta C(T)$ varies between 20 and 300°K then arises. The simplest assumption to make is that it is a linear function of temperature in this range.

Using the above reasoning to obtain $\Delta C(T)$ above 20°K, and taking the temperature dependence of the lattice heat capacity, C_L, of TmE.S. to be the same as that of LaE.S. below 20°K, a C_m was obtained for TmE.S. which had an associated entropy of 10.5 joules/mole. This value seemed quite low in comparison with the fully developed 21.26 joules/mole. Since greater than half of the "experimental" magnetic entropy was developed below 30°K, even with the above assumption concerning $\Delta C(T)$, it is certain that the measured entropy at 20°K contains a considerable fraction of the magnetic entropy at this

temperature. Since Meyer and Smith have no data for HoE.S. or ErE.S., and since their data for DyE.S. and YbE.S. are getting poor at 20°K, the above value of $\Delta C(20°K)$ may be too high, thus leading to a low value of C_m in a range where a large part of the magnetic entropy is developed. It was therefore considered advisable to re-examine the C_L^{20} curve to see if a lower value of $\Delta C(20°K)$ could be justified.

There are three indications that a lower C_L^{20} for TmE.S. and thus a lower $\Delta C(20°K)$ than one obtains using Meyer and Smith's data might be expected: The first is that using this assumption, the "experimental" magnetic heat capacity has a peak at 16°K which compares favorably, to within experimental error, with a Schottky curve calculated for a doubly degenerate level at 32 cm^{-1} above the ground state, and shown as the dotted line in Figure 5. The existence of this level in TmE.S. has been verified by workers in this laboratory and elsewhere. The second is that the region in which my data are compared with Meyer's is one in which his estimates of lattice contributions are becoming poor. For instance, one sees that his observed peak for PrE.S. agrees well with a Schottky curve on the low temperature tail of the peak, but is higher on the higher temperature side. If a contribution from another state at higher temperatures is occurring, this is the direction in which one would expect the experimental curve to vary from the calculated curve. If this is not the case, however, raising

the lattice contribution of the Pr salt would have the effect of lowering the magnetic peak to the calculated value and would tend to make the C_L^{20} versus atomic number curve more linear. Admittedly this effect would be less than 0.1 joule $(\text{mole-deg})^{-1}$ at 20°K, but would be a maximum of 0.4 joule $(\text{mole-deg})^{-1}$ at 12°K.

At the other end of the series, one sees that the observed curve for DyE.S. lies lower than the calculated curve in the region above the peak. It would be hard to understand this in terms of anything but the estimated lattice contribution being too high. In this case, the lattice contribution would have to be decreased by 0.8 joule $(\text{mole-deg})^{-1}$ at 20°K to bring the experimental and calculated curves into agreement. This is still within the claimed limits of accuracy of Meyer's data, and would also have the effect of "linearizing" the C_L^{20} versus atomic number curve.

A lowering of the lattice contribution of YbE.S. could be understood if the measurements of Meyer and Smith include a magnetic contribution that has not been taken into account. Meyer and Smith do say that no Schottky anomaly was detected for the Yb salt, so the next excited level lies at least 60°K above the ground doublet. Since a doublet 60°K above the ground doublet would contribute 7.84 joules $(\text{mole-deg})^{-1}$ to C_m at 20°K, I find their statement misleading. Their claimed accuracy at 20°K is $\pm$ 0.68 joules $(\text{mole-deg})^{-1}$. In order to

contribute less than this at 20°K, a level would have to lie at least 170°K above the ground state. The entire situation regarding the heat capacity data of YbE.S. is somewhat ambiguous. Cooke, et al. (111) carried out the measurements but published no data. They state that an attempt to fit the tail of a Schottky curve with their data showed none existed in the region in which they carried out measurements, i.e. 1-20°K, so the first excited doublet must lie at about 70°K. If they really meant that the peak due to the level would be at 70°K, then the level would lie approximately 150° above the ground state. A doublet 150° above the ground state would contribute approximately 0.8 joule $(\text{mole-deg})^{-1}$ to C_m which is slightly greater than the experimental error claimed by Meyer and Smith, who published the YbE.S. data in the form of a curve of C/T^2 versus T. It appears not impossible that a magnetic contribution exists in YbE.S. at 20°K, and if this is the case, one must necessarily lower the estimated lattice contribution to account for it.

The third positive indication that the lattice heat capacities of the heavier rare earth ethylsulfates are closer to a linear interpolation between the La and Lu salts is the low value of 43.0 joules $(\text{mole-deg})^{-1}$ for C_L^{20} of Y E.S. The unit cell and metal-water distances in Y E.S. are equal to those in ErE.S.[6] to within 0.01Å, and the atomic weight of Y is roughly half that of Er. The latter effects would tend to

lower C_L^{20} relative to ErE.S. One may obtain a rough idea of the lowering due to the mass effect by using the harmonic oscillator approximation for the frequency change, and assuming the average characteristic frequency of the Er ion to be nearly the same as in Er metal (207). Making this calculation, and assuming that the metal atom contributes 3/64 of the total heat capacity of the salt (to obtain a reasonable upper limit), one obtains 1.95 joules $(\text{mole-deg})^{-1}$ for the difference. The difference obtained using the smoothed curve in Figure 4 is 4.3 joules $(\text{mole-deg})^{-1}$. It thus appears reasonable that C_L^{20} of ErE.S. could be at least 2 joules $(\text{mole-deg})^{-1}$ below the value obtained from the interpolation of Meyer and Smith's data.

If a linear interpolation of the lattice heat capacities is made between LaE.S. and LuE.S. at 20°K, the lattice contribution of TmE.S. is lowered from the value obtained using Meyer's data by 2.75 joules $(\text{mole-deg})^{-1}$. It is interesting to note that this lowering gives a value of $\Delta C(T)$ which is lower than the value obtained from my data at 300°K by only 0.4 joules $(\text{mole-deg})^{-1}$. The value of $\Delta C(T)$ obtained using the linear extrapolation between LaE.S. and LuE.S. is $\Delta C(20°K)$ = 1.78 joules $(\text{mole-deg})^{-1}$.

If the value of 1.78 joules $(\text{mole-deg})^{-1}$ for $\Delta C(T)$ is assumed to be constant in the range 20-300°K, a magnetic heat capacity is obtained with an associated magnetic entropy of

18.0 joules (mole) at 300°K. The error in the magnetic entropy caused by neglecting the difference between the value of $\Delta C(20°K)$ and $\Delta C(300°K)$ is less than the error involved in integrating under the magnetic heat capacity curve from 12-300 °K, so the difference in the two $\Delta C(T)$'s was ignored.

The assumption that $\Delta C(T)$ is approximately constant in the range 20-300°K really makes more sense than assuming it to vary from a high value at 20°K to a low value at 300°K for the following reasons: (1) The lattice contribution of these salts at 300°K is only 1/3 of the fully developed value of 3R per atom. (2) If one considers two atomic Debye heat capacity curves with characteristic frequencies such that C at 300°K is approximately R, and ΔC at 300°K is 0.39 joule $(\text{mole-deg})^{-1}$, then these curves are nearly parallel in the range 20-300°K. The value of 0.39 joules $(\text{mole-deg})^{-1}$ is the contribution, per water molecule, to the difference in the lattice heat capacities at 20°K between TmE.S. and LuE.S. (Here the assumption is made that all of the difference in the lattice contribution between TmE.S. and LuE.S. is attributable to the waters of hydration.)

The implication that I wish to make of the above discussion is that C_L^{20} of TmE.S. is closer to the value of 43.3 joules $(\text{mole-deg})^{-1}$ than 45.05 joules $(\text{mole-deg})^{-1}$. Since it would be possible that another peak that would contribute $R\text{Ln}(1 + g)$, where g is the degeneracy of the state

giving rise to the peak, exists below 15°K or above 300°K, in Cp of TmE.S., I would find it hard to close the door to the possibility of Meyer and Smith's C_L^{20}'s being correct. Present spectroscopic evidence indicates, however, that the first level above the ground state is the 32 cm^{-1} state mentioned above. The purpose of this discussion is not to discredit Meyer and Smith's assumptions, but to point out that my data are not inconsistent with their results because of the uncertainty of the magnetic contributions for DyE.S. and YbE.S. at 20°K.

One further remark should be made concerning the heat capacity data reported in this work. Above 35°K, Cm of TmE.S. was seldom greater than one per cent of the total heat capacity and below 35 degrees the measurement error increased to the extent that in no case could the magnetic contribution be obtained to an accuracy of better than 20 per cent. This takes into account the fact that the individual measurements of LuE.S. and TmE.S. were each accurate to 0.1 per cent above 35°K.

The smoothed curve of the magnetic capacity of TmE.S., obtained using a value of 1.78 joules $(mole\text{-}deg)^{-1}$ for $\Delta C(T)$ is shown in Figure 9. The experimental points differed by more than 15 per cent from this curve in only 4 cases.

In Table 3 are given the results obtained for C_m of TmE.S. obtained by subtracting the proper quantity from the

Figure 9. Cm of TmE.S.

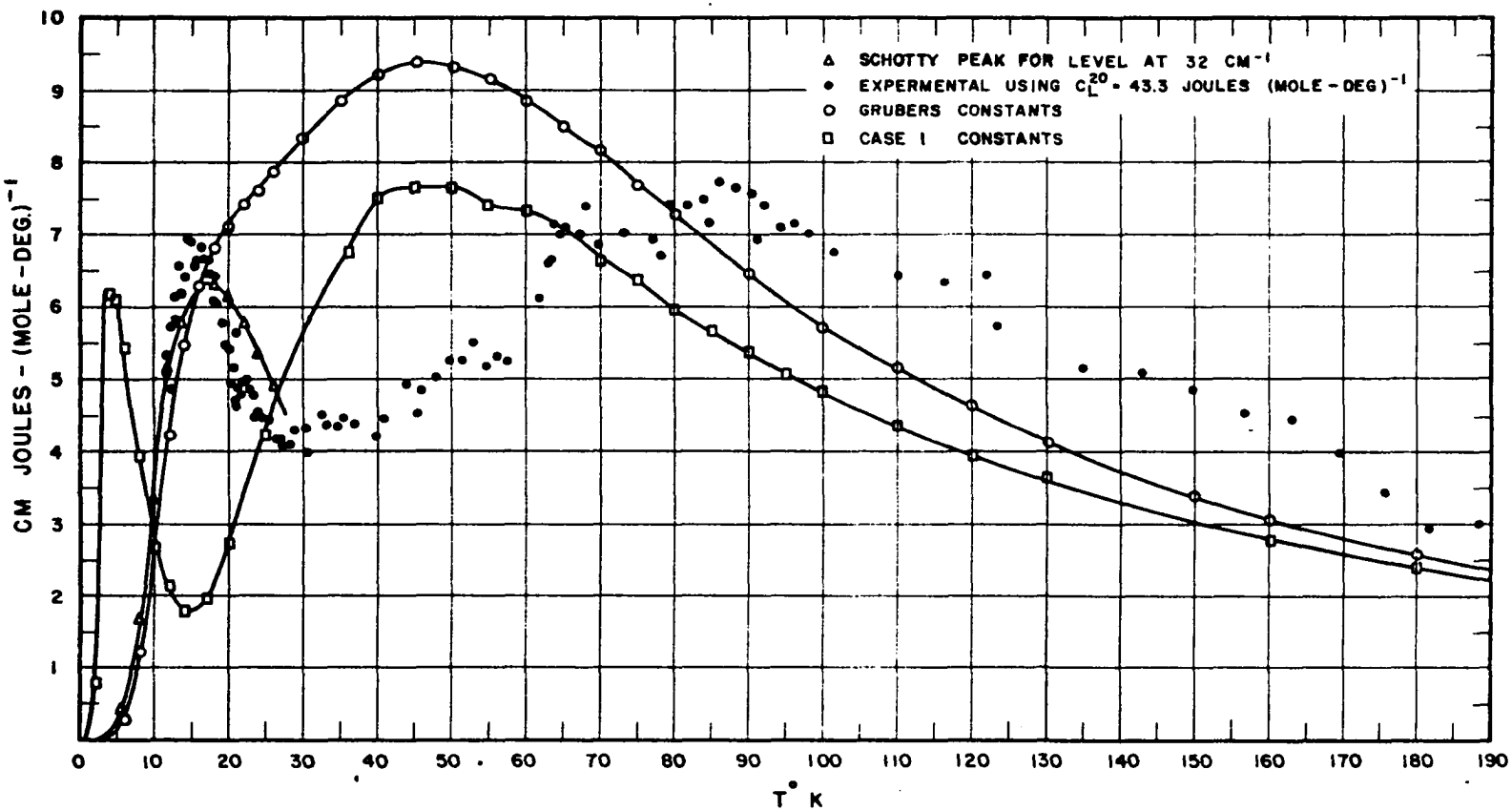
SCHOTTY PEAK FOR LEVEL AT 32 CM⁻¹
EXPERMENTAL USING C_L^{20} = 43.3 JOULES (MOLE - DEG)⁻¹
GRUBERS CONSTANTS
CASE I CONSTANTS
CM JOULES - (MOLE - DEG.)⁻¹
T° K
0
10
20
30
40
50
60
70
80
90
100
110
120
130
140
150
160
170
180
190
1
2
3
4
5
6
7
8
9
10

Table 3. Experimental values of C_m of $Tm(EtSO_4)_3.9H_2O$, joules $(mole\text{-}deg)^{-1}$, values below 20°K obtained using formula 10, values above 20°K obtained using formula 9
1 mole = 706.88 g, 0°C = 273.15°K

T °K	C_m	T °K	C_m	T °K	C_m
11.855	5.32	25.379	4.39	77.068	6.94
11.861	5.07	25.598	4.31	78.252	6.70
12.157	5.74	26.329	4.15	79.399	7.42
12.212	4.86	26.480	4.15	81.664	7.42
12.720	6.14	26.796	5.83	83.868	7.50
12.758	5.82	27.221	4.07	84.640	7.18
13.308	6.57	28.304	4.07	86.017	7.74
13.582	6.19	28.341	4.07	88.117	7.66
14.005	6.43	28.770	4.31	90.175	7.58
14.406	6.92	30.232	4.31	91.156	6.94
14.783	6.90	30.418	3.99	92.193	7.42
15.229	6.56	32.487	4.55	94.175	7.10
15.618	6.82	32.816	4.39	96.122	7.18
16.627	6.67	34.559	4.39	97.641	10.37
16.950	6.46	35.321	4.47	98.040	7.02
17.663	6.39	36.781	4.39	99.932	4.87
17.815	6.41	39.632	4.23	104.140	6.78
17.884	6.09	40.932	4.47	110.325	6.40
18.615	6.01	43.876	4.95	116.250	6.38
19.036	5.76	45.058	4.55	121.953	6.46
19.698	5.48	45.892	4.79	128.528	5.75
20.074	5.43	47.788	5.03	135.917	5.19
20.360	4.95	49.585	5.27	143.037	5.11
20.360	5.19	51.298	5.27	149.918	4.87
20.769	4.63	51.323	5.11	156.592	4.55
20.893	4.71	52.938	5.51	163.038	4.45
20.920	5.67	54.516	5.19	169.402	3.99
21.012	3.19	56.037	5.83	175.575	3.43
21.152	4.87	57.506	5.75	181.610	2.95
21.659	4.79	57.605	5.75	188.292	3.03
21.698	4.95	61.707	6.15	196.891	2.63
21.976	4.95	62.969	6.62	206.454	2.31
21.996	4.95	63.115	6.68		
22.550	5.00	63.747	7.18		
22.870	4.87	64.515	7.02		
23.404	4.79	65.385	7.10		
23.521	4.47	67.251	7.02		
23.782	4.55	68.107	7.42		
24.365	4.47	69.947	6.86		
24.652	4.39	73.340	7.02		

experimental values of $\Delta Q/\Delta T$ of TmE.S. plus the calorimeter can, and performing the required multiplication to obtain the molar C_m. The value of C_L^{20} of TmE.S. is taken to be 1.78 joules $(\text{mole-deg})^{-1}$. Below 20°K, the temperature dependence of the lattice contribution in TmE.S. is taken to be the same as that of LaE.S., which is obtained from Meyer and Smith's data. The points listed in Table 3 below 20°K are thus obtained from the formula

$$C_m = 7.981 \left[\Delta Q/\Delta T \text{ (can + TmE.S.)} - \Delta Q/\Delta T \text{ can} - \frac{C_L(T)}{7.981}\right]. \quad (10)$$

Above 20°K, formula 9 is used to obtain C_m. Table 4 lists the smoothed data of $\Delta Q/\Delta T$ versus T for the can used for both the LuE.S. and TmE.S. measurements. Figure 10 shows the smoothed curve of the heat capacity of TmE.S. Since the heat capacity curves for TmE.S. and LuE.S. are the same to within a few per cent, and the magnetic contribution of TmE.S. is not visible on a scale suitable for being placed in this size cover, the heat capacity curve of LuE.S. is not included. The smoothed values of C_p of LuE.S. are given as a function of temperature in Table 5.

Magnetic Susceptibility Measurements

The results of the perpendicular and parallel susceptibility measurements on TmE.S. are listed in Tables 6 and 7, respectively, and typical experimental points are shown in Figures 11 and 12. Note that rationalized units are

Table 4. $\Delta Q/\Delta T$, joules $(deg)^{-1}$, of the calorimeter can used for heat capacity measurements of TmE.S. and LuE.S. salts - points taken from a smoothed curve

T °K	$\Delta Q/\Delta T$	T °K	$\Delta Q/\Delta T$	T °K	$\Delta Q/\Delta T$
10	0.18	70	15.72	200	31.95
12	0.23	80	18.45	210	32.32
14	0.35	90	20.81	220	32.72
16	0.50	100	22.80	230	33.06
18	0.70	110	24.40	240	33.36
20	0.93	120	25.86	250	33.67
25	1.71	130	27.10	260	33.94
30	2.83	140	28.10	270	34.20
35	4.20	150	29.01	273	34.28
40	5.78	160	29.75	280	34.44
45	7.45	170	30.40	290	34.67
50	9.20	180	30.99	300	34.89
60	12.64	190	31.48	310	35.16

Table 5. Smoothed values of C_p, joules $(mole\text{-}deg)^{-1}$ for $Lu(C_2H_5SO_4)_3 \cdot 9H_2O$* - 1 mole = 712.47 g, 0°C = 273.15°K.

T °K	C_p	T °K	C_p	T °K	C_p
5	0.847	60	204.49	160	484.5
10	8.47	70	238.62	170	508.8
15	22.77	80	271.10	180	528.1
20	42.36	90	304.81	190	555.3
25	63.42	100	329.19	200	577.9
30	85.22	110	356.7	275	745.68
35	107.20	120	383.7	280	756.7
40	128.14	130	409.5	290	779.0
45	148.69	140	435.0	295	802.7
50	168.11	150	459.7		

*Values below 20° obtained assuming the temperature dependence of C_p of LuE.S. is the same as that for LaE.S. measured by Meyer and Smith.

Figure 10. Cp of TmE.S.

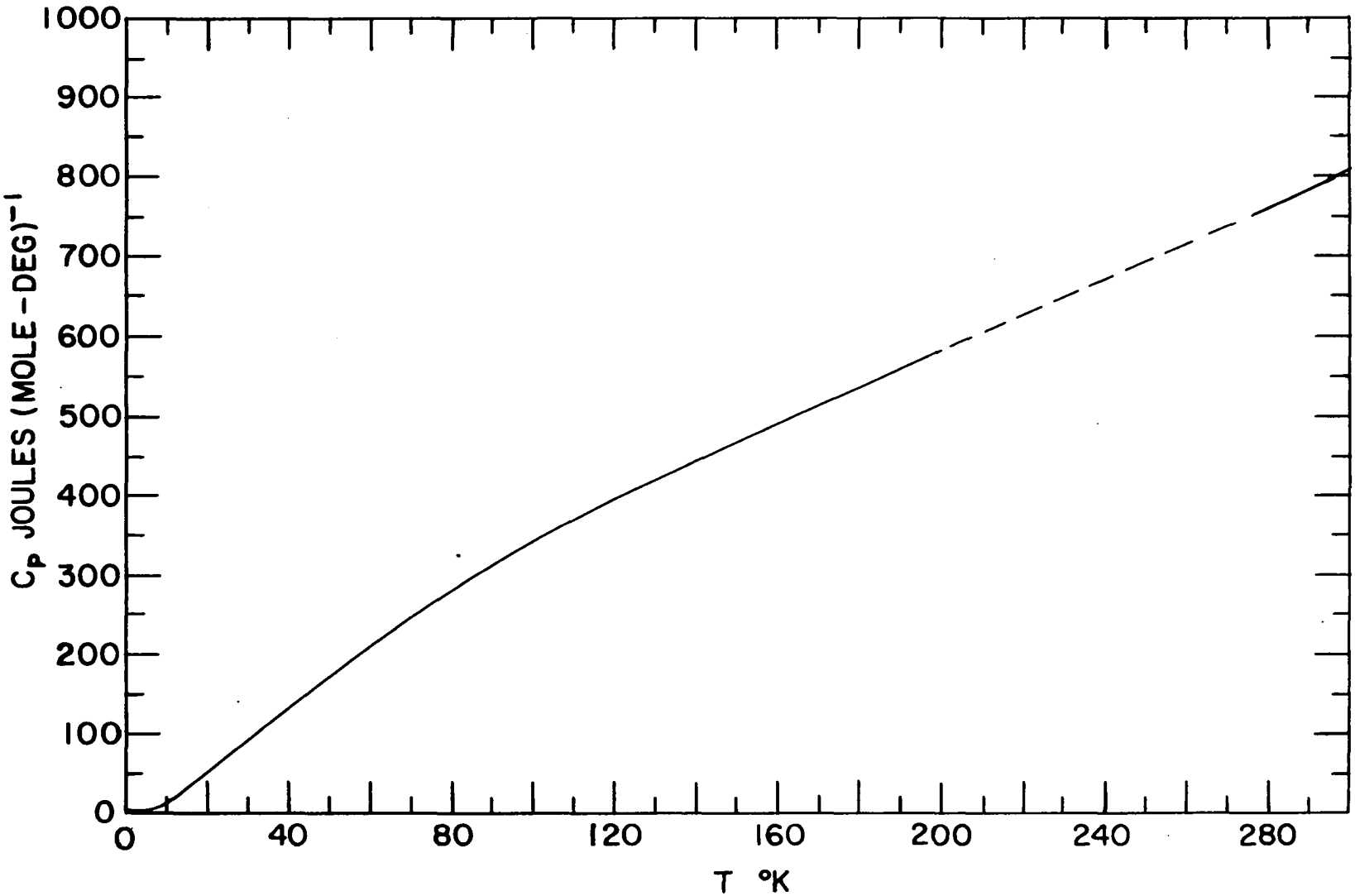
1000
900
800
700
600
500
400
300
200
100
0
C_p JOULES (MOLE-DEG)$^{-1}$
0
40
80
120
160
200
240
280
T °K

Table 6. Experimental values of $\chi_{\perp}^{rat}$ for $Tm(C_2H_5SO_4)_3.9H_2O$ molecular weight = 706.88 g (mole)$^{-1}$, density = 2.00 g (cm^3)$^{-1}$, 0°C = 273.15°K

T °K	$\chi_{\perp}^{rat}x10^2$	T °K	$\chi_{\perp}^{rat}x10^2$	T °K	$\chi_{\perp}^{rat}x10^2$
Crystal No. 3		3.17	1.540	34.4	0.813
		3.34	1.538		
Run 1		3.69	1.538	Crystal No. 2	
		3.86	1.537		
1.57	1.551	4.19	1.533	Run 1	
1.87	1.539	7.83	1.501		
2.11	1.535	8.38	1.487	1.314	1.570
2.48	1.530	9.75	1.463	1.380	1.567
3.32	1.516	10.4	1.442	1.514	1.564
3.62	1.515	11.4	1.420	1.652	1.560
4.19	1.508	12.1	1.399	1.850	1.556
		14.0	1.350	2.025	1.553
Crystal No. 1		14.5	1.329	2.120	1.552
		15.3	1.302	2.373	1.550
Run 1		15.8	1.280	2.681	1.547
		16.5	1.259	2.904	1.545
1.32	1.581	17.0	1.243	3.053	1.544
1.46	1.571	17.4	1.229	3.237	1.542
1.69	1.566	18.1	1.216	3.397	1.541
1.91	1.557	18.3	1.202	3.620	1.539
2.15	1.552	18.7	1.189	3.812	1.538
2.37	1.546	18.9	1.176	4.010	1.537
2.64	1.542	19.4	1.162	4.181	1.535
2.85	1.542	20.4	1.135	4.18	1.534
3.14	1.539	20.9	1.122	5.17	1.524
3.37	1.539	21.1	1.108	6.50	1.520
3.56	1.537	21.5	1.095	7.50	1.512
3.78	1.535	22.0	1.082	8.38	1.504
3.93	1.533	22.4	1.068	9.13	1.492
4.18	1.532	23.0	1.055	9.75	1.481
		23.9	1.028	10.30	1.469
Run 2		24.7	1.014	10.80	1.457
		25.2	1.001	11.20	1.446
1.485	1.578	25.9	0.988	11.80	1.434
1.70	1.570	26.4	0.974	12.44	1.416
1.88	1.561	27.0	0.961	12.73	1.405
2.07	1.557	27.6	0.947	13.27	1.384
2.15	1.554	28.9	0.920	13.64	1.382
2.29	1.553	30.1	0.894	14.08	1.371
2.73	1.467	31.3	0.867	14.42	1.359
3.05	1.542	32.7	0.840	15.08	1.342

Table 6. (Cont.)

T °K	$\chi^{rat}_{\perp} \times 10^2$	T °K	$\chi^{rat}_{\perp} \times 10^2$	T °K	$\chi^{rat}_{\perp} \times 10^2$
Run 1 (Cont.)		66.5	0.487	18.7	1.219
		69.5	0.463	19.2	1.202
15.39	1.330	74.6	0.440	19.8	1.185
15.77	1.319	79.5	0.417	20.5	1.162
16.15	1.307	83.0	0.400	21.2	1.138
16.54	1.296	84.4	0.383	21.9	1.115
16.69	1.284	90.9	0.365	22.4	1.098
17.69	1.272	95.2	0.348	23.1	1.075
17.78	1.255	99.9	0.331	24.2	1.029
18.00	1.249	106.1	0.313	24.9	1.029
18.31	1.238	109.5	0.302	26.0	1.006
18.82	1.221	112.8	0.290	26.7	0.982
19.41	1.203	116.6	0.279	27.3	0.959
19.88	1.186	120.6	0.267	28.6	0.936
20.41	1.169	125.6	0.255	29.8	0.913
20.94	1.151	129.5	0.244	32.2	0.867
21.59	1.134	134.7	0.232	33.3	0.844
22.23	1.117	139.5	0.221	34.6	0.821
22.97	1.093	144.0	0.212	35.4	0.803
23.77	1.070	149.8	0.203	36.5	0.781
24.54	1.047	153.3	0.195	38.1	0.763
25.35	1.024	158.8	0.186	39.1	0.745
26.26	1.000	164.0	0.177	40.3	0.728
27.18	0.978	169.1	0.169	41.5	0.711
28.29	0.955	175.8	0.160	43.3	0.670
30.38	0.914	182.6	0.151	46.4	0.653
30.8	0.891	189.4	0.143	48.1	0.636
32.7	0.868	196.7	0.134	50.1	0.618
33.7	0.845			51.8	0.601
35.0	0.833	Run No. 2		53.2	0.584
36.6	0.799			55.3	0.566
37.8	0.776	12.6	1.422	57.6	0.549
40.5	0.752	13.0	1.399	59.7	0.532
41.5	0.729	13.4	1.387	63.9	0.497
42.5	0.706	13.8	1.375	68.3	0.474
45.4	0.683	14.2	1.364	71.0	0.457
46.2	0.660	14.8	1.347	75.8	0.433
48.5	0.637	15.5	1.323	80.1	0.410
51.3	0.614	16.0	1.306	86.1	0.387
53.1	0.591	16.5	1.289	91.0	0.357
55.7	0.567	17.1	1.271	97.1	0.340
58.5	0.544	17.7	1.254	106.1	0.317
62.1	0.521	18.2	1.237	115.3	0.294

Table 6. (Cont.)

T °K	$\chi^{rat}_{i} \times 10^2$	T °K	$\chi^{rat}_{i} \times 10^2$
Run No. 2 (Cont.)		Run No. 5	
121.4	0.276	1.47	1.561
127.9	0.259	1.97	1.555
134.3	0.242	2.37	1.555
146.3	0.224	2.36	1.545
154.4	0.213	3.36	1.540
		4.20	1.539
Run No. 3		13.5	1.390
		14.5	1.355
80.5	0.405	15.6	1.326
84.1	0.383	17.6	1.275
87.3	0.367	19.6	1.205
99.6	0.323	21.9	1.130
105.0	0.306	23.9	1.072
112.9	0.283	27.1	0.985
120.5	0.265	30.8	0.899
127.8	0.248	34.8	0.812
137.9	0.231	40.4	0.725
145.9	0.217	47.9	0.633
156.4	0.202	54.7	0.574
169.2	0.185	59.6	0.523
181.4	0.173	69.4	0.460
193.7	0.162	78.3	0.414
206.5	0.153	85.0	0.379
		94.0	0.343
Run No. 4		100.8	0.320
		108.7	0.297
80.5	0.407	117.5	0.274
88.2	0.379	127.1	0.251
91.9	0.359	139.8	0.228
102.8	0.330	151.2	0.211
111.4	0.300	162.4	0.195
119.9	0.277	170.1	0.176
132.0	0.254	192.0	0.159
141.1	0.231	202.6	0.147
162.8	0.208		
169.1	0.197		
180.5	0.185		
197.0	0.173		
199.8	0.167		
207.5	0.161		

Table 7. Experimental values of χ^{rat}_{II} for $Tm(C_2H_5SO_4)_3.9H_2O$
molecular weight = 706.88 g, density = 2.00 g $(cm^3)^{-1}$
0°C = 273.15°K

T °K	$\chi^{rat}_{II} \times 10^4$	T °K	$\chi^{rat}_{II} \times 10^4$	T °K	$\chi^{rat}_{II} \times 10^4$
Crystal No. 4		186.1	10.29	6.0	2.81
		191.2	10.29	7.2	1.87
Run 1		196.3	10.91	8.0	1.39
		201.4	10.91	8.6	2.18
32.1	5.30	204.0	10.91	11.4	1.71
33.0	5.46			12.3	1.71
35.2	6.08	Run No. 2		13.0	2.06
36.7	6.08			13.7	2.06
43.4	6.55	30.4	4.37	14.4	2.34
45.8	7.02	31.3	4.37	15.0	2.50
49.7	7.17	32.2	4.37	15.7	2.50
51.6	7.64	33.4	5.14	16.9	2.06
54.3	7.95	34.7	5.77	17.6	2.06
57.2	8.11	35.6	6.92	18.3	2.06
60.6	8.26	36.5	5.92	19.0	2.34
64.0	8.42	37.2	5.92	19.6	2.34
67.2	9.04	38.2	6.08	20.2	2.65
70.3	9.20	39.0	6.24	21.1	2.80
73.4	9.35	40.0	6.39	21.7	3.59
79.5	9.82	41.2	6.24	23.1	3.74
82.4	9.82	41.8	6.39	24.0	4.05
82.4	9.82	42.8	6.55	24.8	4.21
85.3	10.29			25.6	4.36
88.1	10.91	Run No. 3		26.4	4.83
93.7	10.91			27.9	4.99
99.4	11.07	1.40	8.10	29.4	5.12
105.0	11.07	1.46	8.10	32.1	5.30
110.5	11.07	1.61	6.70	34.3	5.62
115.9	11.38	1.75	5.92	36.5	5.77
123.9	11.54	1.91	6.70	38.6	5.92
129.2	11.38	2.05	7.32	40.6	5.92
134.6	11.38	2.17	6.40	42.6	6.40
139.8	10.91	2.37	5.77	44.6	6.40
145.0	10.45	2.63	2.49	46.6	6.55
150.3	10.45	2.82	1.87	58.8	7.80
155.4	10.45	3.12	1.71	62.2	8.42
160.6	10.45	3.34	1.87	65.4	8.88
165.8	9.98	3.57	0.46	68.5	9.20
171.0	9.98	3.79	1.25	71.7	9.20
176.1	9.98	4.01	1.09	74.8	9.20
181.1	9.98	4.19	1.25	77.8	9.35

Table 7. (Cont.)

T °K	$\chi^{rat}_{\parallel} \times 10^4$	T °K	$\chi^{rat}_{\parallel} \times 10^4$	T °K	$\chi^{rat}_{\parallel} \times 10^4$
80.7	9.35	Crystal No. 5		14.25	2.69
83.6	9.35			15.63	3.27
86.5	9.66	Run 1[a]		16.88	3.94
89.3	9.66			18.93	4.03
89.3	9.66	1.37	7.49	20.18	3.65
92.2	9.82	1.52	6.63	20.18	4.32
95.0	10.14	1.76	5.95		
97.8	10.29	1.97	5.76	Run 3[c]	
100.0	10.29	2.13	5.38		
103.5	10.60	2.32	5.67	63.3	5.57
106.2	10.60	2.58	5.19	63.3	5.67
109.0	10.91	2.87	5.57	65.6	4.90
111.7	10.91	3.17	5.19	67.5	6.15
117.2	11.05	3.34	5.09	69.8	5.57
122.5	11.05	3.55	4.60	72.7	6.53
127.8	11.23	3.77	5.28	74.7	6.72
133.1	11.23	4.02	3.52	77.3	6.53
138.4	11.70				
143.7	11.70	Run 2[b]		Run 4[c]	
148.9	12.16				
154.0	12.16	10.0	3.94	63.3	4.91
159.2	12.31	13.95	3.55	63.3	5.91
164.3	12.94	13.95	4.03	63.3	6.48
169.5	13.25	13.95	3.55	66.5	5.78
174.6	13.10	13.95	4.51	68.7	4.51
179.7	13.10	14.38	2.79	71.5	4.51
184.7	12.94	15.50	3.07	73.5	6.10
189.2	12.94	16.63	3.75	75.1	6.77
194.9	12.78	17.87	3.27	77.3	6.72
200.0	12.78	18.80	3.64		
205.1	12.64	20.37	3.74	Run 5[a]	
210.2	12.16				
		Run 3[b]		1.43	6.48
				1.65	7.86
		13.9	3.94	1.84	6.67

[a]Liquid He used as bath and thermometer

[b]Liquid H_2 used as bath and thermometer

[c]Liquid N_2 used as bath and thermometer

Table 7. (Cont.)

T °K	$\chi^{rat}_{\parallel} \times 10^4$	T °K	$\chi^{rat}_{\parallel} \times 10^4$	T °K	$\chi^{rat}_{\parallel} \times 10^4$
2.01	6.28	180	11.10		
2.15	6.09	186.5	9.77		
2.32	5.70	186.5	9.77		
2.57	5.21	193	11.30		
2.66	5.11	193	11.10		
3.81	4.71	202	11.10		
4.02	5.01	202	12.80		
4.20	4.61	206.5	9.30		
4.20	4.42	206.5	9.40		
		206.5	9.90		
Run 6[d]		212	9.30		
		220	8.49		
111	7.86	220	9.25		
112	7.37	229.5	8.78		
112	7.86				
100	6.77	Run 9[e]			
100	6.89				
		173	8.59		
Run 7[e]		190	8.79		
		190	8.28		
145	7.80	190	6.74		
145	11.70	200	8.69		
145	8.78	209	9.10		
155	10.73	220	8.18		
155	9.94	229	9.92		
165	6.83	229	11.40		
170	10.70	229	9.42		
181	11.70	229	10.22		
		229	11.04		
Run 8[e]					
162	11.70				
162	10.80				
166.5	8.80				
166.5	8.80				
170	9.40				
170	9.40				
175	9.30				
180	11.10				

[d]Liquid CH_4 used as bath and thermometer

[e]Liquid C_3H_8 used as bath and thermometer

Figure 11. Rationalized perpendicular susceptibility of TmE.S.

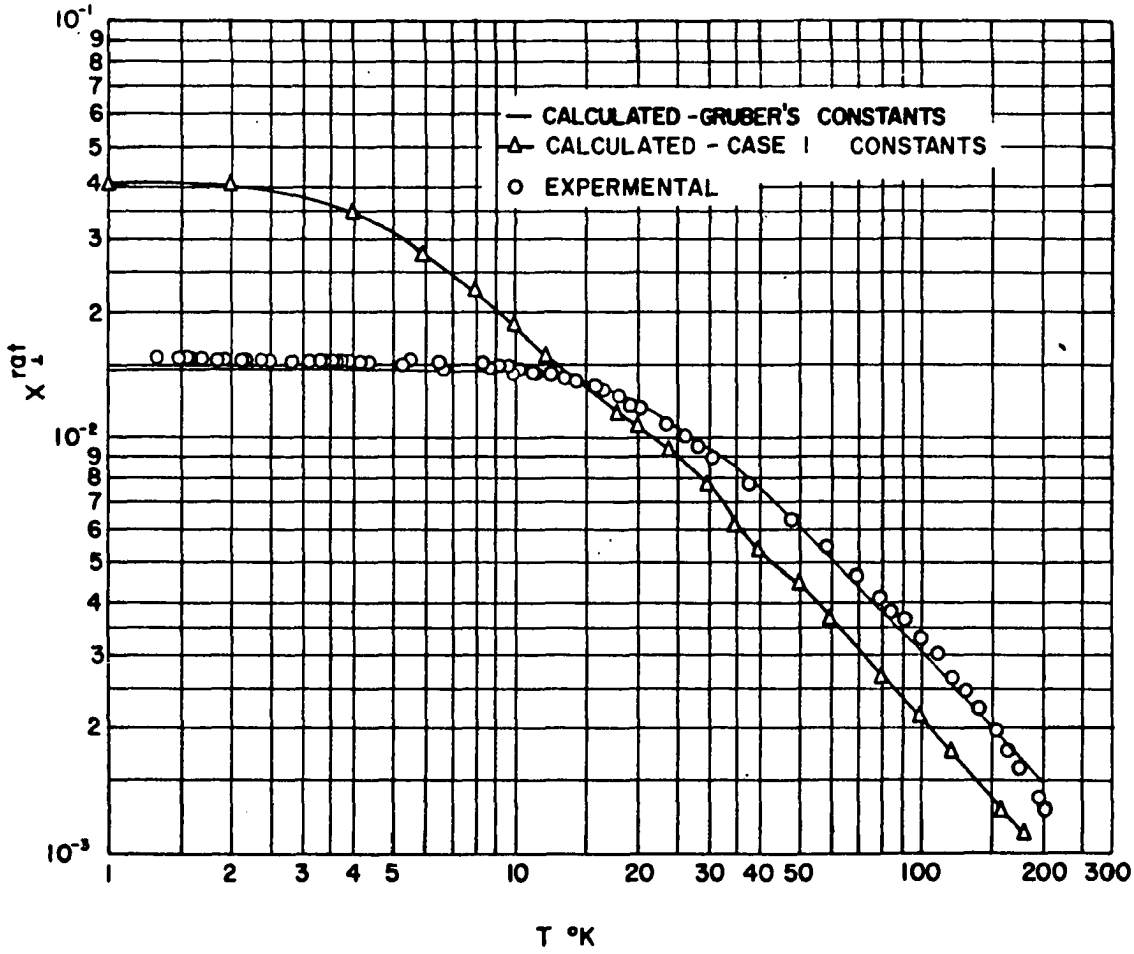
— CALCULATED - GRUBER'S CONSTANTS
-Δ- CALCULATED - CASE I CONSTANTS
O EXPERMENTAL
10^{-1}
10^{-2}
10^{-3}
χ^{rat}_{-1}
1 2 3 4 5 10 20 30 40 50 100 200 300
T °K

Figure 12. Rationalized parallel susceptibility of TmE.S.

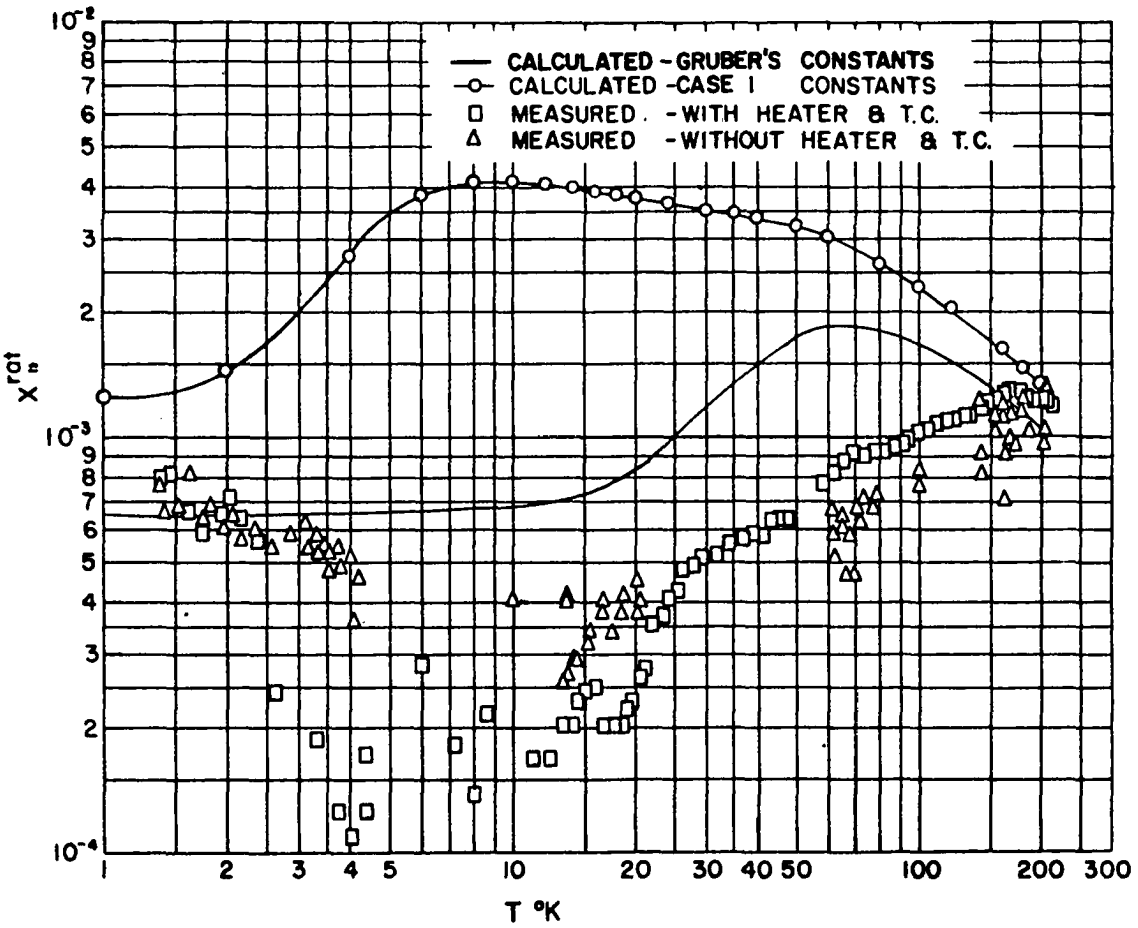
CALCULATED - GRUBER'S CONSTANTS
CALCULATED - CASE I CONSTANTS
MEASURED - WITH HEATER & T.C.
MEASURED - WITHOUT HEATER & T.C.
χ^{rot}_{m}
T °K
10^{-2}
10^{-3}
10^{-4}
1
2
3
4
5
10
20
30
40
50
100
200
300

employed throughout this work. As mentioned under "Experimental Procedure, Magnetic susceptibility measurements", three different crystals were used for the measurements of the perpendicular susceptibility, hereafter referred to as $\chi_{\perp}$, and three crystals were used for measurements of $\chi_{\parallel}$, the parallel susceptibility. The crystals used for $\chi_{\perp}$ measurements were designated as crystals numbers 1, 2, and 3. Measurements below 20°K were made on crystals numbers 1 and 3. Five runs were made above 1.3°K on crystal number 2. The precision of the measurements was one per cent below 20°K, 2 per cent below 100°K, and ranged from 2 to 20 per cent at 100 to 210°K, respectively. The determination of the absolute value of $\chi_{\perp}$ was limited by the coil calibration, knowledge of H_{dipole} below 100°K, and the precision of the measurements above 100°K. The coil calibration was precise to 0.5 per cent. Since the density of the ferric ammonium alum used for the calibration was only known to 0.5 per cent, however, the absolute accuracy of the calibration was only good to one per cent. The limitations, coupled with the precision of the $\chi_{\perp}$ data, made the absolute value of $\chi_{\perp}$ good to 2 per cent below 100°K, neglecting H_{dipole}, and between 2 and 20 per cent from 100 to 200°K.

The absolute value of $\chi_{\perp}$ measured using a calibrated coil is dependent upon the knowledge of the dipole field discussed under "Treatment of Data, Magnetic susceptibility

measurements". This limitation is inherent in the measurement because the difference in the local fields between the salt used for calibration, and the salt whose susceptibility is measured, is ignored. As stated before, $H = H_o + H_{demag.} + H_{dipole}$. For a sphere $H_{demag.} = -M/3\mu_o$. H_{dipole} will be on the order of magnitude of $M/3\mu_o$ (Van Vleck, 204), so that H will differ from H_o by something smaller than $M/3\mu_o$, at most. If one makes the worst assumption possible, namely that $H - H_o = M/3\mu_o = \frac{\chi}{3} Ho$, then the absolute magnitude of a χ determined by neglecting H will be off by $(10^2/3)\chi$ per cent. Since the maximum $\chi_\perp$ measured in this work was 1.5×10^{-2}, the maximum error associated with ignoring the difference in Ho and H will be 0.5 per cent and the total maximum error in the absolute value of $\chi_\perp$ will lie below 3 per cent. Because of the extremity of value assumed for H-Ho, however, it is probable that the value of $\chi_\perp$ obtained experimentally lies within 2 per cent of the true value.

The crystals used for $\chi_{\parallel}$ measurements were designated as crystals numbers 4 and 5. The $\chi_{\parallel}$ measurements on crystal number 4 were badly scattered below 30°K, and were associated with a relatively high value of ΔR_2, the change in the bridge resistive component with the sample in, and out of the coils. Above 30°K the precision improved, and ΔR_2 became comparable to the values obtained in the measurements of $\chi_\perp$. A short in the leads wrapped about the sample holder was determined to be

the cause of the trouble. For this reason, a new, unwired sample holder was constructed, and $\chi_{\parallel}$ of another crystal, crystal number 5, was measured in the range 1.3-4, 13-20, 64-78, 90-110, and 140-210°K. Liquid He, H_2, N_2, CH_4, and C_2H_8 were used as coolant baths and thermometers, as mentioned under "Treatment of Data, Magnetic susceptibility measurements". The scatter of the points taken in the above manner was relatively large, because of the impossibility of keeping the sample coils at a constant temperature. These data served, however, to positively establish the order of magnitude and shape of $\chi_{\parallel}$ below 4°K, and give a rough check of the absolute magnitude above 13°K. None of the points differed by more than 20 per cent from a smoothed curve between 1.3 and 2 °K, and 30 and 200°K. Below 20°K, the points taken with the wired sample container were so irreproducible as to be useless. The He and H_2 range points taken with the unwired container did not deviate from a smoothed curve by more than 30 per cent. One reason for the large experimental scatter in the $\chi_{\parallel}$ measurements was the absolute magnitude of $\chi_{\parallel}$, which was always less than 2×10^{-3} in rationalized units, and which was approximately 2×10^{-4} in the range 4-20°K. The value at 20°K corresponded to a ΔI reading of 0.040 on the bridge, and, in general, the bridge readings were reproducible to 0.005 at best, and about 0.020 at worst. In terms of experimentally determinable absolute magnitudes, therefore, it is not surprising that the

$\chi_{\parallel}$ measurements were imprecise. The absolute magnitude of $\chi_{\parallel}$ therefore, was limited by the precision of the measurements, and in no case was obtained to better than 20 per cent.

DISCUSSION

The Hamiltonian for an ion subject to an electrical potential V, and a magnetic field H, is usually taken to be

$$\mathcal{H} = \sum_i(-h^2 \nabla_i^2/2m + Ze^2/r_i) + \sum_{i>j} e^2/r_{ij} + \sum_i \zeta(r_i)\vec{L}_i\cdot\vec{S}_i - \sum_i \vec{H}\cdot\vec{\mu}_i + \sum_i Ve_i + N \qquad (11)$$

where m is the reduced mass of the electron, ∇^2 is the Laplacian operator, Z is the atomic number, r_i is the distance of the ith electron from the origin, r_{ij} is the distance of the ith from the jth electron, $\zeta(r_i)$ is the spin-orbit coupling parameter, μ_i is the magnetic moment of the ith electron, and N refers to all nuclear interactions. N is small enough compared to the effects we will be interested in to be neglected in this work.

The use of the central field approximation to solve for atomic energy levels in the absence of an electric or magnetic field has been discussed by Conden and Shortley (160). The solution of the problem for trivalent Tm, in the case where the electrostatic repulsion terms are not very much larger than the spin-orbit coupling terms, has been discussed by Spedding (170), and recently recalculated by Gruber and Conway (190) using Spedding's original equations. The matrix elements of an electric potential possessing C_{3h} symmetry have been calculated for the lowest, and next higher J value in the rare earths by Elliot (9) and Elliot and Stevens (11), and the

matrix elements of the magnetic interaction are readily accessible if R-S coupling is assumed, so the solution of the entire problem for trivalent Tm has been, within the limits of the assumptions involved, set up in principle.

It is generally assumed that because the rare earths have magnetic moments at room temperature which are in accord with their lowest J value, R-S coupling is a good approximation in the rare earths. It is also assumed, because Curie's, or the Curie-Weiss law, is followed at room temperature, that the crystal field splittings of the lowest J value are smaller than kT at 300°K. This is to say that the total crystal field splitting of the ground state is on the order of 200 cm^{-1}. Spedding (36) and later workers (190) have found that the first state above ground for trivalent Tm is separated from the ground by about 5,500 cm^{-1}. Second order perturbation theory tells us that the contribution to splittings of the Jth state from higher states goes as the reciprocal of the unperturbed energy difference between the two states, and directly as the sum of the squares of the matrix elements connecting the two states. Since the order of magnitude of the matrix elements connecting two states is less than the total splitting of the individual states, we are dealing with a contribution of approximately $(200^2/5{\cdot}5x10^3)cm^{-1}$ to a splitting of 200 cm^{-1}, or about 2 per cent, from the first excited state in trivalent Tm, which is $^3H_4$, and less from

higher states. This contribution may be ignored in this work, since it will be seen that our knowledge of the crystal field parameters involves errors in the ground state splitting which are at least of the above order of magnitude. The crystal field splitting, then, may as a first approximation, be applied as a perturbation to the lowest state of trivalent Tm. This approximation will limit the dimension of the secular determinant for Tm to 13. As in previous determinations of crystal field splittings at ground states (4), it may be assumed that the ground state is "pure" $^3H_6$, that is, the known deviation from R-S coupling in this ion may be assumed not to appreciably change the splitting of the ground state of the trivalent ion from that calculated using R-S coupling.

To the approximation that the contribution from excited states is negligible and hyperfine splittings are ignored, the splitting caused by a crystal field V and magnetic field H, of the ground state $^3H_6$, is given by

$$|\langle J_z|V + \beta\vec{H}(\vec{L} + 2\vec{S}) - W\delta J_{z/}J'_z\ |J'_z\rangle = 0 \qquad (12)$$

where $|A|$ stands for "the determinant of A", the Dirac notation of matrix elements is used, and J_z ranges from 6 to -6. Here $\beta(\vec{L} + 2\vec{S})$ is $\vec{\mu}$ in the Hamiltonian, where β is the Bohr magneton.

The case with H = 0 will be examined first. The crystal field assumption leads to the restriction that the crystal field potential must satisfy Laplace's equation, a solution of

which is $V = \sum_{L,M} C_L^M r^L Y_L^M$ where Y_L^M is a spherical harmonic. The condition that the potential remain invariant under the operations of the symmetry group of the crystal, which is C_{3h} for the rare earth ethylsulfates, leads to a restriction of the values of l - m to 2n, and m to 3k, where n and k are integers. A matrix element of V between 4f states will be of the form

$$\langle 4, 3, m, m_s|V|4, 3, m', m_s'\rangle = \sum_{l,m} C_l^m \int_0^\infty R_{4f}^2 \, r^l \, r^2 dr \int_\tau \overline{Y_3^m} \, Y_L^M \, Y_3^{m'} \, d\tau \, \delta_{m_s m_s'} \qquad (13)$$

Because of the orthogonality properties of spherical harmonics, this integral will vanish unless $m = m' + M$. Since a product of two spherical harmonics $Y_l^m \cdot Y_{l'}^{m'}$ may be expressed as a sum of spherical harmonics $\sum_{L,M} Y_L^M$ with L always involving $(l - 2i) \pm (l' - 2j)$ where i and j are zero or integers, and since in this case $l = l' (= 3)$, the above sum will be even. Because $\int_\tau Y_L^M \, Y_{L'}^{M'} \, d\tau$ will vanish unless $L = L'$, L in (13) will be even and equal to or less than 6. Therefore, M will have to be even, so M will now be restricted to 6k where k is an integer. The crystal field potentials, then, that we are left with because of the crystal summetry and the dimensionality of 4f wave functions are V_o^o $(= C_o^o \langle r^o \rangle Y_o^o)$, V_2^o, V_4^o, V_6^o, and $V_6^{\pm 6}$. Thus each matrix element of V will be a sum involving one or more of these five terms. V_o^o is independent of L and M, however, and thus does not contribute to the splitting of the ground state. It only contributes an additive constant to all

levels, so it may be ignored in calculations of differences between split levels.

Elliot and Stevens (10), (11), (12) have evaluated the non-vanishing matrix elements of these potentials in the representation which is diagonal in L, S, J^2, and J_Z. They used the fact that within a manifold in which J is constant, the matrix elements of potential operators are equal to a constant times the matrix elements of appropriate angular momentum operators. In Stevens' notation, we have a given J and

$$J_Z \langle J_Z | V_2^0 | J_Z' \rangle = \alpha A_2^0 \left[3J_Z^2 - J(J+1) \right] \text{ where here } A_Z^0 = C_2^0$$

$$\langle r^2 \rangle \langle J_Z | V_4^0 | J_Z \rangle = \beta A_2^0 \left[35J_Z^4 - 30J(J+1)J_Z^2 - + 25J_Z^2 - 6J(J+1) + 3J^2(J+1)^2 \right] \text{where } A_4^0 = C_4^0 \langle r^4 \rangle$$

$$\langle J_Z | V_6^0 | J_Z \rangle = \alpha A_6^0 \left[231J_Z^6 - 315J(J+1)J_Z^4 + 735J_Z^4 + 105J^2 (J+1)^2 J_Z^2 - 525J(J+1)J_Z^2 + 294J_Z^2 - 5J^3 (J+1)^3 + 40J^2 (J+1)^2 - 60J(J+1) \right] S J_Z J_Z' \text{ where } A_6^0 = C_6^0 \langle r^6 \rangle$$

$$\langle J_Z | V_6^6 | J_Z \rangle = \gamma A_6^6 \, 1/2 \left[(Jx + iJy)^6 + (Jx - iJy)^6 \right]$$

V_2^0, V_4^0 and V_6^0 are diagonal in J_Z and symmetric about $J_Z = 0$, and V_6^6 only has elements 6 off the diagonal. It too, is symmetric about $J_Z = 0$. For "pure" $^3H_6$, Stevens has calculated the values of α, β, and γ to be 1/99, 8/3.11.1485, and -5/13.33.2079 respectively. Thus, the diagonal matrix elements of V will be given by a sum of the type $\alpha A_2^0 A + \beta A_4^0 B + \gamma A_6^0 C$ where A, B, and C are functions of J_Z and J. The off diagonal elements of V will be of the form $A_6^6 D$. The values of A, B, C, and D versus (J_Z, J_Z') are given in Table 8.

Table 8. A, B, C, and D within J = 6 for Tm, $^3H_6$, in a C_{3h} crystal field

J_Z	± 6	± 5	± 4	± 3	± 2	± 1	0
J'_Z	± 6	± 5	± 4	± 3	± 2	± 1	0
A	66	33	6	-15	-30	-39	-42
B	60 x 99	-60 x 66	-60 x 96	-60 x 54	660	3840	5640
C	168,300	-420,750	61,200	328,950	168,300	-153,000	-306,000

J_Z	± 6	± 5	± 4	± 3
J'_Z	0	∓ 1	∓ 2	∓ 3
D	$720\sqrt{231}$	$2520\sqrt{66}$	$5040\sqrt{30}$	30,240

To date, there have been two sets of crystal field parameters which have been available for the calculation of the energy levels of thulium in the ethylsulfate. The first, obtained from an extrapolation of these used in the paramagnetic work on the rare earths (4) in the last half of the series are as follows: $A_2^o = 0$. $A_4^o = -40cm^{-1}$. $A_6^o = -30cm^{-1}$. $A_6^6 = 330cm^{-1}$. These will be designated as "Case I constants". The second, obtained by Gruber and Conway (195) from spectroscopic data on TmE.S., are as follows: $A_2^o = 13cm^{-1}$. $A_4^o = -80cm^{-1}$. $A_6^o = 32cm^{-1}$. $A_6^6 = 300cm^{-1}$. These will be called "Gruber's constants". Gruber's constants were chosen to give the best fit with the splitting of the $\mu = 3$ and $\mu = \pm 2$ sublevels in the states $^3F_4$, $^1G_4$, and $^3H_6$, and "reasonable" splitting of the $^3P_2$, $^3F_2$, and $^3H_6$ states. Because of the symmetry of the secular equation, the determinant for calculating the zero magnetic field levels breaks into a cubic and five quadratics. These were hand calculated to give levels for both Elliots' and Gruber's field constants. Gruber and Conway, in addition to producing another set of field constants, also calculated the change in Stevens' α, β and γ, due to off diagonal electrostatic repulsion terms in the Hamiltonian, i.e., due to the breakdown of the R-S coupling. The correction factors are, for the $^3H_6$ state, 1.010, 0.976, and 0.986 for α, β and γ, respectively. These corrected factors were used in the calculation of levels using Gruber's constants. The observed zero magnetic field energy levels versus the levels obtained using Case I and Gruber's constants are tabulated in Table 9.

The energy levels in the presence of a magnetic field will

Table 9. Observed versus calculated energy levels for the ground state of Tm in TmE.S., g = degeneracy of level

Observed	g	Case I constants	g	Gruber's constants	g
0 cm^{-1}	1	0 cm^{-1}	1	0 cm^{-1}	1
32	2	8.17	2	34.78	2
195	2	77.62	2	93.04	1
231	1	83.10	1	100.32	1
		84.06	2	124.36	2
		93.23	1	126.81	2
		113.80	1	177.25	1
		182.73	2	238.55	2
		225.68	1	277.53	1

now be discussed. The energy term is the Hamiltonian involving interaction of electronic moments with a field, H, is $-\sum_i \vec{\mu}_i \cdot \vec{H}$.

Because of the symmetry of the secular determinant for $V + \vec{\mu} \cdot \vec{H}$, the negative sign may be omitted. If R-S coupling is assumed to hold, L and S are good quantum numbers, so $\Sigma \vec{\mu}_i = \beta (\vec{L} + 2\vec{S}) = g\beta\vec{J}$ where g is the Landé splitting factor. Writing $\vec{J}$ in vector notation as $J_x\vec{I} + J_y\vec{J} + J_t\vec{K}$, we see that $\Sigma = g\beta H(aJ_x + bJ_y + cJ_Z)$ where a, b and c are direction cosines for the angles between the x, y, and Z axes, and H respectively. For the axis of quantazation parallel to the crystal c axis, and

H parallel to the c axis, we have a = b = o, c = 1, and $\Sigma_{\parallel} = g\beta J_Z H$. For the perpendicular case in a crystal of c_{3h} symmetry, we have $a^2 + b^2 = 1$, c = 0 and $\Sigma_{\perp} = g\beta H(aJ_x + bJ_y)$ where now Z refers to the crystalline c axis. In the representation in which J^2 and J_Z are diagonal, the non-vanishing matrix elements of J_Z are just J_Z on the diagonal, and the non-vanishing matrix elements of J_x and J_y are

$$\langle J, J_Z \pm 1 \mid Jx \mid J, J_Z \rangle = 1/2\left(\left[J \mp J_Z \right] \left[J \pm J_Z + 1 \right] \right)^{1/2}$$

and

$$\langle J, J_Z \pm 1 \mid Jy \mid J, J_Z \rangle = \mp 1/2\left(\left[J \mp J_Z \right] \left[J \mp J_Z + 1 \right) \right).$$

The matrix elements for $H_{\parallel}$ and $H_{\perp}$ are given in Table 10. The elements given are coefficients of $g\beta H$.

For $H_{\parallel}$, the energy calculation in terms of the crystal field matrix elements, and of G(= $g\beta H$) was carried out as follows: The cubic and 3 quadratics in the secular determinant were each expanded in terms of E and G. E was then set equal to $Eo + bG + cG^2 + \ldots$, the resulting expression expanded, and coefficients of G collected and set to zero. Since the Eo's were known from the zero field calculation, each coefficient of G could be solved for in turn. Thus each energy level was explicitly determined as a function of field.

For $H_{\perp}$, the entire secular determinant was solved on the ISU Cyclone computor for values of G = 1/2, 1, and 2 cm^{-1}. It is possible to show, for $H_{\perp}$, that in the expansion of the secular determinant a and b only occur in the combination

Table 10. Non-vanishing matrix elements of J_Z and aJx + bJy

J_Z	± 6	± 5	± 4	± 3	± 2	± 1	0
J_Z'	± 6	± 5	± 4	± 3	± 2	± 1	0
$\langle\lvert J_Z\rvert\rangle$	± 6	± 5	± 4	± 1	± 2	± 1	0

J_Z	± 6	± 5	± 4	± 3	± 2	± 1
J_Z'	± 5	± 4	± 3	± 2	± 1	0
$\langle\lvert aJx + bJy\rvert\rangle$	$\sqrt{12}(a \mp ib)$	$\sqrt{22}(a \mp ib)$	$\sqrt{30}(a \mp ib)$	$\sqrt{36}(a \mp ib)$	$\sqrt{40}(a \mp ib)$	$\sqrt{42}(a \mp ib)$

$a^2 + b^2$. Therefore, only the coefficients of $(a \pm ib)$ were fed to the computor. It is also possible to show, for H_1, that only even powers of G are involved in the secular determinant expansion. Each level was therefore expressed as $E = Eo + cG^2 + dG^4 + eG^6$.

Three values of E were obtained for the three values of G, so that c, d and e could be solved for. The coefficients of G and G^2 were obtained in this manner for both Case I and Gruber's field constants. The calculation of the magnetic heat capacity and susceptibility were then made using the usual statistical mechanical formulae:

$$Cm = \frac{R}{Z^2}\left[Z \sum_i \left(\frac{Ei}{kT}\right)^2 e^{-Ei/kT} - \left(\sum_i \frac{Ei}{kT} e^{-Ei/kT}\right)^2\right] = \frac{\partial}{\partial T} RT^2 \frac{\partial \, LnZ}{\partial \, T} \qquad (14)$$

where Z is the sum over states, k is Boltzmann's constant, and Ei is the difference between the ground and the ith level, and

$$\chi^{rat} = 4\pi \frac{N}{Z} \Sigma\left(\frac{bi^2}{kT} - 2c_i\right) e^{-ai/kT} = \frac{NkT}{H} \frac{\partial LnZ}{\partial H} \qquad (15)$$

where the ith level is expressed as

$Ei = a_i + b_iH + c_iH^2$ and the standard subterfuge of expanding Z as a function of field is used ((208) pp. 608-619). N is the number of atoms per unit volume, or atoms per mole, depending upon whether a dimensionless, or molar susceptibility is desired. In this work, a dimensionless χ has been calculated. This formula is only valid for $\frac{\beta H}{kT}$ much less

unity - i.e. high temperatures or low fields. For a non-degenerate ground level, ao = bo = 0. The results of the heat capacity and magnetic susceptibility calculations for the two sets of constants are shown in Figures 9, 11 and 12.

From a comparison of calculated with experimental values of the ground state splittings in TmE.S., it is not obvious that either set of field constants yields a successful fitting of experiment with theory. Gruber's values do have among them the observed 32, 195 and 231 cm^{-1}, to within 20 per cent at worst, but this is not surprising since these levels were three of the four pieces of information used to evaluate field constants. The values calculated using the Case I constants appear completely unrealistic. A look at the experimental versus calculated heat capacity curves shows, however, that while Gruber's calculated level at 35 cm^{-1} gives the correct low temperature tail of the heat capacity, the levels below 125 cm^{-1} must certainly be in error. If they existed, the 32 cm^{-1} peak would not show up as a distinct bump at all. The Cm calculated from the Case I constants, while unreal, serves to illustrate the shape of a curve obtained when there is a separation of a factor of ten between the first and succeeding levels above ground - i.e., the Case I constants lead to a level of 8.17 cm^{-1} above ground, and a group of levels starting out 78 cm^{-1}. They thus give a "two peak" structure to Cm. Gruber's first and second excited states are

separated only by a factor of three, and this structure is not obtained. One might thus be led to speculate that the separation between the 32 cm^{-1} and the next highest level would be of the order of five or six times 32, or at about 190 cm^{-1}, which is actually observed. Because of the height of the experimental peak, one might also be led to speculate that there are a number of closely packed levels in the region 190-300 cm^{-1}. Since the absolute magnitude of the second peak is in doubt due to the uncertainty in the lattice heat capacity of TmE.S., however, such speculations have little quantitative value.

The agreement between the calculated and experimental susceptibilities is, as might be expected, poor for the Case I constants. In both the parallel and perpendicular cases, it is obvious that the calculated value of 8.17 cm^{-1} for the first level above ground is causing both curves to break at too low a temperature. Note, however, that the slopes of the calculated and experimental perpendicular susceptibilities do not greatly differ once the two curves have broken from their constant values at 0°K. This is not the case, however, with the calculated and experimental parallel susceptibilities.

For Gruber's constants, the calculated and experimental perpendicular susceptibilities agree to within experimental error, but the difference between the calculated and experimental parallel susceptibilities again points up the indication

that the calculated curve involves too many levels coming in at too low a temperature.

The reason for the really excellent agreement between the calculated and experimental perpendicular susceptibilities is not completely obvious. One thought might be that the perpendicular susceptibility has a particularly simple form of temperature dependence, i.e., $X_\perp = \frac{4\pi N}{Z} \sum_i - 2C_i e^{-Ei/kT}$. The C for the 32 cm^{-1} level has been forced into a realistic value by using this level as one of the field constant determining parameters. Since it turned out to be positive, and possibly fortuitously, as large as any of the other coefficients, it will dominate the susceptibility at the low temperature downward break. That it continues its domination over a rather large temperature range seen from the fact that the sum of the C_i's must equal zero, so for every negative C_i that would tend to raise the susceptibility as its exponential factor approaches unity, there is a positive one that is counteracting this tendency. Since the exponential on the 32 cm^{-1} level is always larger than the others for a given temperature the tendency will be for this level to somewhat over-ride the superimposed effect of the others. I.e., once the correct downward "shove" is given $X_\perp$ at 32 cm^{-1}, the remaining shape of the curve is somewhat predetermined, at least at temperatures less than the total crystal field splitting.

The same type of qualitative argument might be made for the parallel results, except that in this case the temperature dependence is more complicated, in that another parameter and a reciprocal temperature are involved. I.e., in the parallel case a coefficient of the linear term in H exists for the doubly degenerate levels, so each of these will contribute $\frac{4\pi N}{Z}\left(\frac{bi}{kT}^2 - 2c_i\right)e^{-ai/kT}$ to the susceptibility. It also turns out that the C for the 32 cm^{-1} level is less by two orders of magnitude than the c's for the next two higher levels, so that as T increases and the b^2/kT terms become less important, the next higher levels become more important than in the perpendicular case. For comparison, b_i^2 and c_i are given for the parallel case, and c_i is given for the perpendicular case in Table 11. Here, the energy levels are those calculated using Gruber's constants, and the b's and c's are coefficients of $g\beta H$ and $(g\beta H)^2$ respectively. If $g\beta H$ is given in cm^{-1}, b will be dimensionless and c will have the dimensions of $(cm^{-1})^{-1}$.

In retrospect, the following statement might be made: three assumptions are made in the calculation of energy levels of rare earth ions from first principles. These are: (1) the ion core possesses a spherically symmetrical charge distribution (central field approximation), (2) the electrostatic repulsion term is much greater than the spin-orbit coupling term for the ground state (this appears reasonable in view of

Table 11. Coefficients of G and G^2 used in the calculation of $\chi_{\parallel}$ and $\chi_{\perp}$ - Gruber's constants

b_i^2	$\chi_{\parallel}$ c_i	$\chi_{\perp}$ c_i	E_i^0 cm^{-1}
0	-.0267	-.573	0
.0021	-.0521	+.4087	34.78
.0021	-.0521	-.1104	34.78
0	-4.535	-.0661	93.04
0	4.627	-.1515	100.32
.596	-.0521	+.0741	124.36
.596	-.0521	-.2026	124.36
16.25	.0521	+.1267	126.81
16.25	.0521	+.0321	126.81
0	-.0897	+.2708	177.25
5.617	.0521	-.3132	238.55
5.617	.0521	+.0762	238.55
0	+.0897	+.3834	277.53

of the small corrections to Stevens' α, β and r calculated by Gruber and Conway), (3) the Laplacian of the crystal field potential is zero. Using these assumptions and four experimentally determined parameters evaluated from four pieces of experimental information, the agreement between the experimental and calculated ground state splittings in

TmE.S., as evidenced by susceptibility and heat capacity measurements, leaves much to be desired. The perpendicular susceptibility measurements, however, give surprisingly good agreement with the calculated values using Gruber's constants, but it is not obvious that this is due to the corrected calculated energy level structure. Whether the observed disagreement between theory and experiment for TmE.S. lies in a breakdown in one or more of the above three assumptions, or in an improper evaluation of the crystal field constants is yet to be determined. A critical factor in this determination will be whether any four constants exist that can reconcile the experimental thermal, magnetic, and spectral data with calculation. The obviously poor agreement, for TmE.S., between the experimental and calculated Cm, coupled with the "fair" agreement in the calculated and experimental susceptibilities accentuates the fact that it is possible to fit a susceptibility curve with relatively poor values of ground state splitting. It also points up the need for obtaining thermal data in the range 1.4-300°K for all the rare earth ethylsulfates, in order to determine whether or not the previous "good" agreement between experiment and theory below 20°K can be extended to include all the splittings of the ground state. That a great deal of work is yet necessary, theoretically and experimentally in order to get a really good fit between calculated and experimental excited state

splittings, is a conclusion that could easily be defended. A calculation of the crystal field constants from first principles would be interesting as well as informative, and might serve to determine whether or not the currently published values are even in the neighborhood of being correct.

SUMMARY

A description of the construction and operation of a mutual inductance magnetic susceptibility apparatus for measurements in the range 1.4-300°K has been given. Methods used in the treatment of data and calculation of results have been discussed.

The magnetic heat capacity and the single crystal magnetic susceptibilities of TmE.S. have been measured in the range 12-300°K and 1.4-200°K, respectively. The magnetic heat capacity was obtained by using the heat capacity of LuE.S. to evaluate the lattice contribution to TmE.S. Two maxima were observed in the magnetic heat capacity at 19 and 80°K.

The magnetic heat capacity and susceptibilities of TmE.S. have been calculated using the crystalline field approximation and two different sets of crystalline field constants which are currently available from the literature. In neither case was excellent agreement obtained between theory and experiment, although the calculated and experimental perpendicular susceptibilities were in good agreement for the most recently proposed set of field constants. It is not obvious whether the lack of good agreement between experiment and theory is a result of a poor choice of crystal field parameters, a complete failure of the crystal field approximation in this case, or a breakdown of the assumptions involved in calculating the term

intervals and splittings for trivalent Tm. The fair agreement between calculated and experimental susceptibilities, coupled with the complete lack of agreement between calculated and experimental heat capacities points up the need for a further check of previous "good" theoretical and experimental agreement for other rare earth salts with the use of heat capacity data above 20°K.

LITERATURE CITED

1. H. Bethe Ann. Phys. 3, 133 (1929).
2. R. B. Jaynes Phys. Rev. 48, 78 (1935).
3. A. H. Cooke Bull. inst. intern. froid Annex 1955, 178.
4. R. J. Elliot and K. W. H. Stevens Proc. Roy. Soc. (London) A215, 437 (1952).
5. J. H. Van Vleck "Theory of Electric and Magnetic Susceptibilities" Oxford Univ. Press, Oxford, England (1932).
6. F. Hund Z. Physik 33, 855 (1925).
7. J. A. A. Ketelaar Physica 4, 619 (1937).
8. D. R. Fitzwater and R. E. Rundle Z. Krist. 112, 362 (1959).
9. K. W. H. Stevens Proc. Phys. Soc. (London) A65, 209 (1952).
10. R. J. Elliot Rev. Mod. Phys. 25, 167 (1953).
11. R. J. Elliot and K. W. H. Stevens Proc. Roy. Soc. (London) A219, 387 (1953).
12. R. J. Elliot and K. W. H. Stevens Proc. Roy. Soc. (London) A218, 553 (1953).
13. J. Becquerel Le Radium 4, 328 (1907).
14. _____ ibid. 5, 5 (1908).
15. _____ ibid. 6, 327 (1909).
16. _____ Z. Physik 58, 205 (1929).
17. _____ Physica 5, 753 (1938).
18. _____ and H. K. Onnes Le Radium 5, 227 (1908).
19. _____ and _____ Proc. Acad. Amsterdam 10, 592 (1908).

20. _____, _____, and W. J. Dettaas ibid. 29, 264 (1926).

21. _____ and H. K. Onnes Compt. rend. 146, 625 (1908).

22. _____ ibid. 181, 758 (1925).

23. K. F. Herzfeld Physik. Z. 22, 544 (1921).

24. J. Becquerel Proc. Acad. Amsterdam 32, 740 (1929).

25. S. Freed and F. H. Spedding Nature 123, 525 (1929).

26. _____ and _____ Phys. Rev. 34, 945 (1929).

27. S. Freed Phys. Rev. 38, 2122 (1931).

28. F. H. Spedding and G. C. Nutting ibid. 38, 2294 (1931).

29. F. H. Spedding Phys. Rev. 37, 777 (1931).

30. S. Freed and F. H. Spedding ibid. 38, 670 (1931).

31. Yasumttsu Uzmasa Bull. Chem. Soc. Japan. 7, 85 (1932).

32. S. Freed Proc. Roy. Acad. Amsterdam 35, 979 (1932).

33. F. H. Spedding and R. S. Bear Phys. Rev. 46, 308 (1934).

34. W. Prandtl and K. Z. Scheiner Z. anorg. chem. 220, 107 (1934).

35. C. B. Ellis Phys. Rev. 49, 875 (1936).

36. H. A. Bethe and F. H. Spedding Phys. Rev. 52, 454 (1937).

37. F. H. Spedding, H. F. Hamlin, and G. C. Nutting J. Chem. Phys. 5, 172 (1937).

38. A. Merz Ann. Physik (Series 5) 28, 569 (1937).

39. G. Joos and H. Ewald Naturwissenschaften 25, 636 (1937).

40. F. H. Spedding, J. P. Howe, and W. H. Keller J. Chem. Phys. 5, 416 (1937).

41. W. G. Penny and R. Schlapp Phys. Rev. 41, 194 (1932).

42. J. H. Van Vleck J. Phys. Chem. 41, 67 (1937).

43. F. H. Spedding J. Chem. Phys. 5, 160 (1937).

44. F. H. Spedding and H. F. Hamlin J. Chem. Phys. 5, 429 (1937).

45. A. Merz Ann. Physik (Series 5) 28, 569 (1937).

46. H. Ewald Ann. Physik (Series 5) 34, 209 (1939).

47. E. J. Meehan and G. C. Nutting J. Chem. Phys. 7, 1002 (1939).

48. S. Freed, S. I. Weissman, and F. E. Fortress J. Am. Chem. Soc. 63, 1079 (1941).

49. W. F. Meggers Rev. Mod. Phys. 14, 96 (1942).

50. L. J. F. Broer, C. J. Gorter, and J. Hoonschagen Physica 11, 231 (1945).

51. L. J. F. Broer ibid. 12, 642 (1946).

52. D. M. Yost, H. Russell, Jr., and C. S. Garner "The Rare Earth Elements and Compounds" John Wiley and Sons, N.Y., (1947).

53. H. Severin Ann. Physik (Series 6) 1, 41 (1947).

54. H. Severin Z. Physik 125, 445 (1948).

55. J. Hoonschagen and C. J. Gorter Physica 14, 197 (1948).

56. H. Gobrecht Ann. Phys. 7, 88 (1950).

57. S. Freed and C. J. Hochandel J. Chem. Phys. 18, 780 (1950).

58. K. H. Hellwege and H. G. Kahle Z. Physik 129, 62 (1951).

59. H. F. Geisler and K. H. Hellwege ibid. 136, 293 (1953).

60. A. M. Hellwege and K. H. Hellwege ibid. 130, 549 (1951).

61. J. Brochard and K. H. Hellwege ibid. 135, 620 (1953).

62. A. Paskin and J. M. Keller Iowa State Coll. J. Sci. 28, 375 (1954).

63. G. H. Dieke and L. Heroux Phys. Rev. 103, 1227 (1956).

64. S. Freed and E. V. Sayre J. Chem. Phys. 23, 2066 (1955).

65. C. K. Jørgensen J. Chem. Phys. 21, 637 (1955).

66. H. G. Kahle Z. Physik 145, 347 (1956).

67. C. K. Jørgensen Acta Chem. Scand. 11, 981 (1957).

68. B. R. Judd Proc. Roy. Soc. (London) A241, 414 (1957).

69. S. P. Cook and G. H. Dieke J. Chem. Phys. 27, 1213 (1957).

70. U. Johnsen Z. Physik 152, 454 (1958).

71. P. Krumholz Spectrochim. Acta 10, 269 (1958).

72. E. Carlson and G. H. Dieke J. Chem. Phys. 29, 229 (1958).

73. P. P. Feofilov Optica i Spectroscopiva 5, 216 (1958).

74. S. P. Keller J. Chem. Phys. 29, 180 (1958).

75. S. P. Keller and G. D. Pettit ibid. 30, 434 (1959).

76. H. G. Kahle Z. Physik 155, 129 (1959).

77. J. B. Gruber and J. G. Conway J. Chem. Phys. 32, 1180 (1960).

78. E. Wedekind Ber. deut. chem. Ges. B54, 253 (1921).

79. "Collected Papers of H. A. Kramers" North Holland Publishing Co., Amsterdam (1956).

80. C. J. Gorter Nature 128, 68 (1931).

81. W. Klemm, W. Schuth, and M. V. Stackelborg Z. Phys. Chem. B19, 321 (1932).

82. E. H. Williams Phys. Rev. 46, 133 (1934).

83. S. Velayos Anales Soc. espãn fís. guím. 33, 297 (1935).

84. B. Cabrera, S. Velayos, and N. Cabrera Bol. Acad. cienc. exactas, fis-guim nat. (Madrid) 1, No. 2, 1 (1935) and No. 2, 2 (1935).

85. J. Becquerel Compt. rend. 201, 1112 (1935).

86. F. A. Fereday and E. C. Wiersma Physica 2, 575 (1935).

87. L. Mazza and E. Botti Gazz. chim. ital. 66, 552 (1936).

88. B. Cabrera J. phys. radium. 9, 209 (1938).

89. K. S. Krishnan and A. Mookherji Phil. Trans. Roy. Soc. (London) A237, 135 (1938).

90. L. C. Jackson Proc. Roy. Soc. (London) A170, 266 (1939).

91. W. G. Penny and G. S. Kynch ibid. A170, 112 (1939).

92. S. Freed Rev. Mod. Phys. 14, 105 (1942).

93. J. Van den Handel and J. C. Hupse Physica 9, 225 (1942).

94. A. Mukherji Indian J. Phys. 23, 217 (1949).

95. R. A. Satten and D. J. Young J. Chem. Phys. 23, 404 (1955).

96. J. Van den Handel "Encyclopedia of Physics., vol. 2, Low Temperatures" Springer Verlag, Berlin (1956).

97. R. C. Vickery and Ardys Ruben J. Chem. Soc. 1959, 510.

98. A. Mookherji and D. Neogy Current Sci. (India) 28, 12 (1959).

99. Y. Ayant and J. Thomas Compt. rend. 248, 387 (1959).

100. J. Cohen and J. Ducloz J. phys. radium 20, 402 (1959).

101. "Paramagnetic Crystals in Use for Low Temperature Research", in C. J. Gorter, ed. "Progress in Low Temperature Physics" pp. 224-244, Interscience, N.Y., (1955).

102. J. A. Ahlkberg and S. Freed Phys. Rev. 39, 540 (1932).

103. W. F. Giague and C. W. Clark ibid. 54, 3135 (1932).

104. J. A. Ahlkberg and C. W. Clark ibid. 57, 437 (1935).

105. J. A. Ahlkberg, E. R. Blanchard, and W. O. Lundberg J. Chem. Phys. 5, 552 (1937).

106. J. M. Daniels Proc. Phys. Soc. (London) A66, 673 (1953).

107. B. Bleany, H. E. D. Scovil, and R. S. Trenam Phil. Mag. (Series 7) 43, 995 (1952).

108. A. H. Cooke, S. Whitley and W. P. Wolf Proc. Phys. Soc. (London) B68, 415 (1955).

109. A. H. Cooke, H. J. Duffus, and W. P. Wolf Phil. Mag. (Series 7) 44, 623 (1953).

110. H. Sato and R. Kikuchi J. Appl. Phys. 30, 945 (1959).

111. A. H. Cooke, F. R. McKim, H. Meyer, and W. P. Wolf Phil. Mag. (Series 8) 2, 928 (1957).

112. Horst Meyer and P. L. Smith J. Phys. Chem. Solids 9, 285 (1959).

113. H. W. Goldstein, E. F. Nielson, P. N. Walsh, and D. White J. Phys. Chem. 63, 1445 (1959).

114. K. H. Hellwege, U. Johnsen, and W. Pfeffer Z. Physik 154, 301 (1959).

115. H. Bethe Z. Physik 60, 218 (1930).

116. O. M. Jordahl, W. G. Penny, and R. Schlapp Phys. Rev. 40, 637 (1932).

117. R. Schlapp and W. G. Penny Phys. Rev. 42, 666 (1932).

118. J. H. Van Vleck J. Chem. Phys. 3, 807 (1935).

119. G. J. Kynch Trans. Farad. Soc. 33, 1402 (1937).

120. F. H. Spedding J. Chem. Phys. 5, 316 (1937).

121. C. B. Ellis and Harry Hall Phys. Rev. 54, 478 (1938).

122. C. Kittel and J. M. Luttinger Phys. Rev. 73, 162 (1948).

123. J. DeBoer and R. Van Lieshout Physica 15, 570 (1949).

124. R. J. Elliot and K. W. H. Stevens Proc. Phys. Soc. (London) A64, 932 (1951).

125. H. E. D. Scovil and K. W. H. Stevens Proc. Phys. Soc. (London) A65, 954 (1952).

126. B. R. Judd Proc. Roy. Soc. (London) A227, 552 (1955).

127. _____ ibid. A232, 458 (1955).

128. _____ ibid. A241, 122 (1957).

129. W. H. Kleiner J. Chem. Phys. 20, 1784 (1952).

130. Y. Tanabe and S. Sugano J. Phys. Soc. Japan 11, 864 (1956).

131. J. C. Phillips J. Phys. Chem. Solids 11, 226 (1959).

132. R. Lacroix Hely. Phys. Acta 30, 478 (1957).

133. K. H. Hellwege, U. Johnsen, H. Kahle, and G. Schaak Z. Physik 148, 112 (1957).

134. E. V. Sayre, K. M. Sancier, and S. Freed J. Chem. Phys. 49, 242 (1958).

135. N. V. Afanas'eva Optika i Spectroskopiva 5, 629 (1958).

136. W. Low Phys. Rev. 109, 265 (1958).

137. R. Lacroix Arch. Sci. (Geneva) 11, Spec. No. 141 (1958).

138. H. Statz and G. F. Koster Phys. Rev. 115, 1568 (1959).

139. H. S. Jarrett J. Chem. Phys. 31, 1579 (1959).

140. R. L. White and J. P. Andelin, Jr. Phys. Rev. 115, 1435 (1959).

141. R. A. Satten and J. S. Margolis J. Chem. Phys. 32, 573 (1960).

142. R. J. Elliot and K. W. H. Stevens Proc. Phys. Soc. (London) A64, 205 (1951).

143. _____ and _____ ibid. A65, 370 (1952).

144. E. Zavoisky J. Phys. U.S.S.R. 10, 197 (1946).

145. S. A. Al'tshuler, V. YaKurenev, and S. G. Salikhov Doklady Akad. Nauk S.S.S.R. 70, 201 (1950).

146. B. Bleany, R. J. Elliot, H. E. D. Scovil, and R. S. Trenam Phil. Mag. 42, 1062 (1951).

147. B. Bleany and H. E. D. Scovil Proc. Phys. Soc. (London) A64, 204 (1951).

148. G. S. Bogle, H. J. Duffus, and H. E. D. Scovil ibid. A65, 760 (1952).

149. B. Bleany and K. W. H. Stevens Rept. Prog. Phys. 16, 108 (1953).

150. K. D. Bowers and J. Owen ibid. 18, 304 (1955).

151. A. M. Hellwege Z. Phys. 135, 615 (1953).

152. S. A. Al'tshuler, M. M. Zaripov, and L. YaShekun Izvest. Akad. Nauk S.S.S.R. Ser. Fiz. 21, 844 (1957).

153. C. A. Huchinson, Jr., B. R. Judd, and D. F. D. Pope Proc. Phys. Soc. (London) B70, 514 (1957).

154. _____ and E. Wong J. Chem. Phys. 29, 754 (1958).

155. B. R. Judd and E. Wong ibid. 28, 1097 (1958).

156. C. Ryter Helv. Phys. Acta 30, 353 (1957).

157. T. A. Sanadze ,Soviet Phys. [Zhurnal eksperimental 'noĭ i theoreticheskoi fiziki] JETP 6, 801 (1958).

158. On Matsumara, K. Horai, and Z. Miduno J. Phys. Soc. Japan 13, 768 (1958).

159. J. M. Baker and B. Bleany Proc. Roy. Soc. (London) A245, 156 (1958).

160. E. U. Conden and G. H. Shortley "The Theory of Atomic Spectra" Cambridge Univ. Press, Cambridge, England (1935).

161. R. C. Gibbs, D. T. Wilker and H. E. White Phys. Rev. 29 790 (1927).

162. C. P. Snow and F. I. G. Rawlins Proc. Cambridge Phil. Soc. 28, 522 (1932).

163. F. Hund Z. Physik 99, 119 (1936).

164. R. J. Lang Canad. J. Res., Sect. A, 14, 127 (1936).

165. H. Gobrecht Ann. Phys. Lpz. 28, 673 (1937).

166. _____ ibid. 31, 300 (1938).

167. _____ ibid. 31, 755 (1938).

168. _____ Ann. Physik (Series 5) 31, 600 (1937).

169. H. Lang Ann. Physik (Series 5) 31, 609 (1938).

170. F. H. Spedding Phys. Rev. 58, 255 (1940).

171. G. Racah Phys. Rev. 61, 186 (1942).

172. _____ ibid. Rev. 62, 438 (1943).

173. _____ ibid. Rev. 63, 367 (1943).

174. _____ ibid. Rev. 76, 1352 (1949).

175. V. R. Rao Indian J. Phys. 24, 51 (1950).

176. _____ ibid. 24, 296 (1950).

177. _____ ibid. 26, 427 (1952).

178. O. Ishizdu J. Phys. Soc. Japan 5, 145 (1950).

179. G. Racah Letter. Curr. Sci. 21, 67 (1952).

180. R. A. Satten J. Chem. Phys. 21, 637 (1953).

181. _____ ibid. 23, 400 (1955).

182. C. K. Jørgensen J. Chem. Phys. 23, 399 (1955).

183. R. A. Satten Phys. Rev. 85, 775 (1953).

184. E. F. Reilly Phys. Rev. 91, 876 (1953).

185. C. K. Jørgensen Acta Chem. Scand. 9, 540 (1955).

186. B. R. Judd Proc. Roy. Soc. (London) A228, 120 (1955).

187. _____ Proc. Phys. Soc. (London) A69, 157 (1956).

188. J. P. Elliot, B. R. Judd, and W. A. Runciman Proc. Roy. Soc. (London) A240, 509 (1957).

189. V. R. Rao Indian J. Phys. 22, 423 (1958).

190. J. B. Gruber and J. G. Conway J. Chem. Phys. 32, 1178 (1960).

191. B. R. Judd and R. Louden Proc. Roy. Soc. (London) A251, 127 (1959).

192. B. B. Wybourne J. Chem. Phys. 31, 1149 (1959).

193. W. A. Runciman J. Chem. Phys. 30, 1632 (1959).

194. B. G. Wybourne J. Chem. Phys. 32, 639 (1960).

195. J. B. Gruber and J. G. Conway ibid. 32, 1531 (1960).

196. F. H. Spedding Discussions Faraday Soc. 1949, 214 (1949).

197. J. S. Fritz, W. J. Lane, and A. S. Bystroff Anal. Chem. 29, 821 (1957).

198. Ruehrwein and Huffman J. Am. Chem. Soc. 65, 1620 (1943).

199. L. Hartshorn J. Sci. Instr. 2, 145 (1925).

200. V. H. Hesterman "The Effects of Deformation on Superconducting Metals". Unpublished M.S. Thesis, Library, Iowa State University of Science and Technology, Ames, Iowa (1958).

201. L. D. Jennings "Design of Mutual Inductance Bridge for Cryogenic Measurements" [To be published in Review of Scientific Instruments circa September, 1960].

202. F. W. Grober "Inductance Calculations" D. Van Nostrand Co., Inc., N.Y., (1946).

203. R. E. Skochdopole "Low Temperature Heat Capacities of Thorium, Gadolinium, and Erbium". Unpublished Ph.D. Thesis, Library, Iowa State University of Science and Technology, Ames, Iowa (1954).

204. J. H. Van Vleck J. N.Y. Acad. Sci. 40, 289 (1940).

205. C. T. Linder "The Measurement of Low Temperatures" [U.S. Atomic Energy Commission Report] No. R-9433-2-A [Westinghouse Electric Corp. Research Labs., East Pittsburth, Penna.] February 2 (1950).

206. R. I. Copson and Per K. Frolich Ind. Eng. Chem. 21, 1116 (1929).

207. J. A. Hoffman, A. Paskin, K. J. Tauer, and R. J. Weiss J. Phys. Chem. Solids 1, 45 (1956).

208. R. Fowler and E. A. Guggenheim "Statistical Thermodynamics" Cambridge Univ. Press, Cambridge, England, (1952).

ACKNOWLEDGMENTS

The author wishes to express his appreciation to Dr. F. H. Spedding for his suggestion of, permanent interest in, and discussions concerning this problem, and Dr. L. D. Jennings for his guidance and advice in this research. The author wishes to acknowledge the benefit of discussions with Dr. J. M. Keller, Dr. R. E. Rundle, and Dr. C. A. Swenson on the interpretation of the data. He would also like to thank Dr. C. A. Swenson for the use of his facilities in collecting part of the data. The author wishes to thank the following persons: Dr. Jack Powell for preparation of the rare earth oxides; Mr. R. E. Miller, Mr. R. M. Stanton, and Mrs. E. Hill for assistance in some of the measurements and calculations; and Mrs. S. Bystroff for the chemical analysis of the TmE.S. and LuE.S. Finally, the author wishes to express his appreciation to his wife, without whose help the translation phase between the author's writing and the typed rough draft of the thesis could not have been completed.